

**ROLE OF PROTON-COUPLED OLIGOPEPTIDE  
TRANSPORTERS IN SMALL PEPTIDE ABSORPTION  
AND DISPOSITION**

**By**

**Dilara Jappar**

A dissertation submitted in partial fulfillment  
of the requirements for the degree of  
Doctor of Philosophy  
(Pharmaceutical Sciences)  
In The University of Michigan  
2009

Doctoral Committee:

Professor David E. Smith, Chair  
Professor Gordon L. Amidon  
Professor Richard F. Keep  
Professor Steven P. Schwendeman

© Dilara Jappar

All Rights Reserved

2009

## **DEDICATION**

In memory of those Uyghurs who were brutally crushed and killed during the peaceful  
Urumchi demonstration on July 5, 2009

To my loving Mother Rizwan Abaydulla and Father Jappar Rashidin

To my beloved husband Hairat Sabit

Thank you for all your love, support, and sacrifice during my academic journey

## AKNOWLEDGEMENTS

I am greatly obliged to many people who have given me a tremendous amount of support during my academic pursuit. First and foremost, I am very grateful to my advisor Dr. David E. Smith for giving me the great opportunity to work in his laboratory and for providing me with a tremendous amount of support and guidance. His depth of scientific knowledge, right balance of guidance and freedom to explore, and unyielding encouragement have resulted in a tremendous amount of personal growth in me. I am forever indebted to Dr. Smith for his positive role in my professional development.

I would also like to thank my committee members Drs. Gordon Amidon, Richard Keep and Steven Schwendeman for their insightful suggestions and guidance for my research project. It has been a pleasure to work with such knowledgeable and excellent scientists who were sincerely interested in the success of my project and my scientific growth.

I would like to acknowledge Terri Azar, Lynn Alexander (who is greatly missed), Maria Herbel, Jeanne Getty, Barbara Johnson, and Amy Brancheau for their help with the countless administrative matters. I also would like to thank Brandon Ladd from the Upjohn Center for Clinical Pharmacology (Pharmacology Department) for his generous help with the intravenous injections during my *in vivo* studies. I also would like to acknowledge all of my laboratory members for their help. I would like to thank all of the

Upjohn Center for Clinical Pharmacology members for their encouragement and for making my stay at the Upjohn Center a memory rich and fun experience.

I am very fortunate to have such supportive family and friends. Particularly, I am so grateful for my parents' and siblings' unconditional love, support, patience, and encouragement. I also thank my parents for teaching me to believe in excellence and the value of knowledge.

I have been very lucky to go through the experience of graduate school "side by side" with my beloved husband, Hairat Sabit. Knowing each other's daily struggles and challenges definitely made the graduate school experience a unique one for me. His optimistic outlook on life has provided me with a tremendous amount of encouragement during my graduate studies. I am sincerely grateful for his love, support, and continuous encouragement. Last, but not the least, I would also like to thank my second mom, Nancy Gale, for all of her unending love and support.

In concluding, I would like to acknowledge the College of Pharmacy (Upjohn Fellowship, Fred Lyons Fellowship, and Warner Lambert/Parke Davis Fellowship) for the partial support of my research.

## TABLE OF CONTENTS

<b>DEDICATION .....</b>	<b>ii</b>
<b>ACKNOWLEDGEMENTS.....</b>	<b>iii</b>
<b>LIST OF FIGURES.....</b>	<b>vii</b>
<b>LIST OF TABLES.....</b>	<b>xii</b>
<b>LIST OF APPENDICES .....</b>	<b>xiii</b>
<b>ABSTRACT.....</b>	<b>xiv</b>
<b>Chapter 1 .....</b>	<b>1</b>
<b>RESEARCH OBJECTIVES .....</b>	<b>1</b>
<b>Chapter 2 .....</b>	<b>5</b>
<b>BACKGROUND AND LITERATURE REVIEW: .....</b>	<b>5</b>
<b>PROTON-COUPLED OLIGOPEPTIDE TRANSPORTERS.....</b>	<b>5</b>
<b>INTESTINAL PEPTIDE ABSORPTION .....</b>	<b>21</b>
<b>PEPT1 TRANSPORTER.....</b>	<b>28</b>
<b>PHT TRANSPORTERS .....</b>	<b>36</b>
<b>FIGURES .....</b>	<b>39</b>
<b>REFERENCES .....</b>	<b>44</b>
<b>Chapter 3 .....</b>	<b>59</b>
<b>TRANSPORT MECHANISMS OF CARNOSINE IN SKPT CELLS: CONTRIBUTION OF APICAL AND BASOLATERAL MEMBRANE TRANSPORTERS .....</b>	<b>59</b>
<b>ABSTRACT.....</b>	<b>59</b>
<b>INTRODUCTION .....</b>	<b>61</b>
<b>MATERIALS AND METHODS.....</b>	<b>64</b>
<b>RESULTS .....</b>	<b>71</b>
<b>DISCUSSION.....</b>	<b>77</b>

FIGURES .....	83
REFERENCES .....	91
<b>Chapter 4 .....</b>	<b>96</b>
<b>SIGNIFICANCE OF PEPT1 IN THE <i>IN SITU</i> INTESTINAL PERMEABILITY OF GLYCYLSARCOSINE IN WILD-TYPE AND PEPT1 KNOCKOUT MICE.....</b>	<b>96</b>
ABSTRACT.....	96
INTRODUCTION .....	98
MATERIALS AND METHODS.....	101
RESULTS .....	108
DISCUSSION.....	111
FIGURES.....	116
REFERENCES .....	123
<b>Chapter 5 .....</b>	<b>128</b>
<b>SIGNIFICANCE OF PEPT1 ON THE <i>IN VIVO</i> ORAL ABSORPTION AND DISPOSITION OF GLYCYLSARCOSINE IN WILD-TYPE AND PEPT1 KNOCKOUT MICE.....</b>	<b>128</b>
ABSTRACT.....	128
INTRODUCTION .....	130
MATERIALS AND METHODS.....	134
RESULTS .....	140
DISCUSSION.....	146
FIGURES.....	153
REFERENCES .....	171
<b>APPENDICES.....</b>	<b>176</b>

## LIST OF FIGURES

- Figure 2.1** Model of PEPT1 substrate-affinity/transport relationship. The preferred configuration and important conformational features in PEPT1 transporter recognition is summarized. PEPT1 and PEPT2 have very similar not identical structure requirement for affinity/transport. (Adopted from H. Daniel and G. Kottra, *Eur J Physiol.* 447: 610-618, 2004) ..... 39
- Figure 2.2** Model of peptide/mimetics in a single epithelial cell in the intestine and kidney. The peptide transporters PEPT1 and PEPT2 are located at the brush border membrane. They transport small peptide/mimetics from the lumen into the cell. They are energized by  $H^+$  transmembrane gradient and negative membrane potential, which are maintained by sequential action of basolateral  $Na^+/K^+$  ATPase and apical  $Na^+/H^+$  exchangers. Once inside of the cell, the peptide/mimetics are either metabolized into amino acids/metabolites for use or export, or remain as intact. They exit the cell via basolateral amino acid transporters or basolateral peptide transporter accordingly. (Adopted from H. Daniel, *J. Membrane Biol.*, 154:197-203, 1996.)..... 40
- Figure 2.3** Schematic of protein digestion and absorption in the gastrointestinal tract. (Figure adopted from Ganapathy V, Gupta N, and Martindale RG. Protein Digestion and Absorption. In *Physiology of the Gastrointestinal Tract*, 4<sup>th</sup> edition, Johnson LR (ed), Elsevier, Burlington, 2006, pp 1667-1692.) ..... 41
- Figure 3.1** Schematic representation of the SKPT cellular model in which  $CL_{AC}$  and  $CL_{BC}$  represent the influx clearances from the apical and basolateral compartments, respectively, while  $CL_{CA}$  and  $CL_{CB}$  represent the respective efflux clearances to the apical and basolateral compartments (A);  $CL_{AB}$  represents the apical-to-basolateral transepithelial clearance and  $CL_{BA}$  represents the basolateral-to-apical transepithelial clearance (B). The clearance values are those determined experimentally for carnosine in this study (units,  $\mu l/mg/min$ ). ..... 83
- Figure 3.2** RT-PCR analysis of peptide transporter mRNA in SKPT cells, and in kidney, intestine and brain lysates (4  $\mu g$  total RNA). Samples were separated on a 1.5% agarose gel, visualized with ethidium bromide, and screened for PEPT1 and PEPT2 transcripts (A) and for PHT1 and PHT2 transcripts (B).



GAPDH controls for rat brain, intestine, kidney and SKPT cDNA samples are also displayed (C). In each gel, the right-hand lane is a 100 bp DNA ladder. The expected RT-PCR products are shown for each POT under the gel. .... 84

- Figure 3.3** Intracellular accumulation (A) and transcellular transport (B) of 10  $\mu\text{M}$  [ $^3\text{H}$ ]carnosine as a function of time in SKPT cell monolayers at 37°C. The cellular efflux (C) of [ $^3\text{H}$ ]carnosine was determined after preloading the cells from the apical side with 10  $\mu\text{M}$  carnosine for 2 hr at 37°C. For all experiments, the buffer pH was 6.0 in the apical compartment and 7.4 in the basolateral compartment. Data are expressed as mean  $\pm$  SE (n=3-5). ..... 85
- Figure 3.4** Effect of pH on the 15-min uptake of 10  $\mu\text{M}$  [ $^3\text{H}$ ] carnosine in SKPT cell monolayers at 37°C from the apical (A) compartment (basolateral pH maintained at 7.4) and from the basolateral (B) compartment (apical pH maintained at 6.0). Data are expressed as mean  $\pm$  SE (n=3-6). \*\* p < 0.01, as compared to pH 7.4. Relationship between pH and fractional ionization of carnosine (C). ..... 86
- Figure 3.5** Effect of potential inhibitors on the 15-min apical (A) and basolateral (B) uptake of carnosine in SKPT cell monolayers at 37°C. For all experiments, the buffer pH was 6.0 in the apical compartment and 7.4 in the basolateral compartment. Data are expressed as mean  $\pm$  SE (n=3-6). \*\* p < 0.01, as compared to control. .... 87
- Figure 3.6** Effect of concentration on the 15-min uptake of 1-500  $\mu\text{M}$  [ $^3\text{H}$ ]carnosine from the apical (A) and basolateral (B) sides of SKPT cell monolayers at 37°C. For all experiments, the buffer pH was 6.0 in the apical compartment and 7.4 in the basolateral compartment. Data are presented as mean  $\pm$  SE (n=3-6); the inset is a Woolf-Augustinsson-Hofstee plot of the transformed data (V, pmol/mg/15min versus V/S,  $\mu\text{l}/\text{mg}/15\text{min}$ ). ..... 88
- Figure 3.7** Stability of carnosine in the apical, basolateral, and intracellular compartments of SKPT cell monolayers as a function of time (pH 6.0 buffer in apical side and pH 7.4 buffer in basolateral side). Data are presented as mean  $\pm$  SE (n=3). ..... 89
- Figure 4.1** Effective permeability ( $P_{\text{eff}}$ ) of 10  $\mu\text{M}$  [ $^3\text{H}$ ]GlySar during jejunal perfusion of PEPT1<sup>+/+</sup> and PEPT1<sup>-/-</sup> mice. Studies were performed in pH 6.5 perfusion buffer. Data are presented as mean  $\pm$  SE (n=6-9). \*\*\* p < 0.001, for PEPT1 null vs. wild-type. .... 116
- Figure 4.2** Effective permeability ( $P_{\text{eff}}$ ) of 10  $\mu\text{M}$  [ $^3\text{H}$ ]mannitol during jejunal perfusion of PEPT1<sup>+/+</sup> and PEPT1<sup>-/-</sup> mice. Studies were performed in pH 6.5 perfusion buffer. Data are presented as mean  $\pm$  SE (n=4-6). ..... 117

- Figure 4.3** Effective permeability ( $P_{\text{eff}}$ ) of 10  $\mu\text{M}$  [ $^3\text{H}$ ]metoprolol during jejunal perfusion of PEPT1<sup>+/+</sup> and PEPT1<sup>-/-</sup> mice. Studies were performed in pH 6.5 perfusion buffer. Data are presented as mean  $\pm$  SE (n=4-6). ..... 118
- Figure 4.4** Effect of pH on effective permeability ( $P_{\text{eff}}$ ) of 10  $\mu\text{M}$  [ $^3\text{H}$ ]GlySar during jejunal perfusion of wild-type (+/+) mice (A) and PEPT1 null (-/-) mice (C). \*  $p < 0.05$ , compared to pH 7.4. Effect of dimethylamiloride (DMA) (B) on the  $P_{\text{eff}}$  of 10  $\mu\text{M}$  [ $^3\text{H}$ ]GlySar during jejunal perfusion of wild-type mice. Studies were performed in pH 6.5 perfusion buffer (n=4, mean  $\pm$  SE). \*  $p < 0.05$ , compared to control values. .... 119
- Figure 4.5** Concentration-dependent flux of [ $^3\text{H}$ ]GlySar (0.01-20 mM total substrate in perfusate) during jejunal perfusion of wild-type mice. Studies were performed in pH 6.5 buffer (n=4, mean  $\pm$  SE). In panel A,  $C_{\text{in}}$  represents perfusate concentration of GlySar. In panel B,  $C_{\text{w}}$  represent mean “estimated” concentration of GlySar at the intestinal wall. .... 120
- Figure 4.6** Effect of potential inhibitors (25 mM) on the  $P_{\text{eff}}$  of 10  $\mu\text{M}$  [ $^3\text{H}$ ]GlySar during jejunal perfusion of wild-type (+/+) mice (A) and PEPT1 null (-/-) mice (B). Studies were performed in pH 6.5 perfusion buffer (n=4, mean  $\pm$  SE). \*\*  $p < 0.01$ , compared to control values. .... 121
- Figure 4.7** Effective permeability ( $P_{\text{eff}}$ ) of 10  $\mu\text{M}$  [ $^3\text{H}$ ]GlySar during jejunal perfusion of mice and rats. Studies were performed in pH 6.5 perfusion buffer. Data are presented as mean  $\pm$  SE (n=5-6). \*\*\*  $p < 0.001$  for rat vs. mouse. .... 122
- Figure 5.1** Plasma concentrations of GlySar as a function of time over 120 min (A), 240 min (B), and 480 min (C) in PEPT1<sup>+/+</sup> (wild-type) and PEPT1<sup>-/-</sup> (KO) mice following a 1 nmol/g oral gavage dose. Data are expressed as mean  $\pm$  S.E. (n = 4). .... 153
- Figure 5.2** Plasma concentrations of GlySar as a function of time over 120 min (A), 240 min (B), and 480 min (C) in PEPT1<sup>+/+</sup> (wild-type) and PEPT1<sup>-/-</sup> (KO) mice following a 10 nmol/g oral gavage dose. Data are expressed as mean  $\pm$  S.E. (n = 6). .... 154
- Figure 5.3** Plasma concentrations of GlySar as a function of time over 120 min (A), 240 min (B), and 480 min (C) in PEPT1<sup>+/+</sup> (wild-type) and PEPT1<sup>-/-</sup> (KO) mice following a 100 nmol/g oral gavage dose. Data are expressed as mean  $\pm$  S.E. (n = 4). .... 155
- Figure 5.4** Plasma concentrations of GlySar as a function of time over 120 min (A), 240 min (B), and 480 min (C) in PEPT1<sup>+/+</sup> (wild-type) and PEPT1<sup>-/-</sup> (KO) mice following a 1000 nmol/g oral gavage dose. Data are expressed as mean  $\pm$  S.E. (n = 5). .... 156
- Figure 5.5** Plasma concentrations of GlySar as a function of time over 120 min (A), 240 min (B), and 480 min (C) in PEPT1<sup>+/+</sup> (wild-type) and PEPT1<sup>-/-</sup> (KO) mice

following a 5000 nmol/g oral gavage dose. Data are expressed as mean  $\pm$  S.E. (n = 4). ..... 157

- Figure 5.6** Dose-corrected cumulative partial area under the plasma concentration-time curves vs. dose of GlySar in PEPT1<sup>+/+</sup> (wild-type) and PEPT1<sup>-/-</sup> (KO) mice after an oral gavage administration. Data are expressed as mean  $\pm$  S.E. (n = 4-6). \* p < 0.05; \*\*\* p < 0.001 compared with 1 nmol/g dose. .... 158
- Figure 5.7** Cumulative partial AUCs (area under the plasma concentration-time curves) of GlySar as a function of time over 120 min (A), 240 min (B), and 480 min (C) in PEPT1<sup>+/+</sup> (wild-type) and PEPT1<sup>-/-</sup> (KO) mice following a 1 nmol/g oral gavage dose. Data are expressed as mean  $\pm$  S.E. (n = 4). .... 159
- Figure 5.8** Cumulative partial AUCs (area under the plasma concentration-time curves) of GlySar as a function of time over 120 min (A), 240 min (B), and 480 min (C) in PEPT1<sup>+/+</sup> (wild-type) and PEPT1<sup>-/-</sup> (KO) mice following a 10 nmol/g oral gavage dose. Data are expressed as mean  $\pm$  S.E. (n = 6). .... 160
- Figure 5.9** Cumulative partial AUCs (area under the plasma concentration-time curves) of GlySar as a function of time over 120 min (A), 240 min (B), and 480 min (C) in PEPT1<sup>+/+</sup> (wild-type) and PEPT1<sup>-/-</sup> (KO) mice following a 100 nmol/g oral gavage dose. Data are expressed as mean  $\pm$  S.E. (n = 4). .... 161
- Figure 5.10** Cumulative partial AUCs (area under the plasma concentration-time curves) of GlySar as a function of time over 120 min (A), 240 min (B), and 480 min (C) in PEPT1<sup>+/+</sup> (wild-type) and PEPT1<sup>-/-</sup> (KO) mice following a 1000 nmol/g oral gavage dose. Data are expressed as mean  $\pm$  S.E. (n = 5). .... 162
- Figure 5.11** Cumulative partial AUCs (area under the plasma concentration-time curves) of GlySar as a function of time over 120 min (A), 240 min (B), and 480 min (C) in PEPT1<sup>+/+</sup> (wild-type) and PEPT1<sup>-/-</sup> (KO) mice following a 5000 nmol/g oral gavage dose. Data are expressed as mean  $\pm$  S.E. (n = 4). .... 163
- Figure 5.12** Plasma concentration-time profiles of GlySar in PEPT1<sup>+/+</sup> (wild-type) and PEPT1<sup>-/-</sup> (KO) mice after intravenous bolus administration of dipeptide at a dose of 10 nmol/g. Data are expressed as mean  $\pm$  S.E. (n=4-8)..... 164
- Figure 5.13** Tissue concentration (A) and tissue-to-plasma concentration ratio (B) of GlySar in PEPT1<sup>+/+</sup> (wild-type) and PEPT1<sup>-/-</sup> (KO) mice, 60 min after oral gavage administration of dipeptide at 10 nmol/g. Data are expressed as mean  $\pm$  S.E. (n=6). \* p < 0.05; \*\* p < 0.01; \*\*\* p < 0.001 compared with wild-type mice..... 165
- Figure 5.14** Tissue concentration (A) and tissue-to-plasma concentration ratio (B) of GlySar in PEPT1<sup>+/+</sup> (wild-type) and PEPT1<sup>-/-</sup> (KO) mice, 8 h after oral gavage administration of dipeptide at 10 nmol/g. Data are expressed as mean  $\pm$  S.E. (n=6). \* p < 0.05; \*\* p < 0.01; \*\*\* p < 0.001 compared with wild-type mice..... 166

**Figure 5.15** Tissue concentration (A) and tissue-to-plasma concentration ratio (B) of GlySar in PEPT1<sup>+/+</sup> (wild-type) and PEPT1<sup>-/-</sup> (KO) mice, 8 h after intravenous bolus administration of dipeptide at 10 nmol/g. Data are expressed as mean ± S.E. (n=6). \* p < 0.05; \*\* p < 0.01; \*\*\* p < 0.001 compared with wild-type mice. .... 167

**Figure 5.16** Metabolic stability of GlySar in PEPT1<sup>+/+</sup> (wild-type) and PEPT1<sup>-/-</sup> (KO) mice urine over 8 hours (A) and over 24 hours (B) after oral dose administration of dipeptide at 10 nmol/g body weight. Data are presented as mean ± SE (n=4). .... 168

## LIST OF TABLES

<b>Table 2.1</b> Molecular and Functional Features of POTs .....	42
<b>Table 2.2</b> Tissue and Cellular Distribution of POTs.....	43
<b>Table 3.1</b> PCR conditions for Proton-Coupled Oligopeptide Transporter and GAPDH	90
<b>Table 5.1</b> Ration of extent of GlySar systemic exposure in PEPT1 null mice to wild-type at different time point with respect to dose following oral administration (corresponds to Fig 5.1-5.5). .....	169
<b>Table 5.2</b> Dose-corrected slopes of accumulative partial AUC vs. time (Corresponds to Fig 5.7-5.11) .....	170

## **LIST OF APPENDICES**

### **APPENDIX A**

MEASUREMENT OF SKPT INTRACELLULAR VOLUME.....176

### **APPENDIX B**

COMPARISON OF WATER FLUX MEASUREMENTS FOR MOUSE *IN SITU* SINGLE-PASS INTESTINAL PERFUSION.....180

## ABSTRACT

Proton-coupled oligopeptide transporters (POTs) (i.e., PEPT1, PEPT2, PHT1 and PHT2) translocate various small peptide/mimetic across the biological membrane. The first part of this dissertation focuses on investigating the transport properties of carnosine in kidney using SKPT cell cultures as a model of proximal tubular transport. Results demonstrated that carnosine is expected to have a substantial cellular accumulation in kidney due to its high influx clearance across apical membranes by PEPT2, but minimal tubular reabsorption into blood because of very low efflux clearance across basolateral membranes.

Although the role of PEPT1 in intestinal absorption of small peptide/mimetics has been demonstrated previously by *in vitro* models, its relative importance during *in vivo* intestinal absorption is unknown. Therefore, the objective of the second part of this dissertation is to delineate the relative importance of PEPT1 in intestinal absorption and disposition of small peptides/mimetics using wild-type and PEPT1 deficient mice, and glycylsarcosine (GlySar) as a model dipeptide substrate. *In situ* intestinal perfusions and *in vivo* absorption models in mice were used in our investigations. The results from our *in situ* studies show that PEPT1 is responsible for at least 90% of GlySar uptake in the small intestine and the transport protein exhibits low-affinity kinetics. However, during *in vivo* conditions, the extent of reduction in absorption, due to the absence of PEPT1,

was lower than that of the *in situ* model. Specifically, the extent of GlySar absorption was reduced by about 50% due to the absence of PEPT1 transporter during *in vivo* condition. When partial  $AUC_{0-120 \text{ min}}$  was used as an indicator of the rate of absorption, there was a 60% reduction in the rate of GlySar absorption in PEPT1 deficient mice compared to the wild-type animals. With the exception of small intestine, PEPT1 had little effect on the tissue distribution of GlySar. In conclusion, the present studies demonstrate, using both *in situ* and *in vivo* models, that PEPT1 ablation significantly reduces both the rate and extent of oral absorption of small peptide/mimetic substrates (i.e., GlySar). These studies suggest that variability in intestinal PEPT1 (expression and/or activity) should exert a similar fate on peptide-like drugs.



## Chapter 1

### RESEARCH OBJECTIVES

Proton-coupled oligopeptide transporters (POTs) translocate various small peptides and peptidomimetics across the biological membrane via an inwardly directed proton gradient and negative membrane potential. Up to this date, four members to this POT family, PEPT1, PEPT2, PHT1, and PHT2, have been identified in mammals. POTs have significant physiological roles in the absorption and reabsorption of peptide-bound amino nitrogen as well as pharmacological roles in peptidomimetic drug absorption and disposition. Due to their broad substrate specificity, varying capacity, and differential tissue distribution, POTs offer a promising target to drug design in effort to increase drugs' oral bioavailability and/or tissue selection. Current molecular cloning and characterization of POT members have increased our understanding of each peptide transporters' structure, functional property, localization and physiological / pharmacological relevance.

Carnosine ( $\beta$ -alanyl-L-histidine) is a naturally-occurring dipeptide that is highly concentrated in skeletal muscle and brain. Besides being an endogenous substrate, carnosine is also taken exogenously as a dietary supplement for its antioxidant and free radical scavenging properties. Pharmacologically, carnosine has some renoprotective effects including acting as a protective factor in diabetic nephropathy and preventing

ischemia-induced renal injury. Carnosine is known to be transported by all four members of the POTs. Despite carnosine's significant pharmacological importance in the kidney, the renal disposition of this dipeptide has not been elucidated. Previous studies in our lab have demonstrated that expression of PEPT2 in the kidney plays an important role in reabsorption of peptide/mimetics. Therefore, the first research project in this dissertation focused on investigating the transport properties of carnosine in kidney using SKPT cell cultures as a model of proximal tubular transport, and to isolate the functional activities of renal apical and basolateral peptide transporters in this process.

Following the ingestion of dietary protein (70- 100 g per day), proteins are converted into large peptides by gastric and pancreatic proteases in gastrointestinal lumen followed by a further hydrolysis into small peptides (80%) and free amino acids (20%) by various peptidases in the brush border membrane of intestinal epithelium. The final end products of protein digestion are absorbed into the enterocytes predominately in the form of di- and tri-peptides as supposed to free amino acids, suggesting an important role of peptide transporters in absorption of end product of protein meal in intestine. Once inside the enterocytes, the majority of the di- and tripeptides undergo further hydrolysis into their constituent amino acids by cytoplasmic peptidases and exit the epithelial cells via different basolateral amino acid transporters. A small amount of small peptides that are resistant to cytoplasmic peptidases exit the enterocytes intact across the basolateral membrane through a basolateral peptide transporter that has yet to be cloned. Along the intestine, PEPT1 is strongly expressed on the apical membrane of small intestinal enterocyte (i.e., duodenum, jejunum, and ileum) with little or no expression in normal

colon. In addition, human and rat small intestine have been shown to express PHT1 and PHT2 transcripts, where PHT1 is expressed in the villous epithelium of small intestine.

Among three POTs expressed along the intestine (i.e., PEPT1, PHT1, and PHT2), PEPT1 is believed to be the primary POT responsible for small intestinal absorption of small peptides/mimetic and peptide-like therapeutic agents. As a consequence, PEPT1 is the most extensively studied transporter among the POT members. However, most of the previous investigations were relied on non-physiological *in vitro* models that lack an intact blood supply. Moreover, these studies did not reveal much information in respect to the relative importance of PEPT1 in relation to other peptide transporters (or other processes) in intestinal absorption. In addition, PEPT1 is also expressed in other tissues such as kidney, lung, and liver where multiple POT members are expressed with overlapping substrate specificities, thus confounding an accurate assessment of PEPT1 in these tissues.

Utilization of genetically-modified PEPT1 deficient mice offers a powerful tool to assess the relative importance of PEPT1 under the physiological condition for small peptides/mimetics absorption in the small intestine as well as disposition in other tissues. With this in mind, the goal second part of this dissertation project was to delineate the relative importance of PEPT1 in the intestinal absorption and disposition of peptide/mimetics via the utilization of wild-type and PEPT1 deficient mice.

The specific aims of second research project were:

- To define the relative importance of PEPT1 in the intestinal absorption of small peptides by defining the *in situ* intestinal transport properties of

glycylsarcosine (GlySar) in the intestine of PEPT1<sup>+/+</sup> (wild-type) and PEPT1<sup>-/-</sup> (knockout) mice.

- To delineate the relative importance of PEPT1 *in vivo* absorption and disposition of small peptide/mimetic by using glycylsarcosine (GlySar) as a model compound in PEPT1<sup>+/+</sup> (wild-type) and PEPT1<sup>-/-</sup> (knockout) mice.

The results of current dissertation would provide valuable information on understanding the relative significance of PEPT1 in *in vivo* absorption and disposition of small peptide/mimetics (relative to other POTs and/or other processes). Since PEPT1 is highly regulated by various factors (e.g., diets, hormones, growth factors, diurnal rhythm, drugs, and disease states), such understanding would have important implication in predicting intra and inter-individual variability of oral bioavailability of small peptides and peptide-like therapeutic agents.

## **Chapter 2**

### **BACKGROUND AND LITERATURE REVIEW:**

#### **PROTON-COUPLED OLIGOPEPTIDE TRANSPORTERS**

##### **Description and Relative Importance**

Proton-coupled oligopeptide transporters (POT) are membrane proteins that are responsible for translocating small peptides and peptidomimetics across the biological membrane. Thus far, four members in POT super family have been identified, which include PEPT1 (SLC15A1), PEPT2 (SLC15A2), PHT1 (SLC A4), and PHT2 (SLC A3). Unlike many other known mammalian membrane transporters, they are neither ATP nor  $\text{Na}^+$  concentration gradient driven. Rather, they are cotransported with proton energized by inwardly-directed proton concentration gradient and negative membrane potential across the biological membrane. POT transporters transport wide spectrum of di- and tri-peptides as well as a number of peptidomimetics with different conformation, size, polarity, and charges.

PEPT1 was the first peptide transporter that was identified. It was isolated and cloned from rabbit small intestine cDNA library (Fei et al., 1994). Isolation of the rabbit PEPT1 cDNA has lead to the isolation and cloning of PEPT1 from human (Liang et al., 1995), rat (Saito et al., 1995; Miyamoto et al., 1996), and mouse (Fei et al., 2000)

intestinal cDNA library. It has been found that PEPT1 is highly homologous across species. The genomic organization of human PEPT1 shows high similarity with its mouse orthologue (Urtti et al., 2001). PEPT1 protein core mass is predicted to be approximately ~75 kDa (Saito et al., 1995). PEPT2 was the next peptide transporter identified, and it was first cloned from human kidney cDNA library (Liu et al., 1995). PEPT2 was later also cloned from rabbit (Boll et al., 1996), rat (Saito et al., 1996), and mouse (Rubio-Aliaga et al., 2000) kidney cDNA library. Molecular mass of PEPT2 protein is approximately ~107 kDa (Boll et al., 1996). PEPT2 transporter is a high affinity and low capacity transporter, whereas PEPT1 is a low affinity and high capacity transporter. Recently, two additional peptide transporters, PHT1 (Yamashita et al., 1997) and PHT2 (Sakata et al., 2001), were cloned from rat brain cDNA library. Unlike PEPT1 and PEPT2, both PHT1 and PHT2 have shown to transport single amino acid L-histidine in addition to di- and tri-peptides in the same proton gradient manner. There is still lack of information on functional roles of PHT1 and PHT2 in various tissues as well as their substrate specificities and transport mechanisms. Human peptide transporter (HPT-1), a member of cadherin family, has been found in small intestine and shown to transport aminocephalosporins in  $H^+$  gradient dependent manner (Dantzig et al., 1994).

The mammalian peptide transporters have both nutritional (physiological) and pharmacological importance. It was a common belief that protein must be broken down into its free amino acid constituents in the gut lumen before the absorption could take place, and amino acid transporters are responsible for absorption of amino nitrogen in blood circulation. However, later it has been established that more than 50% of plasma amino acid pool is in peptide bound form (Seal and Parker, 1991), suggesting that di- and

tripeptides are absorbed intact in the small intestine; Mathews has demonstrated that digestion of dietary protein in the intestinal lumen results in a mixture of small peptides and free amino acids, and they are absorbed by enterocytes by two separate mechanisms, through intestinal peptide transporter and amino acid transporter, respectively (Mathews, 1975). Therefore, the primary physiological function of POTs in small intestine is to absorb small peptides arising from digestion of dietary protein. Similarly in kidney, PEPT1 and PEPT2 sequentially reabsorb amino acids in peptide-bound form to conserve amino acid nitrogen which would be lost in urine otherwise.

The pharmacological importance of peptide transporters are attributed to their roles in intestinal absorption and systemic exposure of peptidomimetics. The intestinal peptide transporter absorbs orally active  $\beta$ -lactam antibiotics, ACE inhibitor, renin inhibitors, anticancer drug bestatin, and antiviral prodrug valacyclovir, and act as vehicle for their effective intestinal absorption. Systemic exposure and therapeutic efficiency of these drugs are determined not only by their efficient intestinal absorption, but also by their half life in blood circulation. Peptide transporters in kidney reabsorb these peptidomimetics from glomerular filtrate, thus, increasing their half lives in circulation. The peptide transporters can also affect drug distribution and disposition in other organs. They are also good targets to design a prodrug to improve its systemic bioavailability and to alter its pharmacokinetic profile.

### **Molecular Structure of POTs**

Mammalian POT transporters share many structural similarities. Based on hydropathy analysis, POT transporters contain 12 putative transmembrane domains

(TMD) with both N- and C-terminals facing the cytosolic side. They commonly possess an unusually large hydrophilic loop between TMD9 and TMD10. POT proteins vary in size from 572-729 amino acids (Table 2.1). PEPT1 proteins vary from 707 to 710 in amino acids depending on the species, whereas PEPT2 consists of 729 amino acids regardless of the species. POT proteins have a number of potential N-glycosylation (2-7) sites and protein kinase recognition sites (0-3 PKA sites and 1-11 PKC sites) suggesting that POT transporters might be regulated by reversible phosphorylation. The overall molecular structures of POT proteins are summarized in Table 2.1 (Fei et al., 1994; Liang et al., 1995; Liu et al., 1995; Saito et al., 1995; Boll et al., 1996; Miyamoto et al., 1996; Saito et al., 1996; Yamashita et al., 1997; Fei et al., 2000; Rubio-Aliaga et al., 2000; Sakata et al., 2001; Bhardwaj et al., 2006).

PEPT1 and PEPT2 share high homology in amino acid sequence between species (80-90% amino acid identity between human, rat, mouse, and rabbit). However, homology between different peptide transporters in a given species is relatively low. Human PEPT1 and PEPT2 share about 50% amino acid identity, whereas that of rat PHT1 and rat PHT2 is about 50% too. However, peptide/histidine transporters show even less amino acid homology to PEPT transporters, less than 20%. Most of the conserved sequences occur within the putative transmembrane domains, whereas the sequence differences among the species and different transporters occur mostly in loops connecting the putative transmembrane domain, especially in large extracellular loops between TMD9 and TMD10.

HPT-1, isolated from Caco-2 cell line, has been demonstrated to transport aminocephalosporins in H<sup>+</sup> gradient dependent manner. HPT-1 contains a single putative



transmembrane domain (Dantzig et al., 1994). It shows very minimum homology to any known prokaryotic or eukaryotic peptide transporters, about 16% identity and 41% similarity to hPEPT1. However, it has high homology with the cadherin family of cell adhesion protein (Dantzig et al., 1994). On the other hand, some data suggest that HPT-1 is not an actual H<sup>+</sup> coupled oligopeptide transporter but rather a modulator of endogenous oligopeptide transporter in Caco-2 cells (Hediger et al., 1995).

### **Tissue and Cellular Distribution of POTs**

PEPT1 is believed to be the primary peptide transporter in the small intestine that is responsible for absorption of small peptides from the digestion of dietary proteins. PEPT1 mRNA has been detected in the small intestine of a number of mammalian species such as rabbit (Fei et al., 1994), human (Liang et al., 1995), rat (Miyamoto et al., 1996; Shen et al., 1999; Lu and Klaassen, 2006), and mouse (Lu and Klaassen, 2006). PEPT1 protein was also detected in small intestine (Saito et al., 1995; Ogihara et al., 1996; Shen et al., 1999). More specifically, PEPT1 in small intestine is confined to duodenum, jejunum and lesser extent to ileum segments. In small intestine, PEPT1 is localized at the brush border membrane of the differentiated absorptive epithelial cells in villi tips, and not in mucus-secreting goblets cells or less differentiated epithelial cells in the crypts (Ogihara et al., 1996; Walker et al., 1998; Groneberg et al., 2001a). Lower level of expression of PEPT1 mRNA was localized at brush border membrane of kidney proximal tubule cells of rabbit (Fei et al., 1994), human (Liang et al., 1995), rat (Miyamoto et al., 1996; Shen et al., 1999; Lu and Klaassen, 2006), and mouse (Lu and Klaassen, 2006). Mouse renal PEPT1 mRNA was very low compared to that of rats. In contrast, PEPT1 mRNA was detectable in mouse large intestine, but not in rat (Lu and

Klaassen, 2006). Renal PEPT1 protein was detected by western blot in rat (Saito et al., 1995; Shen et al., 1999) and mouse (Shen et al., 2003). In kidney, PEPT1 is confined to brush border of S1 segment of renal proximal tubule (kidney cortex) (Shen et al., 1999). Lower level of PEPT1 mRNA has also been detected in other tissues such as liver, pancreas, lung, bile duct, ovary, placenta, testis, prostate, and even some expression in large intestine and stomach tissue (Fei et al., 1994; Liang et al., 1995; Herrera-Ruiz et al., 2001; Knutter et al., 2002; Lu and Klaassen, 2006). Via utilization of immunofluorescence microscopy and transport studies, PEPT1 was demonstrated to be expressed in membrane of lysosomal compartment of liver cells (Thamotharan et al., 1997), renal cells (Zhou et al., 2000) and pancreatic cells (Bockman et al., 1997), rather than being exclusively confined to plasma membrane.

PEPT2 is primarily localized in the kidney and brain. More specifically, PEPT2 is found in brush border membrane of S2 and S3 segments of renal proximal tubule, the outer stripe of outer medulla (Smith et al., 1998; Shen et al., 1999). PEPT2 mRNA (Liu et al., 1995; Shen et al., 1999) and protein (Shen et al., 1999; Rubio-Aliaga et al., 2000) expression have been detected in the kidney. In brain, PEPT2 mRNA was found to be localized in astrocytes, subependymal cells, ependymal cells, and the epithelial cells of choroid plexus (Berger and Hediger, 1999). Recently PEPT2 protein expression in choroid plexus was confirmed by western blot (Shu et al., 2002). Moreover, PEPT2 is also expressed in lung, muscle, liver, heart, mammary gland, eyes, pituitary gland, spleen, blood vessels, testis, prostate, ovary, and uterus (Boll et al., 1996; Doring et al., 1998a; Lu and Klaassen, 2006). In lung, the expression of PEPT2 mRNA and protein were localized to alveolar type II pneumocytes, bronchial epithelium, and endothelium of

small arteries (Groneberg et al., 2001b). In mammary gland, the PEPT2 is expressed in mammary gland epithelia (Groneberg et al., 2002). In eyes, PEPT2 mRNA is localized in retina (Berger and Hediger, 1999).

Expression of PHT1 mRNA was found in brain, eyes, lung, spleen, liver, heart, kidney, skeletal muscle, thymus, and throughout the GI tract (Yamashita et al., 1997; Botka et al., 2000; Herrera-Ruiz et al., 2001). Specifically, PHT1 was localized in retina of eyes (Ocheltree et al., 2003). In GI tract, hPHT1 protein was detected in stomach, duodenum, jejunum, ileum, and colon by western blot. Immunohistochemical analysis have illustrated that PHT1 is localized at the villous epithelium in the small intestine (Bhardwaj et al., 2006).

PHT2 mRNA is mostly found in lymphatic system, lung, spleen, thymus, and faintly in brain, liver, adrenal gland, heart, and the GI tract (Herrera-Ruiz et al., 2001; Sakata et al., 2001). Unlike other POT members, PHT2 is found in lysosome rather than plasma membrane which was demonstrated by light and electron-microscopic analysis (Sakata et al., 2001). Compared to PEPT1 and PEPT2, relatively little information is available for PHT1 and PHT2 in respect to their physiological roles, substrate specificities, and mechanisms of transport.

Expression of HPT1 is observed in human colon, skeletal muscle, and faintly in the small intestine by RT-PCR and southern-blot analysis (Herrera-Ruiz et al., 2001). A summary of tissue and cellular distributions of POTs is presented in Table 2.2.

### **Protein Structure Activity Relationship**

In order to use POT members as a drug delivery target, it is essential to understand the protein structure and substrate recognition mechanisms of these transporters. Since direct structural approaches, such as crystallization, characterization by NMR or other spectroscopic methods, are limited to transmembrane protein, other methods including site-directed mutagenesis, construction of various chimeras, and computer modeling have been employed to elucidate the protein structure of peptide transporters.

A number of single point mutations have been employed in PEPT1 and PEPT2, which have led to the identification of several essential residues. Since several of H<sup>+</sup> cotransporters are known to contain conserved specific histidyl residues, which are essential for catalytic activity of the transporters, Fei et al have investigated the histidyl residues in hPEPT1 and hPEPT2 using site-directed mutagenesis (Fei et al., 1997). A partial alignment of amino acid sequences of rat, rabbit and human PEPT1 and PEPT2, revealed that His-57, His-121, and His-260 in PEPT1, His-87, His-142, and His-278 in PEPT2 are conserved in all three species. They have found that His-57 in hPEPT1 and His-87 in hPEPT2 are absolutely essential amino acids in transport function of these transporters. Both of these histidyl residues are located near the extracellular surface of the second putative transmembrane domain (Fei et al., 1997). His-57 as the key residue serving as the predominant proton binding sites in hPEPT1 was further confirmed by Uchiyama et al (Uchiyama et al., 2003). Using the same method, Terada and coworkers have shown that His-57 (TMD2) and His-121 (TMD4) in rat PEPT1 are involved in substrate recognition (Terada et al., 1996). Additional studies have also suggested that His-57 and His-121 are intimately involved in the binding of H<sup>+</sup> ion and substrate

recognition in rabbit PEPT1 (Chen et al., 2000). It was also demonstrate that His-57 and its surrounding aromatic residues, such as Tyr-56 and Tyr-64, are essential for normal function of PEPT1 (Chen et al., 2000). This finding is consistent with the concept that aromatic residues stabilize the charges within membrane electric field (Chen et al., 2000). Meredith and coworkers also have reported that Arginine-282 in TMD7 plays a key role in the rabbit PEPT1 proton coupling pathway (Meredith, 2004) and it forms a charge pair with D-341 in TMD8 (Kulkarni et al., 2007; Pieri et al., 2008). Mutation at Trp-294 and Gly-595 significantly reduce substrate uptake, suggesting the involvement of these residues in transport process (Bolger et al., 1998). A combination of transport assays, luminometry and site-directed mutagenesis have suggested that PEPT1 is a multimer, probably a tetramer (Panitsas et al., 2006).

Construction of various chimeras consisting of variable segments of PEPT1 and PEPT2 has helped to identify protein domains that are relevant to substrate binding and transport processes. With this approach, it has been revealed that phenotypical characteristic of PEPT2, such as substrate affinity, substrate specificity, electrophysiological parameters, and pH-dependency, are determined by its first half of the transport protein up to TMD9 or its amino terminal region, not by the large extracellular loop between TMD9 and TMD10 (Doring et al., 1996; Doring et al., 2002). Similar finding was also demonstrate by Terada and coworkers that N-terminal half of the rat PEPT1 and PEPT2 contain both H<sup>+</sup> binding site and substrate recognition site (Terada et al., 2000a). Construction of chimeric PEPT1-PEPT2 protein has also lead to identify the putative substrate binding domains of PEPT1 and PEPT2, which reside in a region comprised of TMD 7, 8 and 9 with their in between loops (Fei et al., 1998).

Bolger and coworkers have demonstrated that computer simulation can be employed to study the structure-function relationship of transmembrane protein (Bolger et al., 1998). Prediction by computer modeling and subsequent site-directed mutagenesis methods have identified that Tyr-167 in TMD5, which is conserved in the peptide transporters from bacteria, fungi, yeast, plant, rabbit and human, plays an essential role in hPEPT1 function, not the steady-state protein level or trafficking of the transporter to the plasma membrane (Yeung et al., 1998).

With substituted cysteine accessibility method (SCAM), it was feasible to evaluate the relative orientation, functional importance, and solvent accessibility of a specific alpha-helical transmembrane segment of hPEPT1. It has been demonstrated that both TMD5 and TMD7 form part of substrate translocation pathway (Kulkarni et al., 2003a; Kulkarni et al., 2003b). For TMD5, the extracellular half of the transmembrane seems to form a classical amphipathic alpha helix and the cytoplasmic half of the transmembrane seems to be highly solvent accessible. Tyr-167, Asn-171, and Ser-174 in TMD5 might play a role in substrate binding, since cysteine mutation of these residues were not tolerated (Kulkarni et al., 2003a). TMD7 seems to be relatively solvent accessible along most of its length, and its cytoplasmic half is more so. It was suggested that the extracellular end of TMD7 may shift following substrate binding, providing the basis for channel opening and substrate translocation. Phe-293, Leu-296, and Phe-297 in TMD7 did not tolerate cysteine mutation, indicating that they might play a structural role in transporter function (Kulkarni et al., 2003b). Moreover, TMD3 also appears to interact with other transmembrane domains (Links et al., 2007).

While it was suggested that N-terminal half of the PEPT1 and PEPT2 contain both the H<sup>+</sup> binding and substrate recognition sites (Terada et al., 2000a), cytosolic C-terminal of the PEPT2 is demonstrated to be involved in apical membrane localization of the protein (Klapper et al., 2006). Recently, it was revealed that Arg-282 in TMD7 and Asp-341 in TMD8 in hPEPT1 form salt bridge, and was proposed that this R282-D341 charge pair might play a role in hPEPT1 translocation mechanism (Kulkarni et al., 2006).

Until crystal structure of PEPT1 becomes available, 3D-structure of PEPT1 will be constantly refined by computer/homology modeling with the support of *in vitro* functional experiments.

### **Substrate Structure Activity Relationship**

PEPT1 and PEPT2 substrate specificities have been intensively studied, but more focus on PEPT1 due to its importance in intestinal absorption of peptides/mimetics. Peptide transporters transport di- and tri-peptides, but not single amino acid or tetrapeptide. They also transport peptidomimetic compounds, such as  $\beta$ -lactam antibiotics (Tamai et al., 1997; Bretschneider et al., 1999), ACE inhibitors (Moore et al., 2000), renin inhibitors (Kramer et al., 1990; Hashimoto et al., 1994), anticancer drug bestatin (Saito and Inui, 1993), antiviral prodrug valacyclovir (Balimane et al., 1998; Ganapathy et al., 1998), and  $\omega$ -amino fatty acids (Doring et al., 1998b). Broad substrate specificity, expression in the intestine and kidney, ability to enhance the permeability of poorly absorbed drugs, and ability to prolong the half-life of drugs make peptide transporters very attractive target for oral drug delivery. In order to design drugs that are targeted at peptide transporters, it is essential to understand their substrate structural requirements.

Conformation, size, charge, hydrophobicity, and side chain flexibility might affect substrate affinity for the peptide transporters. Since three dimensional structures of peptide transporters are still not available, structure-affinity/transport relationship of compounds are usually carried out by inhibition and uptake assays. Inhibition assays usually provide information on recognition and binding strength of ligand, but not the actual translocation of substrate. Uptake studies and two electrode voltage clamp techniques allows the measurement of the actual translocation of a substrate across the biological membrane.

PEPT2 is similar, but not identical to PEPT1 in terms of spectrum of substrates and structure requirement for substrate recognition. Furthermore, most di- and tripeptides as well as peptidomimetic, such as valacyclovir and  $\delta$ -aminolevulinic acid, show higher affinity to PEPT2 compared to PEPT1 regardless of their charges, sizes, and chemical structures (Terada et al., 2000b). PEPT2 is assumed to have 10-15 times higher affinity to its substrates than PEPT1.

Size: Both PEPT1 and PEPT2 transport di- and tripeptides, but not single amino acids or tetra-peptides. Size or molecular weight of peptides does not seem to be a limiting factor. However cyclic dipeptides are not recognized by either PEPT1 or PEPT2 (Terada et al., 2000b). It was postulated that PEPT1 transport all possible 400 dipeptides and 8000 tripeptides. However, Vig and coworker recently have shown that not all dipeptides are substrate for PEPT1 transporter (Vig et al., 2006).

Stereo-selectivity: Studies have demonstrated that both PEPT1 and PEPT2 transporters selectively bind and transport the *trans* conformation of peptide derivatives



(Brandsch et al., 1998; Biegel et al., 2006). PEPT1 also shows much higher affinity to di- and tri-peptides of L-isomers of amino acids than the D-isomers of amino acids (Li et al., 1998). L-Val-L-Val showed highest affinity to PEPT1 followed by D-Val-L-Val, L-Val-D-Val, and D-Val-D-Val in Caco-2 assay. Val-Val-Val with 2 or 3 D-isomers of Val did not show any affinity to PEPT1 (Li et al., 1998).

Charge: Charged dipeptides appear to have a lower affinity compared to structurally similar zwitterionic dipeptides (Brandsch et al., 1999). Vig and coworker have studied the effect of charge on PEPT1 function. They found that dipeptides with one charged side chain have lower PEPT1 activation compared to dipeptides with neutral side chains, and it is further decreased if the both side chain are charged. Dipeptides with acidic side chains at both positions were poor substrate for PEPT1. Furthermore, dipeptides with basic side chains at both positions were not transported by PEPT1. Arg-Arg, Arg-Lys, Lys-Arg, Lys-Lys are not substrates for PEPT1 transporter. Effect of charged amino acid in PEPT1 activation can be summarized as neutral-neutral > charged-neutral ~ neutral-charged > acidic-acidic > basic-basic (Vig et al., 2006). This is the first finding that not all di- and tri-peptides are substrates for PEPT1, and dipeptides with both positively charged amino acids are not transported by PEPT1 transporter.

Peptide Bond: Peptide bond is not an essential structural requirement for the recognition of a substrate either by PEPT1 or PEPT2 (Brandsch et al., 1998; Doring et al., 1998a; Doring et al., 1998b; Ganapathy et al., 1998). Modification of dipeptides, by replacing the peptide bond by ketomethylene (Doring et al., 1998a) or thioxo and replacement of peptide carbonyl oxygen with sulfur (Brandsch et al., 1998), still retained their affinity for PEPT1.  $\omega$ - amino fatty acids with more than four backbone units are

translocated by PEPT1 without significant loss in affinity, further supporting that peptide bond is not essential for recognition by PEPT1 transporter (Doring et al., 1998b). Carbonyl group in small peptide/mimetic is an essential requirement for transport by PEPT1 (Schoenmakers et al., 1999). Peptidomimetic analog without carbonyl group, though do not get transported by PEPT1, still have affinity for PEPT1 shown by inhibition studies (Schoenmakers et al., 1999).

Terminal Group: N-terminal amine and C-terminal carboxyl groups are not absolutely required. Peptidomimetics without  $\alpha$ -amino groups such as captopril, enalapril, and ceftubuten are transported by PEPT1. However, modification of  $\alpha$ -amino group seems to reduce the affinity for both PEPT1 and PEPT2 (Terada et al., 2000b). Methylation or acetylation on carboxyl group of dipeptides strongly reduced dipeptides' affinity for PEPT1, suggesting that negatively charged carboxyl group may be essential for active transport of PEPT1 (Swaan and Tukker, 1997). However, some studies also have shown that modification of C-terminal of Phe-Tyr to amide still retains its affinity to PEPT1 (Meredith et al., 2000). Together, these studies suggest that C-terminal carboxyl group is not absolutely essential for transport; however, modification of it might reduce its affinity to PEPT1.  $\beta$ -lactam antibiotic without an  $\alpha$ -amino group has lower affinity to PEPT1 than  $\beta$ -lactam with an  $\alpha$ -amino group.

Side chain: Hydrophobicity of the side chain seems to be a major determinant in affinity of a substrate. Amino acids with more hydrophobic side chains are preferred over hydrophilic side chains by both PEPT1 and PEPT2 (Brandsch et al., 1999; Tateoka et al., 2001; Knutter et al., 2004; Biegel et al., 2006).

A summary of structural requirement for PEPT1 is illustrated in Figure 2.1. Until three-dimensional structures of the peptide transporters are available, the current model will be refined by trial and error. Nonetheless, the current structure-affinity relationship model might help the rational design of drug and prodrug targeted at peptide transporters.

### **Mechanism of POT-Mediated Transport**

Both PEPT1 and PEPT2 use  $H^+$  concentration gradient and negative inside membrane potential as the driving force for translocating the peptides/mimetics across the biological membrane. Sequential actions of  $Na^+/K^+$  ATPase pump and the  $Na^+/H^+$  exchanger in the small intestine and kidney create an acidic extracellular microclimate.  $Na^+/K^+$  ATPase, located in the basolateral membrane, maintains an inside negative membrane potential and  $Na^+$  concentration gradient across plasma membrane. This generated  $Na^+$  concentration gradient in turn drives the  $Na^+/H^+$  exchanger located in the brush-border membrane to generate and maintains an  $H^+$  concentration gradient across cell membrane. The created inward  $H^+$  electrochemical gradient drives the tertiary active transport of oligopeptides across the plasma membrane (Figure 2.2). The  $H^+$  gradient stimulate the activity of PEPT1 and PEPT2 by increasing their transport rate without affecting their substrate affinity (Brandsch et al., 1997).

Even though PEPT1 and PEPT2 have similar substrate specificities, they have different substrate affinities and mechanisms of transport. Transports by both PEPT1 and PEPT2 are always electrogenic irrespective of the substrate's net charge, and thus proton to substrate ratio differs based on the net charge of substrate. For PEPT1, total charge (substrate plus proton) of +1 is required for transport of each peptide/mimetic. Therefore,

for neutral and cationic dipeptides, the proton to substrate stoichiometric ratio is 1:1. Anionic dipeptides are transported both in their neutral forms at proton to substrate ratio of 1:1 and in their charged forms at ratio of 2:1 where one extra proton is required to quench the negative charge of the anionic dipeptides (Steel et al., 1997; Kottra et al., 2002). Cationic dipeptides are transported preferentially in their deprotonated neutral forms, also in their charged forms in lesser extent. In contrast, PEPT2 stoichiometry is +2 charge for each peptide being transported (Chen et al., 1999). For neutral substrates, the proton to substrate ratio is 2:1. In cases of anionic substrates, one extra proton is required to quench the negative charge resulting in proton to substrate ratio of 3:1 and charge to substrate ratio of 2:1. For cationic substrate, the charge to substrate ratio is 2.4 where they get transported either in its deprotonated (neutral) or its positively charged form (Chen et al., 1999). In all cases, charged molecules present different binding affinity based on extracellular pH. Affinity of anionic substrates increases substantially by decreasing the pH, whereas cationic dipeptides exhibit higher affinity in neutral or slightly alkaline extracellular pH. However, proton binding to the transporter becomes limiting factor for efficient transport at more alkaline pH (Amasheh et al., 1997). In general, the zwitterionic substrates that do not carry a net charge have preferential binding and transport by peptide transporters over charged substrates.

Electrophysiological analysis of pre-steady state current have demonstrated that  $H^+$  and substrates bind to PEPT1 in orderly fashion;  $H^+$  binds to PEPT1 first followed by a change in substrate binding affinity, substrate binding, and then the simultaneous transport of the substrate and  $H^+$  together (Mackenzie et al., 1996). In similar fashion, one  $H^+$  binds to the PEPT2 prior to the substrate binding (Chen et al., 1999). Giant

patch-clamp experiments demonstrated that PEPT1 can transport dipeptides bidirectionally in an electrogenic and proton-coupled symport mode. Under the normal physiological conditions, such as negative inside membrane potential, the external binding site shows higher substrate affinity than the internal binding site, allowing the substrate to be released into the cytosol. However, under certain conditions such as low membrane voltage or absence of pH gradient, PEPT1 may even act as an electrogenic dipeptides-proton efflux symport (Kottra and Daniel, 2001).

## **INTESTINAL PEPTIDE ABSORPTION**

### **Structure of Small Intestine**

Most digestion and absorption of food take place in the small intestine, which consists of duodenum, jejunum, and ileum. Structure of the small intestine is specially adopted for its absorptive function. Its length provides a large surface area for absorption, and which is further increased by its wall structure of villi and microvilli.

Mucus of the intestine forms a series of villi. The large number of villi significantly increases the surface area of the epithelium available for absorption and digestion. The epithelium of the mucosa consists of simple columnar epithelium that contains absorptive cells known as enterocytes, goblet cells (secretes mucus), hormone producing cells, and Paneth cells. The apical membrane of the absorptive cells has microvilli, which further increases the surface area of epithelium. In addition to villi and microvilli, the third feature of the intestine that further increases its surface area is the

circular folds. These folds enhance the absorption by causing chyme to spiral, rather than to move in a straight line as it passes through the small intestine. Since the folds and villi decrease in size in the ileum, most absorption takes place in the duodenum and jejunum. The villi, microvilli and folds all together increase the absorptive surface area of the small intestine by 600 times.

The mucosal wall of the small intestine is arranged into two distinct structures, villi and crypts. Villi project into the lumen covered mostly with mature absorptive enterocytes along with some mucus-secreting goblet cells. Cells in villi only live for a few days, and are shed into the lumen to be digested and absorbed. Therefore, the major function of villi is nutrition absorption. Crypts are moat-like structures of the epithelium around the villi, and are lined mainly with younger epithelial cells, which are involved primarily in secretion. Toward the base of the crypts, there are undifferentiated stem cells, which continuously divide and provide the source of all the epithelial cells in the crypts and on the villi. Crypts also contain mucous-secreting goblet cells, different endocrine epithelial cells, and Paneth cells with large secretory granules. The known functions of crypts include epithelial cell renewal and secretion of ions, water, exocrine, and endocrine. A complete turnover of intestinal epithelium is approximately every 3-7 days (Erickson, 1995).

Molecules passing from the bulk phase of the intestine to epithelial cell apex encounter two distinct regions, the unstirred aqueous layer and the acidic microclimate. The unstirred aqueous layer is known to be a significant barrier to the highly lipophilic molecules. However, water soluble molecules are not significantly impeded by this layer. The thickness of the effective unstirred layer was estimated to be about 530  $\mu\text{m}$  in

rat jejunum (Winne, 1976) and 630  $\mu\text{m}$  in human jejunum (Read et al., 1977). Microclimate of the small intestine, the close vicinity of the external surface of brush border membrane, is significantly more acidic than in the bulk phase of luminal fluid, especially in proximal part of the small intestine. This acidic microclimate is created by sequential action of the basolateral  $\text{Na}^+/\text{K}^+$  ATPase and apical  $\text{Na}^+/\text{H}^+$  exchanger of small intestinal epithelial cell. Hydrogen ions that are pumped into apical space by  $\text{Na}^+/\text{H}^+$  exchangers are trapped by the negatively charged mucopolysaccharide side chain. Thus, mucus impedes the free diffusion of hydrogen ion into the bulk phase and maintains the low pH environment in surface area of the epithelial cells, while the acidity is generated by  $\text{Na}^+/\text{H}^+$  exchanger on the apical side of epithelium (Shiau et al., 1985; Shimada, 1987).

Bulk phase pH in rat and human jejunum fluid is reported to be about 6.5 and 7.1 respectively (Weinstein et al., 1938; Steffansen et al., 1999). In human and animals, the microclimate pH was reported to be 5.5-6.0 (Lucas et al., 1975; Said et al., 1986). Since the intracellular pH in enterocytes is approximately 7.0-7.2 (Kurtin and Charney, 1984), there is a significant  $\text{H}^+$  electrochemical gradient across the plasma membrane to drive the uphill transport of small peptides via PEPT1 into enterocytes. Within the microclimate or surface of epithelium, the upper part of villus is slightly more acidic than the base or crypts in duodenum and jejunum, and no gradient was observed in ileum (Daniel et al., 1989). This pH difference could be attributed to  $\text{H}^+$  secretion from mature enterocytes located on the villus (Daniel et al., 1989).

Microclimate pH can be altered by glucose and sodium content, but not significantly by pH of the bulk phase (Lucas et al., 1980; Hogerle and Winne, 1983;

Shimada, 1987). The microclimate pH is in isohydric with the bulk phase pH when the later is below 5.0. The microclimate is more acidic than the bulk phase if the later is greater than 5.0. When the pH of the bulk phase changes from 5.5 to 8.5, there is only a very minor change in the surface microclimate pH, roughly from 5.5 to 6.2. As the glucose concentration in the bulk phase drops from 10 mM to 2 mM, the surface pH increases significantly. It also increases when the concentration of sodium ion decreases in the bulk phase, and this change is more pronounce in the jejunum than the distal ileum (Lucas et al., 1980; Shimada, 1987).

### **Protein Digestion**

Protein is an important part of our daily diet. A typical western diet usually contains 70-100 g protein per day. In addition to the dietary protein, saliva and gastrointestinal tract also secrete a significant amount of protein (~35 g/day) (Ganapathy et al., 2006). Of this total protein, about 95-98% is completely digested and absorbed in a normal individual (Erickson, 1995). In gastrointestinal lumen, the proteins are converted into large peptides by gastric and pancreatic proteases, which subsequently undergo further hydrolysis by various peptidases on brush border membrane of intestinal epithelium into small peptides (80%) and free amino acids (20%) (Ganapathy et al., 2006). The final end products of protein digestion are absorbed into the enterocytes predominately in the form of di- and tripeptides as supposed to free amino acids (Matthews, 1975). Once inside the enterocytes, the majority of the di- and tripeptides undergo further hydrolysis into their constituent amino acids by cytoplasmic peptidases and exit the epithelial cells via different basolateral amino acid transporters. A small amount of small peptides that are resistant to cytoplasmic peptidases exit the enterocytes



intact across the basolateral membrane through a basolateral peptide transporter that still yet to be cloned (Terada et al., 1999) (Figure 2.3). Furthermore, there are regional differences in small intestinal epithelium in respect to their absorptive capacities for free amino acids and small peptides. While the proximal small intestine has a greater absorption capacity for small peptides compared to the distal small intestine, in contrast, the distal intestine has a greater absorptive capacity for amino acids compared to the proximal small intestine (Matthews et al., 1971). In addition, the activities of brush border membrane peptidase are much higher in the ileal than in the jejunum (Silk et al., 1976), implying an increase in rate of appearance for single amino acids as the luminal content move along the intestine while concentration of small peptides decreases. It was suggested that transporting 2 or 3 amino acids by PEPT1 in a form a small peptide requires the same amount of energy required to transport a single free amino acids (Daniel, 2004). In addition, it was demonstrated that it was faster to transport amino acids in small peptide form in terms of uptake per unit time compared to transporting their constituent amino acids in the free forms (Gilbert et al., 2008).

### **Peptide Transporters in Intestine**

For a long time, it was commonly believed that only amino acids are absorbed by the intestinal epithelial cells. But, it was later found that the end products of protein meal are not exclusively free amino acids, rather a mixture of free amino acids and small peptides (Matthews, 1975). The intestinal epithelium has separate mechanisms for their absorption from the intestinal lumen. There are regional differences in the absorptive capacities for free amino acids and small peptides. The absorption capacity for small peptides is greater in the proximal small intestine than the distal small intestine, whereas

the absorptive capacity for amino acid is greater in the distal small intestine than in the proximal small intestine.

Di- and tri-peptides are carried into the mucosal cells via H<sup>+</sup> dependent peptide transporters. Once inside the epithelium cells, they have two possible fates. Some peptides get digested into their constituent amino acids by cytoplasmic peptidase, followed by transportation across the basolateral membrane into the blood circulation. Undigested di- and tri-peptides are transported intact across the basolateral membrane. Some larger peptides are absorbed by transcytosis after binding to a receptor on the luminal surface of the epithelium.

The primary known peptide transporter in the small intestine is PEPT1. However, recently, some other peptide transporters are also reported to be expressed along the intestine; transcripts of PHT1, PHT2, and HPT1 were found in the intestine (small intestine and colon) (Herrera-Ruiz et al., 2001). PHT1 protein was localized at villous epithelium (Bhardwaj et al., 2006). Nonetheless, these findings do not rule out the possible existence of other peptide transporters in the small intestine.

### **Basolateral Peptide Transporters in Intestine**

When peptides are taken up by the intestinal enterocytes via PEPT1, they diffuse through the cytoplasm and exit into the portal blood across the basolateral membrane as intact dipeptides or as metabolized amino acids constituents. Until 1990, it was commonly believed that only free amino acids entered portal blood from intestinal epithelial cells (Matthews, 1975). However, some recent studies have established that ~50% of the amino acids circulating in the plasma are peptide bond, and majority of

which are in di- and tri-peptides forms (Seal and Parker, 1991). Furthermore, Gardner et al have also reported that about 10% of the amino nitrogen entering the mesenteric blood during absorption of a casein digest *in vivo* was in the form of small peptides (Gardner et al., 1983). These findings suggest the existence of basolateral peptide transporters for exit mechanism of dipeptides from enterocytes.

Studies have indicated that the apical and basolateral sides of human intestinal cell line, Caco-2, have distinct peptide transporters which are active and facilitative transporter systems, respectively (Terada et al., 1999). This basolateral peptide transporter in Caco-2 cells, like PEPT1, has been associated with the translocation of peptide like drugs, such as bestatin (Saito and Inui, 1993), cephalosporins (Inui et al., 1992; Matsumoto et al., 1994) as well as nonpeptidic drugs like  $\delta$ -aminolevulinic acid ( $\delta$ -ALA) and valacyclovir (Irie et al., 2001) in addition to transporting small peptides (Terada et al., 1999). The basolateral peptide transporter was also demonstrated to be pH-independent, incapable of uphill transport (Saito and Inui, 1993) and relatively low affinity compared to the apical dipeptides transporter, PEPT1. However, there have been few contradicting reports suggesting that basolateral peptide transporter is  $H^+$  dependent (Dyer et al., 1990; Thwaites et al., 1993). The kinetic analyses also verified that a single facilitative peptide transporter was involved in the basolateral transport of small peptides/mimetics in Caco-2 cells. Directional studies, influx from basolateral to cytosol and efflux in opposite direction, have also revealed that this basolateral peptide transporter is symmetric in terms of substrate specificity, pH independence for peptide transport, and asymmetric in substrate affinity (Irie et al., 2004). Shepherd et al has suggested a novel 112 kDa protein with no obvious similarity to PEPT1 as a candidate

for basolateral peptide transporters in rat jejunum (Shepherd et al., 2002). Taken together, PEPT1 absorbs substrates from the intestinal luminal to the enterocytes on the apical side, and this basolateral peptide transporter mediates the extrusion of those substrates from the cytosol to the blood stream. Together, PEPT1 and basolateral peptide transporter facilitate the efficient intestinal absorption of small peptides and peptide like drugs.

## **PEPT1 TRANSPORTER**

### **Polymorphism and Splice Variants of PEPT1**

Genetic variations in drug receptors, metabolizing enzymes, and transporters are some of the sources for inter-individual variability in the drug effect and disposition. Since PEPT1 is involved in the carrier mediated uptake of various peptide-like drugs such as  $\beta$ -lactam antibiotics, ACE inhibitors, and antiviral nucleosides L-valacyclovir, polymorphism in PEPT1 could result in variation in therapeutic efficacy of those drugs among different patients. Studies have shown that valacyclovir, a known PEPT1 substrate, have larger inter-individual variability than intra-individual variability in intestinal absorption, suggesting the presence of a genetic variations in PEPT1 (Phan et al., 2003).

Some studies suggest that two human PEPT1 gene polymorphism variants might be involved in susceptibility to bipolar disease (Maheshwari et al., 2002). However,

further investigation is needed to confirm whether or not PEPT1 is causative for this disease.

Recently, by screening a DNA polymorphism discovery panel of 44 ethnically diverse individuals, nine nonsynonymous coding-region single-nucleotide polymorphisms (cSNPs) in human PEPT1 have been identified (Zhang et al., 2004). Among those variants, only one variant, P586L, had a reduced protein expression (western blot), lower plasma membrane expression (immunocytochemical analysis) and reduced transport capacity while maintained a similar affinity to GlySar and other drug substrate as the other variants. This finding suggests that P586 may have a role in translation, degradation and/or membrane insertion of PEPT1 in the plasma membrane (Zhang et al., 2004). This is consistent with other studies, where it was suggested that the C-terminal of the peptide transporters might be involved in membrane localization (Klapper et al., 2006).

A similar study has been performed in Dr. Sadee's lab, where all 23 exons and adjoining intronic regions of PEPT1 were screened in collection of 247 ethnically diverse subjects (Anderle et al., 2006). Of 39 identified variants, 18 are located at exons, and of which only nine are nonsynonymous. Among 9 nonsynonymous SNPs, only one low frequency F28Y variant has an altered affinity to dipeptides without significant change in protein expression level from wild-type. Even though P586L and F28Y have a significant effect on the function of PEPT1, they both are low frequency variants, thus, would have a minimal impact on oral absorption of PEPT1 drug substrates. The two common SNPs in hPEPT1 S117N and G419A were found to maintain the same kinetic properties as the wild-type suggesting that the both variants are not likely to have major

effect on oral drug absorption (Sala-Rabanal et al., 2006). Taken together, PEPT1 seems to have low genetic variability. Its polymorphisms are not expected to be a major factor in inter-individual variability in oral absorption of PEPT1 substrates.

Alternating splicing in hPEPT1 RNA expression leads to the formation of a splice variant hPEPT-RF, which modulates the transport activity of hPEPT1 by serving as a pH-sensing regulatory factor (Saito et al., 1997; Urtti et al., 2001). While hPEPT1 has 23 exons, its splice variant hPEPT1-RF has six. It shares three exons completely and two exons partially with hPEPT1. When expressed alone, the splice variant hPEPT1-RF lacks the peptide transport activity.

### **Regulation of PEPT1**

Changes in functional characteristic and / or expression level of PEPT1 transporter in the small intestine could be possible sources for intra- and inter-individual variability of oral bioavailability of drugs. Such correlation between variation in PEPT1 expression level (both mRNA and protein level) and absorption permeability of peptide-like drugs in small intestine of rat has been established (Chu et al., 2001; Naruhashi et al., 2002). Studies have shown that the expression of PEPT1 transporter is regulated by diets, hormones, growth factors, diurnal rhythm, drugs, and disease states. The mechanisms responsible for these changes in expression level could be attributed to the alteration in PEPT1 gene transcription, intracellular trafficking of PEPT1 protein, or some other unidentified mechanisms.

PEPT1 has number of potential N-glycosylation sites and protein kinase recognition sites, indicating that the transporter can be regulated by reversible

phosphorylation. Studies on Caco-2 has revealed that activation of protein kinase C (PKC) decreases the maximal transport rate ( $V_{\max}$ ) of the PEPT1 without significant change in affinity ( $K_m$ ) (Brandsch et al., 1994).

One potential regulator of expression of any transporter is its own substrates. Studies have demonstrated that treatment of Caco-2 with dipeptides have increased both cellular PEPT1 mRNA and the membrane protein expression without significant change in  $K_m$  value. The mechanism responsible for this change appears to be the regulation of expression gene encoding the PEPT1 (Thamotharan et al., 1998; Walker et al., 1998). These *in vitro* results were confirmed with *in vivo* studies by feeding the rats with varying amount of protein (Erickson et al., 1995; Shiraga et al., 1999). The results showed that high protein meal induces an increase in PEPT1 mRNA which will lead to an increase in the population of PEPT1 transporter (Erickson et al., 1995; Shiraga et al., 1999).

Among different hormones, insulin, epidermal growth factor (EGF), leptin, and thyroid hormones have shown to affect the expression of PEPT1 transporter. When insulin was added to Caco-2 medium at physiological concentration, the uptake of dipeptides in Caco-2 was stimulated; The mechanism that accounts for this increased dipeptides uptake appears to be the increased population of membrane PEPT1 induced by the increased translocation of PEPT1 from preformed cytoplasmic pool (Thamotharan et al., 1999b; Nielsen et al., 2003; Watanabe et al., 2004). EGF had an opposite effect on PEPT1 functional expression based on its duration of exposure. In long-term (> 5 days) treatment of basolateral membrane of Caco-2 with EGF, there was a decrease in PEPT1 protein expression as a result of a decreased PEPT1 mRNA, which leads to a decrease in

dipeptides uptake (Nielsen et al., 2001). However, when the basolateral membrane of Caco-2 was treated with EGF for only short period (< 1h) of time, there was a dose dependent increase in apical uptake of dipeptides (Nielsen et al., 2003). The kinetic analysis revealed that there is an increase in  $V_{max}$  having no significant changes in  $K_m$  and PEPT1 mRNA level (Nielsen et al., 2003). The actual mechanism of the increased PEPT1 function remains to be elucidated. Short-term apical treatment of Caco-2 with leptin and intrajejunal leptin treatment of rat small intestine (mimicking gastric release of leptin) have increased the uptake of dipeptides, and the mechanism appears to be similar to the effect of insulin, which is an increased trafficking of PEPT1 from cytosolic pool to the apical membrane, without altering PEPT1 mRNA level (Buyse et al., 2001). When chronic hyperleptimia was induced in rats, interestingly, PEPT1 mRNA, protein, and dipeptide uptake all seem to increase (Hindlet et al., 2007). The molecular mechanism responsible for these changes appears to be that leptin regulates PEPT1 at both transcriptional level via MAPK and at translational level via ribosomal protein S6 activation (Hindlet et al., 2009).

Treatment of Caco-2 cells with thyroid hormone has induced a decrease in the PEPT1 activity due to a decreased transcription and/or a decreased stability of PEPT1 mRNA (Ashida et al., 2002). Regulation of PEPT1 by thyroid hormone was also confirmed with *in vivo* studies (Ashida et al., 2004). Hyperthyroidism in rat has resulted in a decrease in PEPT1 activity caused by the decreased PEPT1 mRNA and protein expression in the small intestine (Ashida et al., 2004). Hypothyroidism in rats have also lead to an increase in renal PEPT1 mRNA (Lu and Klaassen, 2006).



Pathological conditions, especially in GI tract, have also shown to affect the PEPT1 functional activity. One of the common nutritional conditions is a brief fasting when the patient is severely ill. Fasting, short or prolonged, increases the PEPT1 mRNA expression level, resulting in an increased PEPT1 transporter protein in the brush border membrane of the small intestine (Ogihara et al., 1999; Thamotharan et al., 1999a; Ihara et al., 2000; Naruhashi et al., 2002), resulting altered pharmacokinetic of PEPT1 substrates (Pan et al., 2003). Mechanistic studies have suggested that this fasting induced intestinal PEPT1 expression is mediated by a nuclear receptor, peroxisome proliferator-activated receptor  $\alpha$  (PPAR $\alpha$ ) (Shimakura et al., 2006). Uncontrolled diabetic rats have an increased PEPT1 activity due to the increased stability of PEPT1 mRNA without any changes in transcriptional rate both in the small intestine and kidney (Gangopadhyay et al., 2002). Intestinal resection in patients induces an increase on mRNA and protein level of PEPT1 in colon (Ziegler et al., 2002). Expression of PEPT1 was observed from colon of patients with short bowel syndrome (Ziegler et al., 2002), inflammatory bowel diseases such as ulcerative colitis and Crohn's disease, but not in normal human colon; however, the mechanism responsible for this up-regulation of PEPT1 in colon still remains unclear (Merlin et al., 2001). There is a transcriptional up-regulation of PEPT1 during acute infection with *Cryptosporidium Parvum*, a common cause of diarrheal disease, (Barbot et al., 2003), although the expression of PEPT1 protein remains the same (Marquet et al., 2007). In contrast, there is a decrease in the expression of PEPT1 in jejunal epithelial cells when rats are infected with *Nippostrongylus brasiliensis* (Sekikawa et al., 2003).

There are also a number of pharmacological agents that are known to affect the PEPT1 expression. Studies have suggested that 5-fluorouracil, an anticancer drug that has a deleterious effect on intestinal mucosa, increases the gene expression of PEPT1 (Tanaka et al., 1998; Inoue et al., 2005). Clonidine, an agonist for  $\alpha_2$ -adrenergic receptor, has shown to increase the translocation of preformed cytosolic PEPT1 to apical membrane of Caco-2 cells, resulting in an increased transport activity of PEPT1 (Berlioz et al., 2000), in similar mechanism to insulin (Thamotharan et al., 1999b) and leptin (Buyse et al., 2001). Pentazocine, a  $\sigma$ -ligand receptor, increases the PEPT1 mRNA in Caco-2 cell, and thus, results in an increased population of PEPT1 transporter protein in the plasma membrane leading to an increase in peptide transporter activity (Fujita et al., 1999). Immunosuppressive agent such as tacrolimus and cyclosporine reduce  $V_{max}$  of GlySar uptake on Caco-2 without any effect on  $K_m$  (Motohashi et al., 2001).

In addition to regulation by factors mentioned above, PEPT1 is also regulated by diurnal rhythm (Pan et al., 2002) and this diurnal rhythmic regulation closely is related to feeding schedule (Pan et al., 2003; Pan et al., 2004). Mechanistic studies have suggested that clock controlled gene, albumin D site-binding protein (DBP) plays a major role in this diurnal rhythmic regulation of PEPT1 (Saito et al., 2008).

A thorough understanding of the regulation of PEPT1 transporter will have an implication in nutrition and drug therapy, and may offer explanations to some of the intra- and inter-individual variability in drug responses.

### **Prodrug Approach Using PEPT1 Transporter**

PEPT1 is a very attractive target for the development of prodrug due to its broad substrate specificity and high capacity. A drug with low oral bioavailability can be converted into a prodrug via attachment of a moiety, which can be recognized by PEPT1 transporter in the small intestine. Following the membrane transport, the prodrug can be converted back to its parent drug by hydrolysis in epithelial cells, blood, or liver. PEPT1-targeted prodrugs have a great structural flexibility, and can be either peptidyl or nonpeptidyl prodrugs. Thus far, there are increasing numbers of prodrugs that are targeted at PEPT1. Examples of peptidyl prodrug of PEPT1 include prodrug of  $\alpha$ -methyldopa, a poorly absorbed antihypertensive agent, to  $\alpha$ -methyldopa-Phe,  $\alpha$ -methyldopa-Pro (Hu et al., 1989), and p-glu-L-dopa-pro (Bai, 1995). The Prodrugs of  $\alpha$ -methyldopa have a significantly increased intestinal permeability and an increased oral bioavailability compared to their parent drug. Nonpeptidyl prodrug such as L-valacyclovir, an amino acid ester prodrug of antiviral drug acyclovir, has been shown to be a substrate for PEPT1 in intestine. Through this mechanism, L-valacyclovir improved the oral bioavailability of acyclovir 3-5 times (Balimane et al., 1998; Ganapathy et al., 1998). L-valine ester prodrug of ganciclovir, valganciclovir, is also shown to be transported by PEPT1 (Sugawara et al., 2000). Therefore, PEPT1-targeted prodrug therapy is a promising strategy to improve the intestinal absorption and thus the oral bioavailability of poorly absorbed drugs.

### **Experimental Models to Study PEPT1**

Due to the importance of PEPT1 transporter in the intestinal absorption of peptides/mimetics, PEPT1 has been studied extensively in various experimental conditions. Most of the previous studies were *in vitro* models that lacked intact blood

supplies such as PEPT1 expression in *Xenopus laevis* oocytes (Fei et al., 1994; Liang et al., 1995; Fei et al., 2000) and in various cell lines, such as LLC-PK1, CHO, HeLa, and MDCK cells, by transient or stable transfection. Other *in vitro* models that did not differentiate the effect of PEPT1 from other possible peptide transporters include Caco-2 cell line, brush border membrane vesicle, and Ussing chamber with the small intestine. *In-situ* rat intestinal perfusion has also been utilized in PEPT1 studies. Although this model has an intact blood supply, it does not differentiate PEPT1 transporter from other possible peptide transporters in the small intestine.

## **PHT TRANSPORTERS**

### **Functional Characteristic of PHT Transporter**

Peptide-histidine transporter 1 (PHT1) was first cloned from the rat brain (Yamashita et al., 1997) cDNA library. Rat PHT1 is predicted to have 572 amino acid residues with estimated core molecular mass of 64.9 kDa. Recently, the human orthologue of PHT1 was also cloned and characterized (Bhardwaj et al., 2006). The putative hPHT1 is 86.5% identical to rPHT1 and 48.4% identical to rPHT2. The human PHT1 is predicted to have 577 amino acids with estimated molecular weight of 62 kDa. The structural analysis of hPHT1 and rPHT1 suggest that PHT1 protein contains 12 transmembrane domains with both N- and C- terminals facing the cytosolic side. Functional characteristics of rPHT1 and hPHT1 were evaluated by expression in *Xenopus laevis* oocytes and transient transfection of COS-7 cells, respectively. Both studies

demonstrated that PHT1 transports histidine and carnosine with high affinity in a proton-dependent and  $\text{Na}^+$  concentration gradient independent manner. The transport of histidine by PHT1 was inhibited by various dipeptides and tripeptides, but not single amino acids, suggesting that PHT1 also transports di- and tripeptides (Yamashita et al., 1997; Bhardwaj et al., 2006). One interesting finding was that of COS-7 cells transfected with hPHT1 did not show much affinity for GlySar (Bhardwaj et al., 2006). Peptide-histidine transporter 2 (PHT2) was cloned from rat brain cDNA library (Sakata et al., 2001) and rPHT2 is predicted to encode a protein of 582 amino acid.

PHT1 is distributed in various tissues. The PHT1 mRNA was found in brain, eyes, skeletal muscle, kidney, liver, heart, lung, spleen, colon, thymus, and throughout the GI tract (Yamashita et al., 1997; Botka et al., 2000; Herrera-Ruiz et al., 2001; Ocheltree et al., 2003). In the GI tract, the hPHT1 protein was detected in the stomach, duodenum, jejunum, ileum, and colon. Immunohistochemical analyses demonstrated that PHT1 is localized at villous epithelium of small intestine (Bhardwaj et al., 2006). PHT2 mRNA is mostly found in lymphatic system, lung, spleen, thymus, and faintly in brain, liver, adrenal gland, heart, and the GI tract (Herrera-Ruiz et al., 2001; Sakata et al., 2001). Unlike other POT members, PHT2 is found in lysosome rather than plasma membrane which was demonstrated by light and electron-microscopic analysis (Sakata et al., 2001).

The functional roles of PHT1 and PHT2 have been evaluated in several tissues including brain and eyes. In evaluation of functional activity of PHT1 and PHT2 in brain, synaptosomes from rat cerebral cortex were prepared, and the presence of PHT1 and PHT2 mRNA were confirmed by RT-PCR (Fujita et al., 2004). They have found that

the uptake of histidine into synaptosomes was independent of a transmembrane pH gradient and was not inhibited by GlySar, suggesting that the uptake of histidine was not mediated by PHT1 and PHT2, but rather by various kinds of amino acid transporters. Furthermore, the uptake of GlySar into synaptosomes was not inhibited by the presence of histidine, confirming that PHT1 and PHT2 were not responsible for the uptake of GlySar into synaptosomes from the cerebral cortex of rat (Fujita et al., 2004). The functional activity of PHT1 and PHT2 was also investigated in rat neonatal astrocytes (Xiang et al., 2006). The uptake of carnosine, a known substrate for both PEPT2 and PHT1, was not affected by L-histidine, a PHT1 and PHT2 substrate, suggesting that PHT1 and PHT2 were not functionally active in astrocytes (Xiang et al., 2006). The functional activity of PHT1 was also investigated in retina (Ocheltree et al., 2003). PHT1 mRNA was expressed in retinal pigment epithelium (RPE), a human retinal epithelium cell line ARPE-19, and neural retina (Ocheltree et al., 2003). However, the uptake of GlySar in retinal epithelium cell line ARPE-19 was not inhibited by the presence of 1 mM L-histidine. This suggests that, despite the presence of mRNA, PHT1 is not functionally active on the apical membrane of retinal epithelium (Ocheltree et al., 2003).

## FIGURES

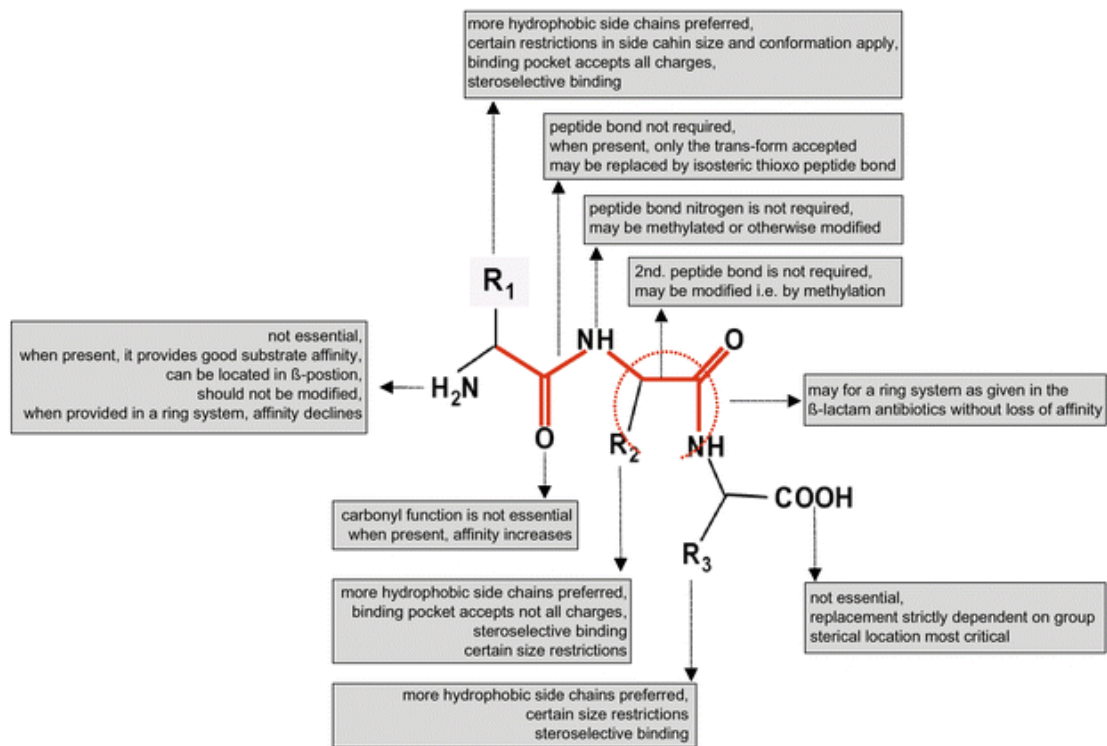


**Figure 2.1** Model of PEPT1 substrate-affinity/transport relationship. The preferred configuration and important conformational features in PEPT1 transporter recognition is summarized. PEPT1 and PEPT2 have very similar not identical structure requirement for affinity/transport. (Adopted from H. Daniel and G. Kottra, *Eur J Physiol.* 447: 610-618, 2004)

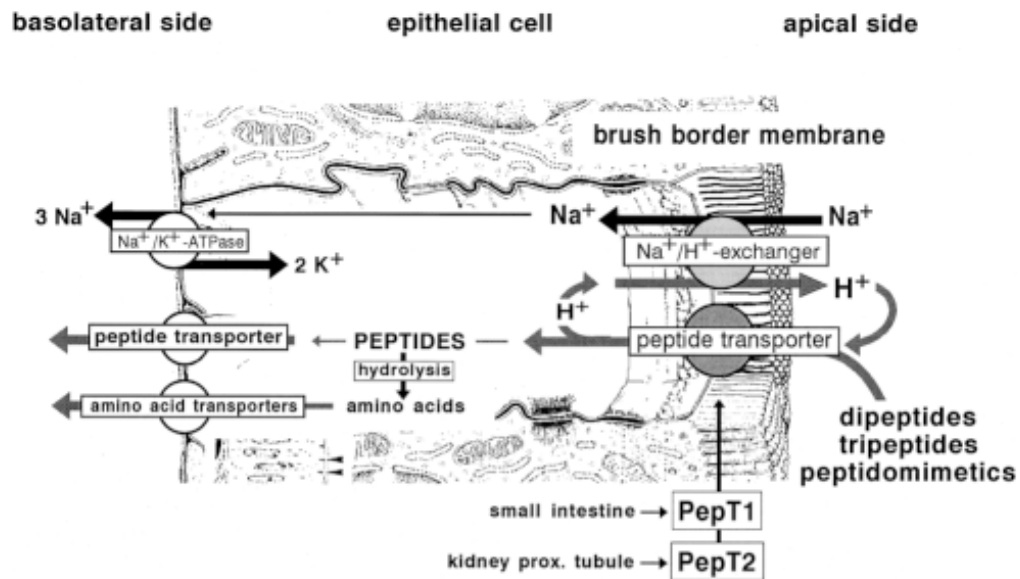


**Figure 2.2** Model of peptide/mimetics in a single epithelial cell in the intestine and kidney. The peptide transporters PEPT1 and PEPT2 are located at the brush border membrane. They transport small peptide/mimetics from the lumen into the cell. They are energized by  $\text{H}^+$  transmembrane gradient and negative membrane potential, which are maintained by sequential action of basolateral  $\text{Na}^+/\text{K}^+$  ATPase and apical  $\text{Na}^+/\text{H}^+$  exchangers. Once inside of the cell, the peptide/mimetics are either metabolized into amino acids/metabolites for use or export, or remain as intact. They exit the cell via basolateral amino acid transporters or basolateral peptide transporter accordingly. (Adopted from H. Daniel, *J. Membrane Biol.*, 154:197-203, 1996.)



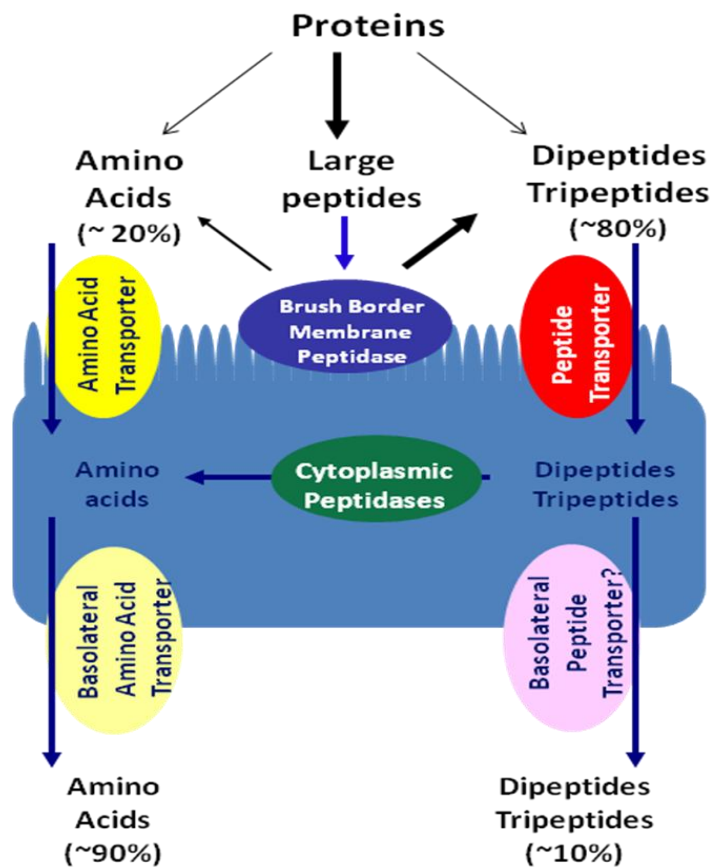


**Figure 2.3** Schematic of protein digestion and absorption in the gastrointestinal tract. (Figure adopted from Ganapathy V, Gupta N, and Martindale RG. Protein Digestion and Absorption. In Physiology of the Gastrointestinal Tract, 4<sup>th</sup> edition, Johnson LR (ed), Elsevier, Burlington, 2006, pp 1667-1692.)

**Table 2.1** Molecular and Functional Features of POTs

Features	PEPT1				PEPT2				PHT1		PHT2
Human gene name	SLC15A1				SLC15A2				SLC15A4		SLC15A3
Mammalian species	Rabbit	Human	Rat	Mouse	Human	Mouse	Rat	Rabbit	Rat	Human	Rat
Amino acids	707	708	710	709	729	729	729	729	572	577	582
Protein Kinase A site	1	0	1	1	0	0	3	0	0	2	2
Protein Kinase C site	1	2	1	1	5	2	3	4	11	11	4
Glycosylation site	4	7	5	6	3	2		5	4	4	3
Transmembrane domain	12				12				12		12
Coupling ion	Cotransport /H <sup>+</sup>				Cotransport /H <sup>+</sup>				Cotransport /H <sup>+</sup>		Cotransport /H <sup>+</sup>
Amino acid in substrate	2-3				2-3				2-3		2
Transport of L-Histidine	No				No				Yes		Yes
Substrate affinity	Low				High				High		?
<i>K<sub>m</sub></i> value	mM				μM				μM		?
Stereoselectivity	L > D				L > D						
Amino acid identity between species	81% human vs. rabbit 83% human vs. rat 83% human vs. mouse 77% rat vs. rabbit				82% human vs. mouse 82% mouse vs. rabbit 92% mouse vs. rat				86.5 % human vs. rat		
Amino acid identity between POTs					~ 50% PEPT2 vs. PEPT1				17% PHT1 vs. PEPT1 12% PHT1 vs. PEPT2		49% PHT2 vs. PHT1 22% PHT2 vs. PEPT1 24% PHT2 vs. PEPT2

**References for Table 2.1 include:** Fei et al., 1994; Liang et al., 1995; Liu et al., 1995; Saito et al., 1995; Boll et al., 1996; Miyamoto et al., 1996; Saito et al., 1996; Yamashita et al., 1997; Fei et al., 2000; Rubio-Aliaga et al., 2000; Sakata et al., 2001; Bhardwaj et al., 2006).

**Table 2.2** Tissue and Cellular Distribution of POTs

POT isoform	Tissue	Species	RNA	Protein	Localization
<b>PEPT1</b>	Small intestine	Rabbit, Human, Rat, Mouse	Y	Y	Brush border of enterocytes
	Kidney	Rabbit, Human, Rat, Mouse	Y	Y	Brush border membrane of epithelium cells of S1 segment of proximal tubule and lysosome
	Liver	Rabbit, Human	Y		lysosome
	Pancreas	Human		Y	Lysosome acinar cells
	Placenta	Human	Y		
	Testis	Rat	Y		
	Ovary	Mouse	Y		
	Lung	Mouse	Y		Epithelial cells
	Prostate	Human	Y		
	Bile duct		Y	Y	Apical membrane of cholangicytes
<b>PEPT2</b>	Kidney	Rat, Mouse, Rabbit	Y	Y	Brush border membrane of epithelium cells of S2 and S3 segment of proximal tubule
	Brain	Rat	Y	Y	astrocytes, subependymal cells, ependymal cells and epithelial cells of choroid plexus
	Lung	Rabbit, Rat	Y	Y	Apical membrane of alveolar type II pneumocytes and bronchial epithelium and endothelium of small arteries
	Liver	Rabbit	Y		
	Heart	Rabbit	Y		
	Mammary gland	Rat	Y	Y	Epithelial cells of glands and ducts
	Eye		Y		Retina epithelium
	<b>PHT1</b>	Brain	Rat, Human	Y	
Eye	Rat, Bovine, Human	Y			
Lung	Rat	Y			
Spleen	Rat	Y			
GI tract	Rat	Y			
Skeletal muscle	Human	Y			
Kidney	Human	Y			
Heart	Human	Y			
Liver	Human	Y			
Colon	Human	Y			
Thymus	Human	Y			
Small intestine	Human	Y	Y	At villous epithelium	
<b>PHT2</b>	Lung	Rat	Y		lysosome
	Spleen	Rat	Y		
	Thymus	Rat	Y		
	Brain	Rat	Y		
	Liver	Rat	Y		
	Adrenal glad	Rat	Y		
	Heart	Rat	Y		
	Small intestine	Rat	Y		
<b>HPT1</b>	Colon	Human	Y		
	Skeletal muscle	Human	Y		
	Small intestine	Human, Rat	Y		

**Reference for Table 2.2 includes:** (Fei et al., 1994; Liang et al., 1995; Liu et al., 1995; Saito et al., 1995; Boll et al., 1996; Miyamoto et al., 1996; Ogihara et al., 1996; Saito et al., 1996; Bockman et al., 1997; Thamocharan et al., 1997; Yamashita et al., 1997; Doring et al., 1998a; Smith et al., 1998; Walker et al., 1998; Berger and Hediger, 1999; Shen et al., 1999; Botka et al., 2000; Fei et al., 2000; Rubio-Aliaga et al., 2000; Zhou et al., 2000; Groneberg et al., 2001a; Groneberg et al., 2001b; Herrera-Ruiz et al., 2001; Sakata et al., 2001; Groneberg et al., 2002; Knutter et al., 2002; Shu et al., 2002; Ocheltree et al., 2003; Shen et al., 2003; Bhardwaj et al., 2006; Lu and Klaassen, 2006).

## REFERENCES

Amasheh S, Wenzel U, Boll M, Dorn D, Weber W, Clauss W and Daniel H (1997) Transport of charged dipeptides by the intestinal H<sup>+</sup>/peptide symporter PepT1 expressed in *Xenopus laevis* oocytes. *J Membr Biol* **155**:247-256.

Anderle P, Nielsen CU, Pinsonneault J, Krog PL, Brodin B and Sadee W (2006) Genetic variants of the human dipeptide transporter PEPT1. *J Pharmacol Exp Ther* **316**:636-646.

Ashida K, Katsura T, Motohashi H, Saito H and Inui K (2002) Thyroid hormone regulates the activity and expression of the peptide transporter PEPT1 in Caco-2 cells. *Am J Physiol Gastrointest Liver Physiol* **282**:G617-623.

Ashida K, Katsura T, Saito H and Inui K (2004) Decreased activity and expression of intestinal oligopeptide transporter PEPT1 in rats with hyperthyroidism in vivo. *Pharm Res* **21**:969-975.

Bai JP (1995) pGlu-L-Dopa-Pro: a tripeptide prodrug targeting the intestinal peptide transporter for absorption and tissue enzymes for conversion. *Pharm Res* **12**:1101-1104.

Balimane PV, Tamai I, Guo A, Nakanishi T, Kitada H, Leibach FH, Tsuji A and Sinko PJ (1998) Direct evidence for peptide transporter (PepT1)-mediated uptake of a nonpeptide prodrug, valacyclovir. *Biochem Biophys Res Commun* **250**:246-251.

Barbot L, Windsor E, Rome S, Tricottet V, Reynes M, Topouchian A, Huneau JF, Gobert JG, Tome D and Kapel N (2003) Intestinal peptide transporter PepT1 is over-expressed during acute cryptosporidiosis in suckling rats as a result of both malnutrition and experimental parasite infection. *Parasitol Res* **89**:364-370.

Berger UV and Hediger MA (1999) Distribution of peptide transporter PEPT2 mRNA in the rat nervous system. *Anat Embryol (Berl)* **199**:439-449.

Berlioz F, Maoret JJ, Paris H, Laburthe M, Farinotti R and Roze C (2000) alpha(2)-adrenergic receptors stimulate oligopeptide transport in a human intestinal cell line. *J Pharmacol Exp Ther* **294**:466-472.

Bhardwaj RK, Herrera-Ruiz D, Eltoukhy N, Saad M and Knipp GT (2006) The functional evaluation of human peptide/histidine transporter 1 (hPHT1) in transiently transfected COS-7 cells. *Eur J Pharm Sci* **27**:533-542.

- Biegel A, Knutter I, Hartrodt B, Gebauer S, Theis S, Luckner P, Kottra G, Rastetter M, Zebisch K, Thondorf I, Daniel H, Neubert K and Brandsch M (2006) The renal type H(+)/peptide symporter PEPT2: structure-affinity relationships. *Amino Acids* **31**:137-156.
- Bockman DE, Ganapathy V, Oblak TG and Leibach FH (1997) Localization of peptide transporter in nuclei and lysosomes of the pancreas. *Int J Pancreatol* **22**:221-225.
- Bolger MB, Haworth IS, Yeung AK, Ann D, von Grafenstein H, Hamm-Alvarez S, Okamoto CT, Kim KJ, Basu SK, Wu S and Lee VH (1998) Structure, function, and molecular modeling approaches to the study of the intestinal dipeptide transporter PepT1. *J Pharm Sci* **87**:1286-1291.
- Boll M, Herget M, Wagener M, Weber WM, Markovich D, Biber J, Clauss W, Murer H and Daniel H (1996) Expression cloning and functional characterization of the kidney cortex high-affinity proton-coupled peptide transporter. *Proc Natl Acad Sci U S A* **93**:284-289.
- Botka CW, Wittig TW, Graul RC, Nielsen CU, Higaka K, Amidon GL and Sadee W (2000) Human proton/oligopeptide transporter (POT) genes: identification of putative human genes using bioinformatics. *AAPS PharmSci* **2**:E16.
- Brandsch M, Brandsch C, Ganapathy ME, Chew CS, Ganapathy V and Leibach FH (1997) Influence of proton and essential histidyl residues on the transport kinetics of the H+/peptide cotransport systems in intestine (PEPT 1) and kidney (PEPT 2). *Biochim Biophys Acta* **1324**:251-262.
- Brandsch M, Knutter I, Thunecke F, Hartrodt B, Born I, Borner V, Hirche F, Fischer G and Neubert K (1999) Decisive structural determinants for the interaction of proline derivatives with the intestinal H+/peptide symporter. *Eur J Biochem* **266**:502-508.
- Brandsch M, Miyamoto Y, Ganapathy V and Leibach FH (1994) Expression and protein kinase C-dependent regulation of peptide/H<sup>+</sup> co-transport system in the Caco-2 human colon carcinoma cell line. *Biochem J* **299** ( Pt 1):253-260.
- Brandsch M, Thunecke F, Kullertz G, Schutkowski M, Fischer G and Neubert K (1998) Evidence for the absolute conformational specificity of the intestinal H+/peptide symporter, PEPT1. *J Biol Chem* **273**:3861-3864.
- Bretschneider B, Brandsch M and Neubert R (1999) Intestinal transport of beta-lactam antibiotics: analysis of the affinity at the H+/peptide symporter (PEPT1), the uptake into Caco-2 cell monolayers and the transepithelial flux. *Pharm Res* **16**:55-61.

Buyse M, Berlioz F, Guilmeau S, Tsocas A, Voisin T, Peranzi G, Merlin D, Laburthe M, Lewin MJ, Roze C and Bado A (2001) PepT1-mediated epithelial transport of dipeptides and cephalixin is enhanced by luminal leptin in the small intestine. *J Clin Invest* **108**:1483-1494.

Chen XZ, Steel A and Hediger MA (2000) Functional roles of histidine and tyrosine residues in the H(+)-peptide transporter PepT1. *Biochem Biophys Res Commun* **272**:726-730.

Chen XZ, Zhu T, Smith DE and Hediger MA (1999) Stoichiometry and kinetics of the high-affinity H<sup>+</sup>-coupled peptide transporter PepT2. *J Biol Chem* **274**:2773-2779.

Chu XY, Sanchez-Castano GP, Higaki K, Oh DM, Hsu CP and Amidon GL (2001) Correlation between epithelial cell permeability of cephalixin and expression of intestinal oligopeptide transporter. *J Pharmacol Exp Ther* **299**:575-582.

Daniel H (2004) Molecular and integrative physiology of intestinal peptide transport. *Annu Rev Physiol* **66**:361-384.

Daniel H, Fett C and Kratz A (1989) Demonstration and modification of intervillous pH profiles in rat small intestine in vitro. *Am J Physiol* **257**:G489-495.

Dantzig AH, Hoskins JA, Tabas LB, Bright S, Shepard RL, Jenkins IL, Duckworth DC, Sportsman JR, Mackensen D, Rosteck PR, Jr. and et al. (1994) Association of intestinal peptide transport with a protein related to the cadherin superfamily. *Science* **264**:430-433.

Doring F, Dorn D, Bachfischer U, Amasheh S, Herget M and Daniel H (1996) Functional analysis of a chimeric mammalian peptide transporter derived from the intestinal and renal isoforms. *J Physiol* **497** ( Pt 3):773-779.

Doring F, Martini C, Walter J and Daniel H (2002) Importance of a small N-terminal region in mammalian peptide transporters for substrate affinity and function. *J Membr Biol* **186**:55-62.

Doring F, Walter J, Will J, Focking M, Boll M, Amasheh S, Clauss W and Daniel H (1998a) Delta-aminolevulinic acid transport by intestinal and renal peptide transporters and its physiological and clinical implications. *J Clin Invest* **101**:2761-2767.

Doring F, Will J, Amasheh S, Clauss W, Ahlbrecht H and Daniel H (1998b) Minimal molecular determinants of substrates for recognition by the intestinal peptide transporter. *J Biol Chem* **273**:23211-23218.

Dyer J, Beechey RB, Gorvel JP, Smith RT, Wootton R and Shirazi-Beechey SP (1990) Glycyl-L-proline transport in rabbit enterocyte basolateral-membrane vesicles. *Biochem J* **269**:565-571.

Erickson RH (1995) Peptide Metabolism at Brush-Border Membranes, in: *Peptide-Based Drug Design* (Taylor MD and Amidon GL eds), pp 23-45, American Chemical Society, Washington DC.

Erickson RH, Gum JR, Jr., Lindstrom MM, McKean D and Kim YS (1995) Regional expression and dietary regulation of rat small intestinal peptide and amino acid transporter mRNAs. *Biochem Biophys Res Commun* **216**:249-257.

Fei YJ, Kanai Y, Nussberger S, Ganapathy V, Leibach FH, Romero MF, Singh SK, Boron WF and Hediger MA (1994) Expression cloning of a mammalian proton-coupled oligopeptide transporter. *Nature* **368**:563-566.

Fei YJ, Liu JC, Fujita T, Liang R, Ganapathy V and Leibach FH (1998) Identification of a potential substrate binding domain in the mammalian peptide transporters PEPT1 and PEPT2 using PEPT1-PEPT2 and PEPT2-PEPT1 chimeras. *Biochem Biophys Res Commun* **246**:39-44.

Fei YJ, Liu W, Prasad PD, Kekuda R, Oblak TG, Ganapathy V and Leibach FH (1997) Identification of the histidyl residue obligatory for the catalytic activity of the human H<sup>+</sup>/peptide cotransporters PEPT1 and PEPT2. *Biochemistry* **36**:452-460.

Fei YJ, Sugawara M, Liu JC, Li HW, Ganapathy V, Ganapathy ME and Leibach FH (2000) cDNA structure, genomic organization, and promoter analysis of the mouse intestinal peptide transporter PEPT1. *Biochim Biophys Acta* **1492**:145-154.

Fujita T, Kishida T, Wada M, Okada N, Yamamoto A, Leibach FH and Ganapathy V (2004) Functional characterization of brain peptide transporter in rat cerebral cortex: identification of the high-affinity type H<sup>+</sup>/peptide transporter PEPT2. *Brain Res* **997**:52-61.

Fujita T, Majikawa Y, Umehisa S, Okada N, Yamamoto A, Ganapathy V and Leibach FH (1999) sigma Receptor ligand-induced up-regulation of the H<sup>(+)</sup>/peptide transporter PEPT1 in the human intestinal cell line Caco-2. *Biochem Biophys Res Commun* **261**:242-246.

Ganapathy ME, Huang W, Wang H, Ganapathy V and Leibach FH (1998) Valacyclovir: a substrate for the intestinal and renal peptide transporters PEPT1 and PEPT2. *Biochem Biophys Res Commun* **246**:470-475.

Ganapathy V, Gupta N and Martindale RG (2006) Protein Digestion and Absorption, in: *Physiology of the Gastrointestinal Tract* (Johnson LR ed), pp 1667-1692, Elsevier, Burlington.

Gangopadhyay A, Thamocharan M and Adibi SA (2002) Regulation of oligopeptide transporter (Pept-1) in experimental diabetes. *Am J Physiol Gastrointest Liver Physiol* **283**:G133-138.

Gardner ML, Lindblad BS, Burston D and Matthews DM (1983) Trans-mucosal passage of intact peptides in the guinea-pig small intestine in vivo: a re-appraisal. *Clin Sci (Lond)* **64**:433-439.

Gilbert ER, Wong EA and Webb KE, Jr. (2008) Board-invited review: Peptide absorption and utilization: Implications for animal nutrition and health. *J Anim Sci* **86**:2135-2155.

Groneberg DA, Doring F, Eynott PR, Fischer A and Daniel H (2001a) Intestinal peptide transport: ex vivo uptake studies and localization of peptide carrier PEPT1. *Am J Physiol Gastrointest Liver Physiol* **281**:G697-704.

Groneberg DA, Doring F, Theis S, Nickolaus M, Fischer A and Daniel H (2002) Peptide transport in the mammary gland: expression and distribution of PEPT2 mRNA and protein. *Am J Physiol Endocrinol Metab* **282**:E1172-1179.

Groneberg DA, Nickolaus M, Springer J, Doring F, Daniel H and Fischer A (2001b) Localization of the peptide transporter PEPT2 in the lung: implications for pulmonary oligopeptide uptake. *Am J Pathol* **158**:707-714.

Hashimoto N, Fujioka T, Toyoda T, Muranushi N and Hirano K (1994) Renin inhibitor: transport mechanism in rat small intestinal brush-border membrane vesicles. *Pharm Res* **11**:1448-1451.

Hediger MA, Kanai Y, You G and Nussberger S (1995) Mammalian ion-coupled solute transporters. *J Physiol* **482**:7S-17S.

Herrera-Ruiz D, Wang Q, Gudmundsson OS, Cook TJ, Smith RL, Faria TN and Knipp GT (2001) Spatial expression patterns of peptide transporters in the human and rat gastrointestinal tracts, Caco-2 in vitro cell culture model, and multiple human tissues. *AAPS PharmSci* **3**:E9.

Hindlet P, Bado A, Farinotti R and Buyse M (2007) Long-term effect of leptin on H<sup>+</sup>-coupled peptide cotransporter 1 activity and expression in vivo: evidence in leptin-deficient mice. *J Pharmacol Exp Ther* **323**:192-201.



Hindlet P, Bado A, Kamenicky P, Delomenie C, Bourasset F, Nazaret C, Farinotti R and Buyse M (2009) Reduced intestinal absorption of dipeptides via PepT1 in mice with diet-induced obesity is associated with leptin receptor down-regulation. *J Biol Chem* **284**:6801-6808.

Hogerle ML and Winne D (1983) Drug absorption by the rat jejunum perfused in situ. Dissociation from the pH-partition theory and role of microclimate-pH and unstirred layer. *Naunyn Schmiedebergs Arch Pharmacol* **322**:249-255.

Hu M, Subramanian P, Mosberg HI and Amidon GL (1989) Use of the peptide carrier system to improve the intestinal absorption of L-alpha-methyldopa: carrier kinetics, intestinal permeabilities, and in vitro hydrolysis of dipeptidyl derivatives of L-alpha-methyldopa. *Pharm Res* **6**:66-70.

Ihara T, Tsujikawa T, Fujiyama Y and Bamba T (2000) Regulation of PepT1 peptide transporter expression in the rat small intestine under malnourished conditions. *Digestion* **61**:59-67.

Inoue M, Terada T, Okuda M and Inui K (2005) Regulation of human peptide transporter 1 (PEPT1) in gastric cancer cells by anticancer drugs. *Cancer Lett* **230**:72-80.

Inui K, Yamamoto M and Saito H (1992) Transepithelial transport of oral cephalosporins by monolayers of intestinal epithelial cell line Caco-2: specific transport systems in apical and basolateral membranes. *J Pharmacol Exp Ther* **261**:195-201.

Irie M, Terada T, Okuda M and Inui K (2004) Efflux properties of basolateral peptide transporter in human intestinal cell line Caco-2. *Pflugers Arch* **449**:186-194.

Irie M, Terada T, Sawada K, Saito H and Inui K (2001) Recognition and transport characteristics of nonpeptidic compounds by basolateral peptide transporter in Caco-2 cells. *J Pharmacol Exp Ther* **298**:711-717.

Klapper M, Daniel H and Doring F (2006) Cytosolic COOH terminus of the peptide transporter PEPT2 is involved in apical membrane localization of the protein. *Am J Physiol Cell Physiol* **290**:C472-483.

Knutter I, Hartrodt B, Theis S, Foltz M, Rastetter M, Daniel H, Neubert K and Brandsch M (2004) Analysis of the transport properties of side chain modified dipeptides at the mammalian peptide transporter PEPT1. *Eur J Pharm Sci* **21**:61-67.

Knutter I, Rubio-Aliaga I, Boll M, Hause G, Daniel H, Neubert K and Brandsch M (2002) H<sup>+</sup>-peptide cotransport in the human bile duct epithelium cell line SK-ChA-1. *Am J Physiol Gastrointest Liver Physiol* **283**:G222-229.

- Kotra G and Daniel H (2001) Bidirectional electrogenic transport of peptides by the proton-coupled carrier PEPT1 in *Xenopus laevis* oocytes: its asymmetry and symmetry. *J Physiol* **536**:495-503.
- Kotra G, Stamford A and Daniel H (2002) PEPT1 as a paradigm for membrane carriers that mediate electrogenic bidirectional transport of anionic, cationic, and neutral substrates. *J Biol Chem* **277**:32683-32691.
- Kramer W, Girbig F, Gutjahr U, Kleemann HW, Leipe I, Urbach H and Wagner A (1990) Interaction of renin inhibitors with the intestinal uptake system for oligopeptides and beta-lactam antibiotics. *Biochim Biophys Acta* **1027**:25-30.
- Kulkarni AA, Davies DL, Links JS, Patel LN, Lee VH and Haworth IS (2006) A Charge Pair Interaction Between Arg282 in Transmembrane Segment 7 and Asp341 in Transmembrane Segment 8 of hPepT1. *Pharm Res*.
- Kulkarni AA, Davies DL, Links JS, Patel LN, Lee VH and Haworth IS (2007) A charge pair interaction between Arg282 in transmembrane segment 7 and Asp341 in transmembrane segment 8 of hPepT1. *Pharm Res* **24**:66-72.
- Kulkarni AA, Haworth IS and Lee VH (2003a) Transmembrane segment 5 of the dipeptide transporter hPepT1 forms a part of the substrate translocation pathway. *Biochem Biophys Res Commun* **306**:177-185.
- Kulkarni AA, Haworth IS, Uchiyama T and Lee VH (2003b) Analysis of transmembrane segment 7 of the dipeptide transporter hPepT1 by cysteine-scanning mutagenesis. *J Biol Chem* **278**:51833-51840.
- Kurtin P and Charney AN (1984) Intestinal ion transport and intracellular pH during acute respiratory alkalosis and acidosis. *Am J Physiol* **247**:G24-31.
- Li J, Tamura K, Lee CP, Smith PL, Borchardt RT and Hidalgo IJ (1998) Structure-affinity relationships of Val-Val and Val-Val-Val stereoisomers with the apical oligopeptide transporter in human intestinal Caco-2 cells. *J Drug Target* **5**:317-327.
- Liang R, Fei YJ, Prasad PD, Ramamoorthy S, Han H, Yang-Feng TL, Hediger MA, Ganapathy V and Leibach FH (1995) Human intestinal H<sup>+</sup>/peptide cotransporter. Cloning, functional expression, and chromosomal localization. *J Biol Chem* **270**:6456-6463.
- Links JL, Kulkarni AA, Davies DL, Lee VH and Haworth IS (2007) Cysteine scanning of transmembrane domain three of the human dipeptide transporter: implications for substrate transport. *J Drug Target* **15**:218-225.

Liu W, Liang R, Ramamoorthy S, Fei YJ, Ganapathy ME, Hediger MA, Ganapathy V and Leibach FH (1995) Molecular cloning of PEPT 2, a new member of the H<sup>+</sup>/peptide cotransporter family, from human kidney. *Biochim Biophys Acta* **1235**:461-466.

Lu H and Klaassen C (2006) Tissue distribution and thyroid hormone regulation of Pept1 and Pept2 mRNA in rodents. *Peptides* **27**:850-857.

Lucas ML, Lei FH and Blair JA (1980) The influence of buffer pH, glucose and sodium ion concentration on the acid microclimate in rat proximal jejunum in vitro. *Pflugers Arch* **385**:137-142.

Lucas ML, Schneider W, Haberich FJ and Blair JA (1975) Direct measurement by pH-microelectrode of the pH microclimate in rat proximal jejunum. *Proc R Soc Lond B Biol Sci* **192**:39-48.

Mackenzie B, Loo DD, Fei Y, Liu WJ, Ganapathy V, Leibach FH and Wright EM (1996) Mechanisms of the human intestinal H<sup>+</sup>-coupled oligopeptide transporter hPEPT1. *J Biol Chem* **271**:5430-5437.

Maheshwari M, Christian SL, Liu C, Badner JA, Detera-Wadleigh S, Gershon ES and Gibbs RA (2002) Mutation screening of two candidate genes from 13q32 in families affected with Bipolar disorder: human peptide transporter (SLC15A1) and human glypican5 (GPC5). *BMC Genomics* **3**:30.

Marquet P, Barbot L, Plante A, Huneau JF, Gobert JG and Kapel N (2007) Cryptosporidiosis induces a transient upregulation of the oligopeptides transporter (PepT1) activity in neonatal rats. *Exp Biol Med (Maywood)* **232**:454-460.

Matsumoto S, Saito H and Inui K (1994) Transcellular transport of oral cephalosporins in human intestinal epithelial cells, Caco-2: interaction with dipeptide transport systems in apical and basolateral membranes. *J Pharmacol Exp Ther* **270**:498-504.

Matthews DM (1975) Intestinal absorption of peptides. *Physiol Rev* **55**:537-608.

Matthews DM, Crampton RF and Lis MT (1971) Sites of maximal intestinal absorptive capacity for amino acids and peptides: evidence for an independent peptide uptake system or systems. *J Clin Pathol* **24**:882-883.

Meredith D (2004) Site-directed mutation of arginine 282 to glutamate uncouples the movement of peptides and protons by the rabbit proton-peptide cotransporter PepT1. *J Biol Chem* **279**:15795-15798.

Meredith D, Temple CS, Guha N, Sword CJ, Boyd CA, Collier ID, Morgan KM and Bailey PD (2000) Modified amino acids and peptides as substrates for the intestinal peptide transporter PepT1. *Eur J Biochem* **267**:3723-3728.

Merlin D, Si-Tahar M, Sitaraman SV, Eastburn K, Williams I, Liu X, Hediger MA and Madara JL (2001) Colonic epithelial hPepT1 expression occurs in inflammatory bowel disease: transport of bacterial peptides influences expression of MHC class 1 molecules. *Gastroenterology* **120**:1666-1679.

Miyamoto K, Shiraga T, Morita K, Yamamoto H, Haga H, Taketani Y, Tamai I, Sai Y, Tsuji A and Takeda E (1996) Sequence, tissue distribution and developmental changes in rat intestinal oligopeptide transporter. *Biochim Biophys Acta* **1305**:34-38.

Moore VA, Irwin WJ, Timmins P, Lambert PA, Chong S, Dando SA and Morrison RA (2000) A rapid screening system to determine drug affinities for the intestinal dipeptide transporter 2: affinities of ACE inhibitors. *Int J Pharm* **210**:29-44.

Motohashi H, Katsura T, Saito H and Inui K (2001) Effects of tacrolimus and cyclosporin A on peptide transporter PEPT1 in Caco-2 cells. *Pharm Res* **18**:713-717.

Naruhashi K, Sai Y, Tamai I, Suzuki N and Tsuji A (2002) PepT1 mRNA expression is induced by starvation and its level correlates with absorptive transport of cefadroxil longitudinally in the rat intestine. *Pharm Res* **19**:1417-1423.

Nielsen CU, Amstrup J, Nielsen R, Steffansen B, Frokjaer S and Brodin B (2003) Epidermal growth factor and insulin short-term increase hPepT1-mediated glycylsarcosine uptake in Caco-2 cells. *Acta Physiol Scand* **178**:139-148.

Nielsen CU, Amstrup J, Steffansen B, Frokjaer S and Brodin B (2001) Epidermal growth factor inhibits glycylsarcosine transport and hPepT1 expression in a human intestinal cell line. *Am J Physiol Gastrointest Liver Physiol* **281**:G191-199.

Ocheltree SM, Keep RF, Shen H, Yang D, Hughes BA and Smith DE (2003) Preliminary investigation into the expression of proton-coupled oligopeptide transporters in neural retina and retinal pigment epithelium (RPE): lack of functional activity in RPE plasma membranes. *Pharm Res* **20**:1364-1372.

Ogihara H, Saito H, Shin BC, Terado T, Takenoshita S, Nagamachi Y, Inui K and Takata K (1996) Immuno-localization of H<sup>+</sup>/peptide cotransporter in rat digestive tract. *Biochem Biophys Res Commun* **220**:848-852.

- Ogihara H, Suzuki T, Nagamachi Y, Inui K and Takata K (1999) Peptide transporter in the rat small intestine: ultrastructural localization and the effect of starvation and administration of amino acids. *Histochem J* **31**:169-174.
- Pan X, Terada T, Irie M, Saito H and Inui K (2002) Diurnal rhythm of H<sup>+</sup>-peptide cotransporter in rat small intestine. *Am J Physiol Gastrointest Liver Physiol* **283**:G57-64.
- Pan X, Terada T, Okuda M and Inui K (2003) Altered diurnal rhythm of intestinal peptide transporter by fasting and its effects on the pharmacokinetics of ceftibuten. *J Pharmacol Exp Ther* **307**:626-632.
- Pan X, Terada T, Okuda M and Inui K (2004) The diurnal rhythm of the intestinal transporters SGLT1 and PEPT1 is regulated by the feeding conditions in rats. *J Nutr* **134**:2211-2215.
- Panitsas KE, Boyd CA and Meredith D (2006) Evidence that the rabbit proton-peptide co-transporter PepT1 is a multimer when expressed in *Xenopus laevis* oocytes. *Pflugers Arch* **452**:53-63.
- Phan DD, Chin-Hong P, Lin ET, Anderle P, Sadee W and Guglielmo BJ (2003) Intra- and interindividual variabilities of valacyclovir oral bioavailability and effect of coadministration of an hPEPT1 inhibitor. *Antimicrob Agents Chemother* **47**:2351-2353.
- Pieri M, Hall D, Price R, Bailey P and Meredith D (2008) Site-directed mutagenesis of Arginine<sup>282</sup> suggests how protons and peptides are co-transported by rabbit PepT1. *Int J Biochem Cell Biol* **40**:721-730.
- Read NW, Barber DC, Levin RJ and Holdsworth CD (1977) Unstirred layer and kinetics of electrogenic glucose absorption in the human jejunum in situ. *Gut* **18**:865-876.
- Rubio-Aliaga I, Boll M and Daniel H (2000) Cloning and characterization of the gene encoding the mouse peptide transporter PEPT2. *Biochem Biophys Res Commun* **276**:734-741.
- Said HM, Blair JA, Lucas ML and Hilburn ME (1986) Intestinal surface acid microclimate in vitro and in vivo in the rat. *J Lab Clin Med* **107**:420-424.
- Saito H and Inui K (1993) Dipeptide transporters in apical and basolateral membranes of the human intestinal cell line Caco-2. *Am J Physiol* **265**:G289-294.
- Saito H, Motohashi H, Mukai M and Inui K (1997) Cloning and characterization of a pH-sensing regulatory factor that modulates transport activity of the human H<sup>+</sup>/peptide cotransporter, PEPT1. *Biochem Biophys Res Commun* **237**:577-582.

Saito H, Okuda M, Terada T, Sasaki S and Inui K (1995) Cloning and characterization of a rat H<sup>+</sup>/peptide cotransporter mediating absorption of beta-lactam antibiotics in the intestine and kidney. *J Pharmacol Exp Ther* **275**:1631-1637.

Saito H, Terada T, Okuda M, Sasaki S and Inui K (1996) Molecular cloning and tissue distribution of rat peptide transporter PEPT2. *Biochim Biophys Acta* **1280**:173-177.

Saito H, Terada T, Shimakura J, Katsura T and Inui K (2008) Regulatory mechanism governing the diurnal rhythm of intestinal H<sup>+</sup>/peptide cotransporter 1 (PEPT1). *Am J Physiol Gastrointest Liver Physiol* **295**:G395-402.

Sakata K, Yamashita T, Maeda M, Moriyama Y, Shimada S and Tohyama M (2001) Cloning of a lymphatic peptide/histidine transporter. *Biochem J* **356**:53-60.

Sala-Rabanal M, Loo DD, Hirayama BA, Turk E and Wright EM (2006) Molecular interactions between dipeptides, drugs and the human intestinal H<sup>+</sup> -oligopeptide cotransporter hPEPT1. *J Physiol* **574**:149-166.

Schoenmakers RG, Stehouwer MC and Tukker JJ (1999) Structure-transport relationship for the intestinal small-peptide carrier: is the carbonyl group of the peptide bond relevant for transport? *Pharm Res* **16**:62-68.

Seal CJ and Parker DS (1991) Isolation and characterization of circulating low molecular weight peptides in steer, sheep and rat portal and peripheral blood. *Comp Biochem Physiol B* **99**:679-685.

Sekikawa S, Kawai Y, Fujiwara A, Takeda K, Tegoshi T, Uchikawa R, Yamada M and Arizono N (2003) Alterations in hexose, amino acid and peptide transporter expression in intestinal epithelial cells during *Nippostrongylus brasiliensis* infection in the rat. *Int J Parasitol* **33**:1419-1426.

Shen H, Smith DE, Keep RF, Xiang J and Brosius FC, 3rd (2003) Targeted disruption of the PEPT2 gene markedly reduces dipeptide uptake in choroid plexus. *J Biol Chem* **278**:4786-4791.

Shen H, Smith DE, Yang T, Huang YG, Schnermann JB and Brosius FC, 3rd (1999) Localization of PEPT1 and PEPT2 proton-coupled oligopeptide transporter mRNA and protein in rat kidney. *Am J Physiol* **276**:F658-665.

Shepherd EJ, Lister N, Affleck JA, Bronk JR, Kellett GL, Collier ID, Bailey PD and Boyd CA (2002) Identification of a candidate membrane protein for the basolateral peptide transporter of rat small intestine. *Biochem Biophys Res Commun* **296**:918-922.

Shiau YF, Fernandez P, Jackson MJ and McMonagle S (1985) Mechanisms maintaining a low-pH microclimate in the intestine. *Am J Physiol* **248**:G608-617.

Shimada T (1987) Factors affecting the microclimate pH in rat jejunum. *J Physiol* **392**:113-127.

Shimakura J, Terada T, Saito H, Katsura T and Inui K (2006) Induction of intestinal peptide transporter 1 expression during fasting is mediated via peroxisome proliferator-activated receptor alpha. *Am J Physiol Gastrointest Liver Physiol* **291**:G851-856.

Shiraga T, Miyamoto K, Tanaka H, Yamamoto H, Taketani Y, Morita K, Tamai I, Tsuji A and Takeda E (1999) Cellular and molecular mechanisms of dietary regulation on rat intestinal H<sup>+</sup>/Peptide transporter PepT1. *Gastroenterology* **116**:354-362.

Shu C, Shen H, Teuscher NS, Lorenzi PJ, Keep RF and Smith DE (2002) Role of PEPT2 in peptide/mimetic trafficking at the blood-cerebrospinal fluid barrier: studies in rat choroid plexus epithelial cells in primary culture. *J Pharmacol Exp Ther* **301**:820-829.

Silk DB, Nicholson A and Kim YS (1976) Hydrolysis of peptides within lumen of small intestine. *Am J Physiol* **231**:1322-1329.

Smith DE, Pavlova A, Berger UV, Hediger MA, Yang T, Huang YG and Schnermann JB (1998) Tubular localization and tissue distribution of peptide transporters in rat kidney. *Pharm Res* **15**:1244-1249.

Steel A, Nussberger S, Romero MF, Boron WF, Boyd CA and Hediger MA (1997) Stoichiometry and pH dependence of the rabbit proton-dependent oligopeptide transporter PepT1. *J Physiol* **498** ( Pt 3):563-569.

Steffansen B, Lepist EI, Taub ME, Larsen BD, Frokjaer S and Lennernas H (1999) Stability, metabolism and transport of D-Asp(OBzl)-Ala--a model prodrug with affinity for the oligopeptide transporter. *Eur J Pharm Sci* **8**:67-73.

Sugawara M, Huang W, Fei YJ, Leibach FH, Ganapathy V and Ganapathy ME (2000) Transport of valganciclovir, a ganciclovir prodrug, via peptide transporters PEPT1 and PEPT2. *J Pharm Sci* **89**:781-789.

Swaan PW and Tukker JJ (1997) Molecular determinants of recognition for the intestinal peptide carrier. *J Pharm Sci* **86**:596-602.

Tamai I, Nakanishi T, Hayashi K, Terao T, Sai Y, Shiraga T, Miyamoto K, Takeda E, Higashida H and Tsuji A (1997) The predominant contribution of oligopeptide

transporter PepT1 to intestinal absorption of beta-lactam antibiotics in the rat small intestine. *J Pharm Pharmacol* **49**:796-801.

Tanaka H, Miyamoto KI, Morita K, Haga H, Segawa H, Shiraga T, Fujioka A, Kouda T, Taketani Y, Hisano S, Fukui Y, Kitagawa K and Takeda E (1998) Regulation of the PepT1 peptide transporter in the rat small intestine in response to 5-fluorouracil-induced injury. *Gastroenterology* **114**:714-723.

Tateoka R, Abe H, Miyauchi S, Shuto S, Matsuda A, Kobayashi M, Miyazaki K and Kamo N (2001) Significance of substrate hydrophobicity for recognition by an oligopeptide transporter (PEPT1). *Bioconjug Chem* **12**:485-492.

Terada T, Saito H, Mukai M and Inui KI (1996) Identification of the histidine residues involved in substrate recognition by a rat H<sup>+</sup>/peptide cotransporter, PEPT1. *FEBS Lett* **394**:196-200.

Terada T, Saito H, Sawada K, Hashimoto Y and Inui K (2000a) N-terminal halves of rat H<sup>+</sup>/peptide transporters are responsible for their substrate recognition. *Pharm Res* **17**:15-20.

Terada T, Sawada K, Irie M, Saito H, Hashimoto Y and Inui K (2000b) Structural requirements for determining the substrate affinity of peptide transporters PEPT1 and PEPT2. *Pflugers Arch* **440**:679-684.

Terada T, Sawada K, Saito H, Hashimoto Y and Inui K (1999) Functional characteristics of basolateral peptide transporter in the human intestinal cell line Caco-2. *Am J Physiol* **276**:G1435-1441.

Thamotharan M, Bawani SZ, Zhou X and Adibi SA (1998) Mechanism of dipeptide stimulation of its own transport in a human intestinal cell line. *Proc Assoc Am Physicians* **110**:361-368.

Thamotharan M, Bawani SZ, Zhou X and Adibi SA (1999a) Functional and molecular expression of intestinal oligopeptide transporter (Pept-1) after a brief fast. *Metabolism* **48**:681-684.

Thamotharan M, Bawani SZ, Zhou X and Adibi SA (1999b) Hormonal regulation of oligopeptide transporter pept-1 in a human intestinal cell line. *Am J Physiol* **276**:C821-826.

Thamotharan M, Lombardo YB, Bawani SZ and Adibi SA (1997) An active mechanism for completion of the final stage of protein degradation in the liver, lysosomal transport of dipeptides. *J Biol Chem* **272**:11786-11790.



- Thwaites DT, Brown CD, Hirst BH and Simmons NL (1993) Transepithelial glycylsarcosine transport in intestinal Caco-2 cells mediated by expression of H(+)-coupled carriers at both apical and basal membranes. *J Biol Chem* **268**:7640-7642.
- Uchiyama T, Kulkarni AA, Davies DL and Lee VH (2003) Biophysical evidence for His57 as a proton-binding site in the mammalian intestinal transporter hPepT1. *Pharm Res* **20**:1911-1916.
- Urtti A, Johns SJ and Sadee W (2001) Genomic structure of proton-coupled oligopeptide transporter hPEPT1 and pH-sensing regulatory splice variant. *AAPS PharmSci* **3**:E6.
- Vig BS, Stouch TR, Timoszyk JK, Quan Y, Wall DA, Smith RL and Faria TN (2006) Human PEPT1 pharmacophore distinguishes between dipeptide transport and binding. *J Med Chem* **49**:3636-3644.
- Walker D, Thwaites DT, Simmons NL, Gilbert HJ and Hirst BH (1998) Substrate upregulation of the human small intestinal peptide transporter, hPepT1. *J Physiol* **507** (Pt 3):697-706.
- Watanabe K, Terada K, Jinriki T and Sato J (2004) Effect of insulin on cephalixin uptake and transepithelial transport in the human intestinal cell line Caco-2. *Eur J Pharm Sci* **21**:87-95.
- Weinstein L, Weiss JE and Gillespie RW (1938) The Influence Of Diet On The L. Acidophilus Content And H-Ion Concentration Of The Intestine. *J Bacteriol* **35**:515-525.
- Winne D (1976) Unstirred layer thickness in perfused rat jejunum in vivo. *Experientia* **32**:1278-1279.
- Xiang J, Hu Y, Smith DE and Keep RF (2006) PEPT2-mediated transport of 5-aminolevulinic acid and carnosine in astrocytes. *Brain Res*.
- Yamashita T, Shimada S, Guo W, Sato K, Kohmura E, Hayakawa T, Takagi T and Tohyama M (1997) Cloning and functional expression of a brain peptide/histidine transporter. *J Biol Chem* **272**:10205-10211.
- Yeung AK, Basu SK, Wu SK, Chu C, Okamoto CT, Hamm-Alvarez SF, von Grafenstein H, Shen WC, Kim KJ, Bolger MB, Haworth IS, Ann DK and Lee VH (1998) Molecular identification of a role for tyrosine 167 in the function of the human intestinal proton-coupled dipeptide transporter (hPepT1). *Biochem Biophys Res Commun* **250**:103-107.

Zhang EY, Fu DJ, Pak YA, Stewart T, Mukhopadhyay N, Wrighton SA and Hillgren KM (2004) Genetic polymorphisms in human proton-dependent dipeptide transporter PEPT1: implications for the functional role of Pro586. *J Pharmacol Exp Ther* **310**:437-445.

Zhou X, Thamocharan M, Gangopadhyay A, Serdikoff C and Adibi SA (2000) Characterization of an oligopeptide transporter in renal lysosomes. *Biochim Biophys Acta* **1466**:372-378.

Ziegler TR, Fernandez-Estivariz C, Gu LH, Bazargan N, Umeakunne K, Wallace TM, Diaz EE, Rosado KE, Pascal RR, Galloway JR, Wilcox JN and Leader LM (2002) Distribution of the H<sup>+</sup>/peptide transporter PepT1 in human intestine: up-regulated expression in the colonic mucosa of patients with short-bowel syndrome. *Am J Clin Nutr* **75**:922-930.

## Chapter 3

# TRANSPORT MECHANISMS OF CARNOSINE IN SKPT CELLS: CONTRIBUTION OF APICAL AND BASOLATERAL MEMBRANE TRANSPORTERS

### ABSTRACT

**Purpose.** The aim of this study was to investigate the transport properties of carnosine in kidney using SKPT cell cultures as a model of proximal tubular transport, and to isolate the functional activities of renal apical and basolateral transporters in this process.

**Methods.** The membrane transport kinetics of 10  $\mu\text{M}$  [ $^3\text{H}$ ]carnosine was studied in SKPT cells as a function of time, pH, potential inhibitors and substrate concentration. A cellular compartment model was constructed in which the influx, efflux and transepithelial clearances of carnosine were determined. Peptide transporter expression was probed by RT-PCR.

**Results.** Carnosine uptake was 15-fold greater from the apical than basolateral surface of SKPT cells. However, the apical-to-basolateral transepithelial transport of carnosine was severely rate-limited by its cellular efflux across the basolateral membrane. The high-affinity, proton-dependence, concentration-dependence and inhibitor specificity of carnosine supports the contention that PEPT2 is responsible for its apical uptake. In

contrast, the basolateral transporter is saturable, inhibited by PEPT2 substrates but non-concentrative, thereby, suggesting a facilitative carrier.

**Conclusions.** Carnosine is expected to have a substantial cellular accumulation in kidney but minimal tubular reabsorption in blood because of its high influx clearance across apical membranes by PEPT2 and very low efflux clearance across basolateral membranes.

**Key Words:** PEPT2; SKPT; carnosine; transport mechanisms; cellular kinetics

## INTRODUCTION

Proton-coupled oligopeptide transporters (POTs) are membrane proteins that translocate various small peptides and peptide-like drugs across the biological membrane via an inwardly-directed proton gradient and negative membrane potential. At present, four members of the POT family, namely PEPT1, PEPT2, PHT1 and PHT2, have been identified in mammals (Herrera-Ruiz and Knipp, 2003; Daniel and Kottra, 2004). POTs have significant physiological roles in the absorption and reabsorption of peptide-bound amino nitrogen as well as pharmacological roles in drug absorption and disposition (e.g.,  $\beta$ -lactam antibiotics, angiotensin-converting enzyme inhibitors, renin inhibitors, bestatin and valacyclovir). PEPT1, cloned from a rabbit small intestine cDNA library (Fei et al., 1994), has been characterized as a high-capacity, low-affinity transporter. In addition to its expression in apical membranes of S1 segments in proximal tubule (i.e., kidney cortex), PEPT1 is highly expressed in apical membranes of small intestine (Shen et al., 1999; Groneberg et al., 2001). PEPT2, cloned from a human kidney cDNA library (Liu et al., 1995), is a low-capacity, high-affinity transporter that is primarily localized in the brush border of S3 segments in proximal tubule (i.e., outer stripe of outer medullar) (Liu et al., 1995; Shen et al., 1999; Rubio-Aliaga et al., 2000), as well as in brain, choroid plexus, eye, lung and mammary gland (Groneberg et al., 2002). In spite of the sequential expression of PEPT1 and PEPT2 in renal proximal tubules, studies have definitively shown that PEPT2 accounts for the vast majority of reabsorption for the model dipeptide glycylsarcosine (GlySar) and the  $\beta$ -lactam antibiotic cefadroxil in kidney (Takahashi et al., 1998; Inui et al., 2000; Ocheltree et al., 2005; Shen et al., 2007).

Two additional peptide transporters, PHT1 (Yamashita et al., 1997) and PHT2 (Sakata et al., 2001), have been cloned from a rat brain cDNA library. Unlike PEPT1 and PEPT2, they transport a single amino acid, L-histidine, in addition to the proton-stimulated transport of di/tripeptides. While PHT1 mRNA is abundantly expressed in rat brain and eye, PHT2 mRNA is abundant in rat lung, spleen, thymus and immunocytes. Unlike other POT family members, PHT2 protein was found subcellularly in the lysosomes of transfected cell lines rather than in the plasma membrane, as demonstrated by light and electron-microscopic analyses (Sakata et al., 2001). Compared to PEPT1 and PEPT2, relatively little is known about PHT1 and PHT2 with respect to their physiological roles, substrate specificities, precise localization and directionality of transport.

Functional studies have indicated the presence of distinct basolateral peptide transporters in the small intestine (Terada et al., 1999) and kidney (Terada et al., 2000). In this regard, the intestinal basolateral peptide transporter, expressed in the Caco-2 cells, was suggested as a facilitative efflux transporter that assists in the efficient absorption of small peptides/mimetics by mediating their extrusion from cell to blood (Terada et al., 1999; Sawada et al., 2001; Irie et al., 2004). In contrast, the renal basolateral peptide transporter, expressed in MDCK cells, was suggested as an influx transporter facilitating the clearance of small peptides/mimetics from the blood circulation (Sawada et al., 2001). Thus far, none of these basolateral peptide transporters have been cloned and, hence, they are not well characterized compared to current members of the POT family.

Carnosine ( $\beta$ -alanyl-L-histidine) is a naturally-occurring dipeptide that is highly concentrated in skeletal muscle and brain. Besides being an endogenous substrate,

carnosine is also taken exogenously as a dietary supplement for its antioxidant and free radical scavenging properties (Aruoma et al., 1989; Hartman et al., 1990). In the body, carnosine prevents glycation and the cross-linking of proteins by deleterious aldehydes and ketones (Hipkiss et al., 1998), further protecting the cell against oxidative damage. The potential benefit of carnosine is limited by its susceptibility to hydrolysis by tissue and serum carnosinase, but not  $\alpha$ -peptidase (Hipkiss, 1998), resulting in degradation to its constituent amino acids (i.e.,  $\beta$ -alanine and L-histidine). Pharmacologically, carnosine has some renoprotective effects including acting as a protective factor in diabetic nephropathy (Janssen et al., 2005) and preventing ischemia-induced renal injury (Fujii et al., 2003; Fujii et al., 2005; Kurata et al., 2006). Carnosine is transported by all of the POTs (Yamashita et al., 1997; Sakata et al., 2001; Son et al., 2004; Teuscher et al., 2004; Bhardwaj et al., 2006).

Even though carnosine has significant pharmacological importance in the kidney, the renal disposition of this dipeptide has not been elucidated. Therefore, the aim of this study was to investigate the transport properties of carnosine in kidney using SKPT cell cultures as a model of proximal tubular transport, and to isolate the functional activities of renal apical and basolateral transporters in this process.

## MATERIALS AND METHODS

### Reagents

[<sup>3</sup>H]Carnosine (10 Ci/mmol) and [<sup>14</sup>C]D-mannitol (53 mCi/mmol) were purchased from Moravek Biochemicals (Brea, CA). Primers for the PCR analyses were obtained from Invitrogen Life Technologies (Carlsbad, CA). The epithelial cell line SKPT-0193 C1.2, established by SV40 transformation of isolated rat kidney proximal tubule cells, was kindly provided by Dr. Ulrich Hopfer (Case Western Reserve University, Cleveland, OH). All other chemicals were from standard sources and were of the highest quality available.

### Cell Cultures

SKPT cells were grown on 75 cm<sup>2</sup> cell culture flasks and cultured in 1:1 DMEM (without glucose)/HAM'S F12 medium supplemented with 5% fetal bovine serum, 5 µg/ml apotransferrin, 5 µg/ml insulin, 4 µg/ml dexamethasone, 10 ng/ml epidermal growth factor, 15 mM HEPES, 0.06% NaHCO<sub>3</sub>, 50 µM ascorbic acid, 20 nM selenium and 1% penicillin G (100 unit/ml)/streptomycin (100 µg/ml). As described previously (Shu et al., 2001), cells were subcultured every 3-5 days by treatment with 0.05% trypsin and 0.53 mM EDTA at 37°C. SKPT cells were seeded on collagen-coated (5 µg/cm<sup>2</sup>) 12-transwell filter inserts (12 mm diameter, 0.4 µm pore size) at 10<sup>5</sup> cells /well density (10<sup>5</sup> cell /cm<sup>2</sup>), and the culture medium was changed every other day. At 24 hr prior to experimentation, antibiotics were removed from the culture medium. SKPT cells were



used 4 days after the initial seeding. Transepithelial electrical resistance was measured prior to the experiments to ensure the integrity of cell monolayers.

### **Reverse Transcription-Polymerase Chain Reaction (RT-PCR) Analyses**

RT-PCR was used to identify the expression of specific POT mRNA in SKPT cells. In brief, total RNA was isolated from SKPT cells using an RNeasy Mini Kit (Qiagen, Valencia, CA). The RNA was then reverse-transcribed in a 40  $\mu$ l reaction mixture containing 200 U of Moloney murine leukemia virus reverse transcriptase and random primers. cDNA was amplified with specific primers for all four oligopeptide transporters by PCR. The primers were designed using the Vector NTI program (Invitrogen, Carlsbad, CA), and PCR was performed in a 60- $\mu$ L reaction mixture containing 2 U of *Taq* DNA polymerase, 4 pmol each of the 5' and 3' primers for each POT, 0.2  $\mu$ g of cDNA sample, 1.5 mM MgCl<sub>2</sub>, and 0.5 mM deoxytriphosphate nucleotide mixture. Glyceraldehyde 3-phosphate dehydrogenase (GAPDH) was used as a control for PCR analyses. The positive controls for oligopeptide transporters were rat small intestine (PEPT1), rat kidney (PEPT2), and rat brain (PHT1 and PHT2). The amplified products were separated on a 1.5 % agarose gel and visualized with ethidium bromide. Primers and PCR conditions for each POT are listed in the supplementary material (Table 3.1).

### **Carnosine Intracellular Accumulation and Transepithelial Transport Studies**

The uptake buffer consisted of 25 mM MES/Tris (pH 6.0) or 25 mM HEPES/Tris (pH 7.4), each containing 140 mM NaCl, 5.4 mM KCl, 1.8 mM CaCl<sub>2</sub>, 0.8 mM MgSO<sub>4</sub> and 5 mM glucose. For intracellular accumulation and transepithelial transport

experiments, the cell monolayers were washed and preincubated apically with 0.4 ml of pH 6.0 buffer and basolaterally with 1.2 ml of pH 7.4 buffer for 10 min at 37°C. The buffers were then removed and fresh buffer (0.4 ml pH 6.0 or 1.2 ml pH 7.4 containing [<sup>3</sup>H]carnosine and [<sup>14</sup>C]mannitol; 10 μM each) was added to the apical or basolateral compartments, respectively, in the absence and presence of potential inhibitors. Control buffer of 1.2 ml pH 7.4 or 0.4 ml pH 6.0 was added to the opposite compartment (i.e., no carnosine, mannitol or inhibitor). Cells were then incubated for the indicated length of time at 37°C. For transepithelial flux experiments, a 100-μl aliquot was collected from the opposite compartment from where drug was placed, and the radioactivity counted. For intracellular accumulation experiments, media were aspirated from both compartments and the monolayers were then washed 4 times from both sides with ice-cold buffer. The filters with monolayers were detached from the chamber, placed in a scintillation vial, and the cells were solubilized with 0.2 M NaOH and 1% SDS. Radioactivity was measured in solubilized cells (and buffer) with a dual-channel liquid scintillation counter (Beckman LS 6000 SC; Beckman Coulter Inc., Fullerton, CA). Protein concentrations were measured using the Bio-Rad DC protein assay (Bio-Rad Laboratories, Hercules, CA) with bovine serum albumin as the standard. Mannitol was used to correct the uptake data of carnosine due to filter binding and extracellular content (Teuscher et al., 2000; Teuscher et al., 2004), as well as the transepithelial transport of carnosine due to paracellular flux (Shu et al., 2002).

### **Efflux Studies**

SKPT monolayers were loaded by incubating the cells apically with [<sup>3</sup>H]carnosine and [<sup>14</sup>C]mannitol (10 μM each) for 2 hr at 37°C. Following incubation, monolayers

were washed four times from both sides with ice-cold buffer (no substrate present). The monolayers were then incubated at 37°C with control buffer in both compartments (i.e., 0.4 ml of pH 6.0 buffer in the apical side and 1.2 ml of pH 7.4 buffer in the basolateral side). At specified times, 100- $\mu$ l and 300- $\mu$ l aliquots were taken from the apical and basolateral compartments, respectively, and replaced with fresh buffer. Radioactivity was measured in the buffer samples with a dual-channel liquid scintillation counter, and efflux was expressed as a percentage relative to carnosine's initial concentration in cells after the 2-hr loading period.

### **Substrate Stability Studies**

Carnosine stability was evaluated in the apical, basolateral and intracellular compartments of SKPT cells. Following apical or basolateral incubations of [<sup>3</sup>H]carnosine (10  $\mu$ M) for 5, 10, 15, 60, 120, 180 and 300 min at 37°C, media were collected from the donor and receiver sides for analysis. The monolayers were washed four times with ice-cold buffer, and the filters with monolayers were detached from the chamber. The cells were mixed with 0.5 ml of Milli-Q water and then lysed by sonication for 30 sec x 5 times. An equal volume of acetonitrile was added to the cell lysates, vortexed for 5 sec, and centrifuged at 14,000 g for 10 min at 4°C. Cell supernatants were concentrated under cryovacuum (SpeedVac concentrator SVC 200H with Refrigerated Condensation Trap RT 4104, Savant Instrument Inc, Farmingdale, NY) and analyzed, along with buffer samples, by high-performance liquid chromatography (Model 515 Pump, Water, Milford, MA) with radiochromatography detection (Flo-One 500TR, PerkinElmer Life and Analytical Sciences, Boston, MA). Sample components were separated using a reversed-phase column (Supelco Discovery® C-18, 5  $\mu$ m, 250 cm

× 4.6 mm, Supelco Park, Bellefonte, PA) subjected to a mobile phase of 0.1 M NaH<sub>2</sub>PO<sub>4</sub> and 0.075 % heptafluorobutyric acid, pumped isocratically at 1 ml /min. Retention times for histidine and carnosine were 4.4 min and 7.9 min, respectively, under ambient conditions. Carnosine stability was determined by its recovery and the appearance of histidine following the specified incubation periods.

### **Kinetic Analyses**

The influx and efflux clearances of carnosine across SKPT cell membranes are depicted by the three-compartment model in Fig. 3.1A. Variations in the amount of carnosine with time are described in each compartment according to the following mass balance equations (Sun and Pang, 2008):

$$\frac{dX_A}{dt} = CL_{CA} \cdot C_C - CL_{AC} \cdot C_A \quad (1)$$

$$\frac{dX_B}{dt} = CL_{CB} \cdot C_C - CL_{BC} \cdot C_B \quad (2)$$

$$\frac{dX_C}{dt} = CL_{AC} \cdot C_A + CL_{BC} \cdot C_B - (CL_{CA} + CL_{CB}) \cdot C_C \quad (3)$$

where X<sub>A</sub>, X<sub>B</sub> and X<sub>C</sub> (pmol/mg protein) are the amounts of carnosine, respectively, in the apical, basolateral and cellular compartments; C<sub>A</sub>, C<sub>B</sub> and C<sub>C</sub> (pmol/μl) are the respective concentrations of carnosine in the apical, basolateral and cellular compartments; CL<sub>AC</sub> and CL<sub>BC</sub> (μl/min/mg protein) represent the influx clearances from the apical and basolateral compartments, respectively, to the cellular compartment; and

$CL_{CA}$  and  $CL_{CB}$  represent the respective efflux clearances from the cellular compartment to the apical and basolateral compartments. The transepithelial transport of carnosine is depicted in Fig. 3.1B and can be described by:

$$\frac{dX_A}{dt} = CL_{BA} \cdot C_B \quad \text{B-to-A directional transport} \quad (4)$$

$$\frac{dX_B}{dt} = CL_{AB} \cdot C_A \quad \text{A-to-B directional transport} \quad (5)$$

where  $CL_{AB}$  and  $CL_{BA}$  represent the transcellular clearances of carnosine from the apical to basolateral compartment and from the basolateral to apical compartment, respectively. Finally, the transcellular clearance can be described by:

$$CL_{AB} = CL_{AC} \cdot f_{efflux.B} \quad (6)$$

$$CL_{BA} = CL_{BC} \cdot f_{efflux.A} \quad (7)$$

where  $f_{efflux.A}$  and  $f_{efflux.B}$  represent the fraction of carnosine effluxed from the cellular compartment to the apical and basolateral compartments, respectively, at steady state.

A Michaelis-Menten model was used to fit the concentration-dependent uptake data of carnosine, where  $V$  is the initial uptake rate,  $V_{max}$  is the maximal rate of saturable uptake,  $K_m$  is the Michaelis constant, and  $S$  is the substrate concentration (Eq. 8). The unknown parameters (i.e.,  $V_{max}$  and  $K_m$ ) were determined by nonlinear regression analysis (GraphPad Prism v4.0; GraphPad Software, Inc. San Diego, CA) and a weighting factor of unity. The quality of fit was determined by evaluating the coefficient of determination ( $r^2$ ), the standard error of parameter estimates, and the residual plots.

$$V = \frac{V_{\max} \cdot S}{K_m + S} \quad (8)$$

While other transport models were attempted (i.e., saturable component plus linear term; two saturable components), they did not fit the data as well as a saturable component alone.

### **Statistical Analyses**

All data were reported as mean  $\pm$  SE. Cellular uptakes of carnosine were standardized for the total amount of protein (mg) in SKPT cells. Statistical differences were determined between groups by analysis of variance followed by Dunnett's test for pairwise comparisons with the control group (GraphPad Prism, v4.0; GraphPad Software, Inc., La Jolla, CA). A probability of  $p \leq 0.05$  was considered significant.

## **RESULTS**

### **RT-PCR Analyses of POT Expression in SKPT Cells**

Specific POT transcripts were sought in SKPT cells and kidney lysates (Fig. 3.2), while intestinal lysates served as a positive control for PEPT1 mRNA and brain lysates served as a positive control for PHT1 or PHT2 mRNA. Although kidney lysates expressed all four members of the POT family, only PEPT2 and PHT1 transcripts were expressed in SKPT cells. GAPDH, which served as a housekeeper gene, was strongly expressed in all samples. Given the predominant role of PEPT2 in renal reabsorption (Takahashi et al., 1998; Inui et al., 2000; Ocheltree et al., 2005; Shen et al., 2007), the presence of PEPT2 mRNA in SKPT cells suggests that this cell line was a good model to study the proximal tubular transport of peptides (e.g., carnosine) in kidney. The presence of PHT1 mRNA in SKPT cells also allows us to evaluate whether this peptide-histidine transporter has a functional role in the disposition of small peptides in kidney.

### **Time Course of Carnosine Intracellular Accumulation and Transepithelial Transport**

As observed Fig. 3.3A, the apical uptake of carnosine was substantially greater than its uptake from the basolateral surface of SKPT cell monolayers ( $\approx$  15-fold). It was also observed that carnosine uptake was linear for 60 min at the apical surface and for 30 min at the basolateral surface. As a result, initial rates were determined at 15 min for both apical and basolateral uptakes in subsequent experiments. At 180-300 min, the

apical uptake of carnosine reached a plateau value of approximately 220 pmol/mg protein. Using the experimentally determined value for intracellular volume of SKPT cells (i.e.,  $2.0 \pm 0.1$   $\mu\text{l}/\text{mg}$  of protein, see appendix A), and given that the extracellular medium concentration of carnosine was 10  $\mu\text{M}$ , the intracellular to extracellular concentration ratio of carnosine was 11, indicating the presence of active uptake process(es) at the apical membrane (possibly PEPT2 and/or PHT1). However, when carnosine was introduced from the basolateral compartment, the uptake reached a plateau value of only 15 pmol/mg protein. This result translated into an intracellular to extracellular concentration ratio of only 0.8, indicating the absence of a concentrative mechanism for carnosine uptake at the basolateral membrane.

In contrast to its intracellular accumulation, the apical-to-basolateral transcellular flux of carnosine was smaller than its basolateral-to-apical transcellular flux ( $\approx$  2-fold) (Fig. 3.3B). This finding suggests that although carnosine preferentially accumulates in the cell from the apical surface, its basolateral efflux is very limited thereby driving carnosine back to the apical compartment. This aspect is further examined in the efflux studies below.

### **Efflux of Carnosine**

In order to test our interpretation of the transcellular transport data and to better understand the fate of carnosine once inside the cell, the efflux of carnosine was evaluated after 2 hr of apical preloading. As shown in Fig. 3.3C, about 40% of carnosine was effluxed from the cell to the apical compartment at 60 min and about 4% of cellular carnosine was effluxed to the basolateral compartment. When a single exponential term



was used to fit the efflux-time profile [i.e.,  $Y = Y_{ss} \cdot (1 - e^{-K_{eff} \cdot t})$ ], we found that 66% of carnosine was effluxed from the cellular to apical compartment while only 4.7% of carnosine was effluxed to the basolateral compartment at steady state (i.e.,  $f_{efflux.A} = 0.66$  and  $f_{efflux.B} = 0.047$ , respectively). This finding is in accordance with the transepithelial transport data, which suggested a very minimal efflux of carnosine across the basolateral membrane.

### **Kinetics Analysis of Carnosine Cellular Transport**

Based on the slopes of the transport versus time profiles depicted in Fig. 3.3B, the A-to-B transepithelial rate of carnosine was 1.99 pmol/min/mg protein while the B-to-A transepithelial rate of carnosine was 3.74 pmol/min/mg protein. Given that these studies were performed with 10  $\mu$ M concentrations in the donor compartment, and according to Eqs. 4 and 5, the transepithelial clearances were calculated as:  $CL_{AB} = 0.20$   $\mu$ l/min/mg and  $CL_{BA} = 0.37$   $\mu$ l/min/mg. With a knowledge of the fractional effluxes of carnosine to both apical and basolateral compartments (see efflux studies above), and the transepithelial clearances determined here, the influx clearances of carnosine were determined according to Eqs. 6 and 7, in which:  $CL_{AC} = 4.25$   $\mu$ l/min/mg and  $CL_{BC} = 0.57$   $\mu$ l/min/mg. Finally, the efflux clearances of carnosine were calculated according to Eqs. 1 and 2 (now that all other parameters are known), such that:  $CL_{CA} = 0.69$   $\mu$ l/min/mg and  $CL_{CB} = 0.018$   $\mu$ l/min/mg. All clearance values are summarized in the cellular models shown in Fig. 3.1.

### **Proton-Dependent Uptake of Carnosine**

To determine whether the uptake of carnosine was stimulated by an inwardly-directed proton gradient, we evaluated the uptake of carnosine from both membrane surfaces at various pH values. This was achieved by varying pH of the donor side from 5.5 to 7.4 while keeping the apical side at pH 6.0 for basolateral uptakes and the basolateral side at pH 7.4 for apical uptakes. As shown on Fig. 3.4A, the apical uptake of carnosine demonstrated a marked dependency on extracellular pH values and was maximal at pH 6.5, which is consistent with the proton-substrate symport characteristics of the PEPT2 and PHT1. In contrast, the basolateral uptake of carnosine (Fig 3.4B) was more insensitive to changes in external pH (maximal at pH 6.5;  $p > 0.05$  for all comparisons). Carnosine is a basic dipeptide with pKa values of 2.76, 6.78 and 9.36 (Nielsen et al., 2002). Therefore, as the pH of the environment increases from 5.5 to 7.4, carnosine becomes less basic (Fig. 3.4C). Thus, at pH 5.5 carnosine is 95% ionized ( $\text{NH}_3^+$ ), at pH 6.5 carnosine is 65% ionized ( $\text{NH}_3^+$ ), and at pH 7.4 carnosine is 15-20% ionized ( $\text{NH}_3^+$ ). While higher pH values would favor an increased passive uptake of carnosine, the PEPT2-mediated of dipeptide is not favored due to a reduction in proton motive force. Moreover, pH may also affect the protonation state of the peptide transporter protein. The multiple influences of pH, along with membrane potential, should be considered when drawing conclusions about peptide transporter activity.

### **Effect of Potential Inhibitors**

Specificity of carnosine transport at the apical and basolateral membranes of SKPT cells was evaluated by co-incubating the substrate with potential inhibitors. In particular, the PEPT2-mediated uptake of carnosine was probed by performing studies in the absence and presence of GlySar, while the PHT1-mediated uptake of carnosine was

probed with histidine. As shown in Fig. 3.5A, the apical uptake of carnosine was unaffected by 1, 2 and 5 mM of histidine (a potent inhibitor of PHT1). In contrast, 1 and 2 mM of GlySar (a classic inhibitor of PEPT2) reduced the apical uptake of carnosine by 90%. Self-inhibition experiments revealed that 1 and 2 mM of unlabeled substrate inhibited the apical uptake of radiolabeled carnosine by 96%. At the basolateral membrane, carnosine uptake was unaffected by 1 mM of histidine but reduced by 90-99% in the presence of 1 mM of GlySar, unlabeled carnosine (self-inhibition), or cefadroxil (Fig. 3.5B).

### **Concentration-Dependent Uptake of Carnosine**

The concentration dependency of carnosine was characterized at both the apical and basolateral surfaces of SKPT cells. At the apical membrane, carnosine uptake was saturable (Fig. 3.6A) with Michaelis-Menten parameters of  $V_{\max}=659\pm 27$  pmol/mg/15min and  $K_m=49\pm 8$   $\mu$ M. Carnosine was also found to have saturable transport kinetics at the basolateral membrane (Fig. 3.6B) where the  $V_{\max}=27.4\pm 1.3$  pmol/mg/15min and  $K_m=108\pm 10$   $\mu$ M. Linear transformations of the data, as shown in Woolf-Augustinsson-Hofstee plot inserts, suggest the involvement of a single specific transporter for the uptake of carnosine at each membrane. However, compared to the apical transporter (i.e., PEPT2), the basolateral transporter has a 24-fold lower capacity and a 2-fold lower affinity. The results are consistent with the previous cellular accumulation, transepithelial transport and pH-dependent findings, in which different transport systems appear to be involved for carnosine at the apical and basolateral membranes of SKPT cells.

### **Stability of Carnosine**

As shown in Fig. 3.7, carnosine remained intact in the donor compartment, whether introduced from the apical or basolateral side, for up to 300 min of incubation. However, there was some degradation of carnosine in the intracellular compartment after the first hour of incubation. In this regard, carnosine was > 94% intact for the first 15 min of incubation while being about 87% intact at 60 min and 81% intact at 300 min of incubation. Overall, these findings indicate that carnosine was mostly intact during the intracellular accumulation, transepithelial transport and efflux experiments, and completely stable for those experiments in which incubation times were only 15 min (i.e., carnosine  $\pm$  inhibitors, pH-dependent and concentration-dependent studies).

## DISCUSSION

Carnosine, a naturally-occurring dipeptide and dietary supplement, has been shown to have some renoprotective qualities (Fujii et al., 2003; Fujii et al., 2005; Janssen et al., 2005; Kurata et al., 2006) yet no studies have delineated its mechanism of transport in kidney. In the present study, several new findings were revealed with respect to the transport mechanisms of carnosine in SKPT cells. Specifically, we have demonstrated that: 1) PEPT2 is the only peptide transporter responsible for the apical uptake of carnosine; the basolateral transporter is saturable, inhibited by dipeptide/mimetic substrates but non-concentrative, thereby, suggesting a facilitative carrier, 2) PHT1 mRNA is expressed in rat kidney lysates and SKPT monolayers, however, this peptide/histidine transporter is functionally inactive at both the apical and basolateral membranes of the cell, and 3) the apical-to-basolateral transepithelial transport of carnosine is severely rate-limited by its cellular efflux across the basolateral membrane (i.e.,  $CL_{CB}/CL_{AC}$  ratio=0.004). In contrast, the basolateral-to-apical transepithelial transport of carnosine is rate-limited to a minor extent by its cellular influx at the basolateral membrane (i.e.,  $CL_{BC}/CL_{CA}$  ratio=0.8). Thus, the directionality of transcellular kinetics can more fully be appreciated by understanding all of the influx and efflux parameters for a given substrate in the cellular compartment model (Fig. 3.1).

Our findings regarding the influx and efflux clearances of carnosine in SKPT cells are in agreement with studies using GlySar as a model substrate in this cell line. In particular, Bravo et al. (Bravo et al., 2005) reported similar apical-to-basolateral and basolateral-to-apical fluxes of GlySar even though the apical uptake of dipeptide was

about 5x greater than its basolateral uptake in SKPT cells. In the study by Neumann et al. (Neumann et al., 2004) the transepithelial apical-to-basolateral flux of GlySar was only 28% higher than its reverse flux (i.e., basolateral to apical direction) in SKPT cells despite the apical uptake of GlySar being about 3.5x greater than its basolateral uptake. The values in our study were 2-fold and 12-fold, respectively, for the preferential basolateral-to-apical flux (Fig. 3.3B) and apical intracellular accumulation (Fig. 3.3A) of carnosine. To account for the anomaly between transcellular transport and apical uptake, Bravo et al. (Bravo et al., 2005) speculated that a low basolateral transport activity may limit the carrier-mediated transepithelial flux of GlySar in SKPT cells. Our kinetic analysis agrees with this assessment and has demonstrated that carnosine is effluxed at a much slower rate across the basolateral versus apical membrane of SKPT cells (Fig. 3.3C).

The efflux studies suggest that once carnosine enters the epithelial cells of kidney proximal tubule from the luminal side, the dipeptide accumulates substantially within the cell rather than being transported to the blood side. Carnosine may then recycle back to the luminal compartment. Our results show that carnosine has an 11-times greater concentration in SKPT cells as compared to medium and that its cell-to-apical efflux is about 10 times greater than the substrate's cell-to-basolateral efflux. We reported a similar finding for carnosine in rat choroid plexus primary cell cultures (Teuscher et al., 2004), where its intracellular to extracellular concentration ratio was approximately 135 to 1 and apical efflux was about 4 times greater than basolateral efflux.

The SKPT cell line, derived from rat kidney proximal tubule cells, has been used previously as a model system to study the mechanism of peptide/mimetic transport in

epithelial cells of kidney proximal tubule. In this regard, functional, Northern blot and immunoblot analyses have demonstrated conclusively that SKPT cells express the high-affinity, low-capacity (i.e., “renal”) peptide transporter PEPT2 but not PEPT1 (Brandsch et al., 1995; Ganapathy et al., 1995; Shu et al., 2001). Moreover, confocal laser scanning microscopy showed immunostaining of PEPT2 in the apical but not basolateral membrane (Bravo et al., 2004). The current study has corroborated these findings, but has also shown the functional activity of a renal basolateral peptide transporter in SKPT cells (Figs. 3.4B, 3.5B and 3.6B) and the presence of the peptide/histidine transporter PHT1 in this cell line as well as rat kidney lysates (Fig. 3.2). While several studies have reported on the accumulation of GlySar in SKPT cells (Brandsch et al., 1995; Ganapathy et al., 1995; Brandsch et al., 1997; Ganapathy et al., 1997; Ganapathy et al., 1998; Sugawara et al., 2000), only apical uptake was investigated and a non-physiologic, synthetic dipeptide was used as a model substrate. Moreover, the potential roles of the renal basolateral peptide transporter and PHT1 were not appreciated at that time and, as a result, studies were not appropriately designed to probe whether or not other peptide transporters might be involved in renal trafficking of peptides at the plasma membrane.

The high-affinity uptake of carnosine at the apical membrane of SKPT cells (i.e.,  $K_m=49 \mu\text{M}$ ) is comparable to the PEPT2-mediated uptake of carnosine in rat choroid plexus primary cell cultures ( $K_m=34 \mu\text{M}$ ) (Teuscher et al., 2004) and whole tissue ( $K_m=39 \mu\text{M}$ ) (Teuscher et al., 2001), and rat neonatal astrocytes ( $K_m=43 \mu\text{M}$ ) (Xiang et al., 2006). This finding, along with the proton-dependence, concentration-dependence and inhibitor specificity of carnosine in SKPT monolayers, supports the contention that PEPT2 is responsible for its uptake at the apical surface of these cells. On the other hand,

the saturable but non-concentrative uptake of carnosine at the basolateral membrane, along with its preferred uptake over efflux at this membrane (i.e.,  $CL_{BC}/CL_{CB}$  ratio=32), would suggest that the basolateral transporter of carnosine is facilitative in the inward direction. Based on functional experiments in MDCK cells, Inui and coworkers (Terada et al., 2000; Sawada et al., 2001; Terada and Inui, 2004) reported that the renal basolateral peptide transporter was distinct from that of known peptide transporters (i.e., PEPT1 and PEPT2) and the intestinal basolateral peptide transporter. They also suggested that the basolateral peptide transporter was facilitative and that it was involved in the cellular uptake, but not cellular efflux, of small peptides in the MDCK cell line. MDCK cells, however, display features of distal tubules or collecting ducts (Handler, 1986) as opposed to proximal tubules where peptide reabsorption occurs (Shen et al., 1999). Moreover, although MDCK cells express a proton-peptide cotransporter at the apical membrane, its kinetic characteristics are that of PEPT1 and not PEPT2 (Brandsch et al., 1995). As a result, the SKPT cell line appears to have greater relevance to peptide transport in kidney. Notwithstanding these differences in experimental model, the precise nature of the renal basolateral transporter is uncertain as long as the clone of this protein remains unavailable.

In conclusion, despite the substantial cellular uptake of carnosine by PEPT2 at the apical membrane, this dipeptide is expected to have minimal tubular reabsorption into blood due to its very limited efflux across the basolateral membrane. This is important because, once inside the cell, carnosine may accumulate (as intact dipeptide or constituent amino acids) and have beneficial renoprotective properties. Although cellular uptake of carnosine at the renal basolateral transporter is fairly low when compared to



luminal uptake, secretion across the cell may be possible, although minor, because of its favorable efflux kinetics at the apical membrane. These findings elucidate, for the first time, a complete picture of the cellular kinetics of carnosine in SKPT cells and, more importantly, the influence of influx and efflux clearances on transepithelial transport. Future studies will be performed with carnosine in wild-type and PEPT2 null mice to further probe the *in vivo* pharmacokinetics and pharmacodynamics of this naturally-occurring dipeptide and dietary nutrient supplement. Moreover, a greater effort should be made on cloning and characterizing the renal basolateral peptide transporter.

**ABBREVIATIONS:** GAPDH, glyceraldehyde 3-phosphate dehydrogenase; GlySar, glycylsarcosine; PEPT, peptide transporter; PHT, peptide/histidine transporter; POTs, proton-coupled oligopeptide transporters; SKPT, spontaneous hypertensive rat kidney proximal tubule.

## FIGURES

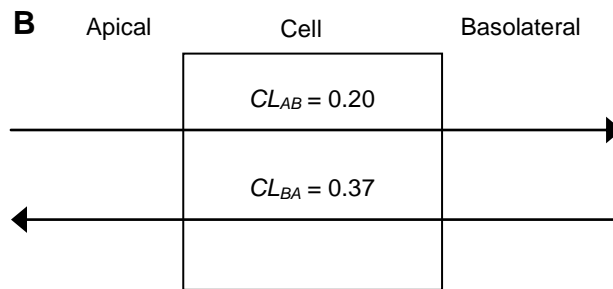
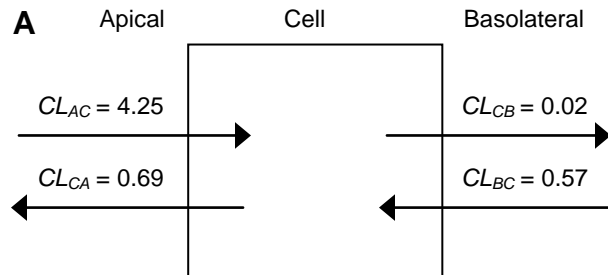


**Figure 3.1** Schematic representation of the SKPT cellular model in which  $CL_{AC}$  and  $CL_{BC}$  represent the influx clearances from the apical and basolateral compartments, respectively, while  $CL_{CA}$  and  $CL_{CB}$  represent the respective efflux clearances to the apical and basolateral compartments (A);  $CL_{AB}$  represents the apical-to-basolateral transepithelial clearance and  $CL_{BA}$  represents the basolateral-to-apical transepithelial clearance (B). The clearance values are those determined experimentally for carnosine in this study (units,  $\mu\text{l}/\text{mg}/\text{min}$ ).

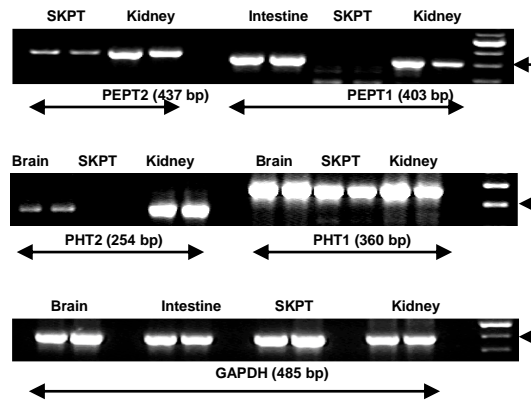


**Figure 3.2** RT-PCR analysis of peptide transporter mRNA in SKPT cells, and in kidney, intestine and brain lysates (4  $\mu$ g total RNA). Samples were separated on a 1.5% agarose gel, visualized with ethidium bromide, and screened for PEPT1 and PEPT2 transcripts (A) and for PHT1 and PHT2 transcripts (B). GAPDH controls for rat brain, intestine, kidney and SKPT cDNA samples are also displayed (C). In each gel, the right-hand lane is a 100 bp DNA ladder. The expected RT-PCR products are shown for each POT under the gel.

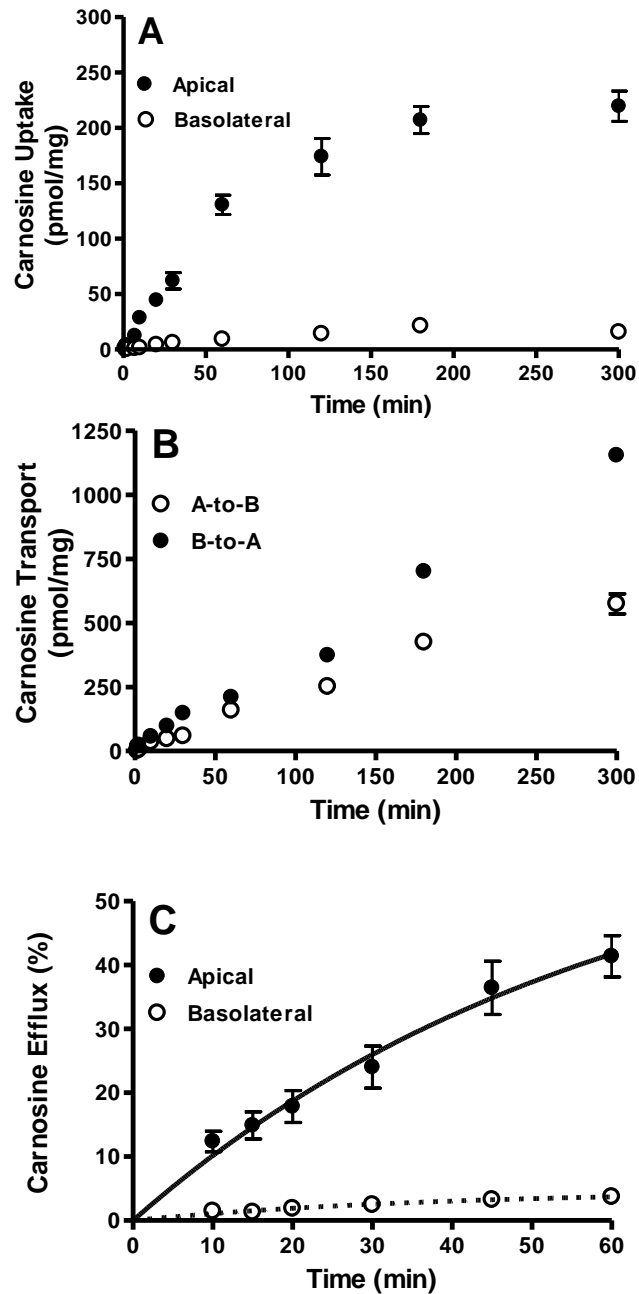


**Figure 3.3** Intracellular accumulation (A) and transcellular transport (B) of 10  $\mu\text{M}$  [ $^3\text{H}$ ]carnosine as a function of time in SKPT cell monolayers at 37°C. The cellular efflux (C) of [ $^3\text{H}$ ]carnosine was determined after preloading the cells from the apical side with 10  $\mu\text{M}$  carnosine for 2 hr at 37°C. For all experiments, the buffer pH was 6.0 in the apical compartment and 7.4 in the basolateral compartment. Data are expressed as mean  $\pm$  SE (n=3-5).

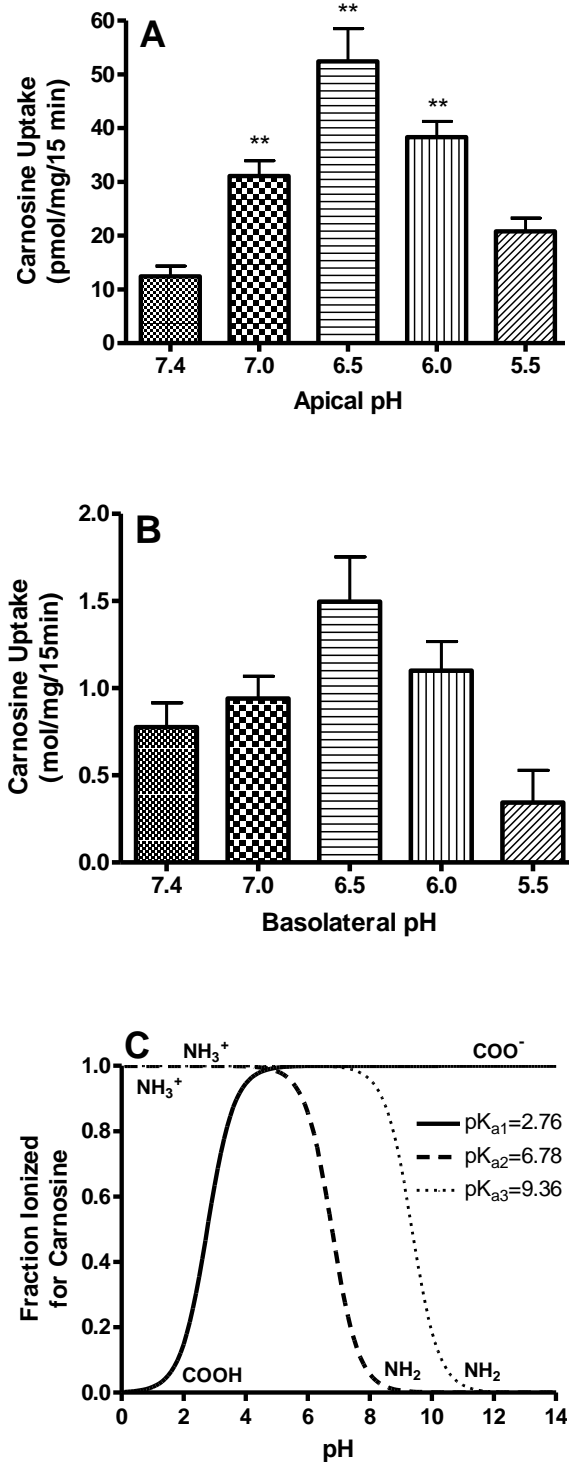


**Figure 3.4** Effect of pH on the 15-min uptake of 10  $\mu\text{M}$  [ $^3\text{H}$ ] carnosine in SKPT cell monolayers at 37°C from the apical (A) compartment (basolateral pH maintained at 7.4) and from the basolateral (B) compartment (apical pH maintained at 6.0). Data are expressed as mean  $\pm$  SE (n=3-6). \*\* p < 0.01, as compared to pH 7.4. Relationship between pH and fractional ionization of carnosine (C).

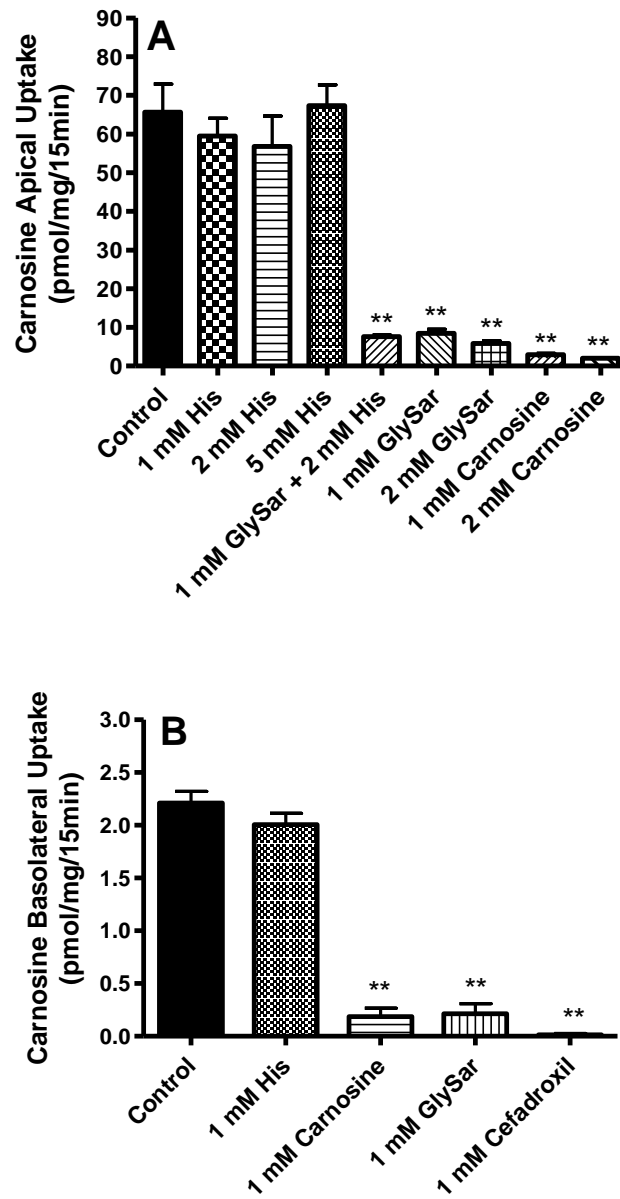


**Figure 3.5** Effect of potential inhibitors on the 15-min apical (A) and basolateral (B) uptake of carnosine in SKPT cell monolayers at 37°C. For all experiments, the buffer pH was 6.0 in the apical compartment and 7.4 in the basolateral compartment. Data are expressed as mean  $\pm$  SE (n=3-6). \*\* p < 0.01, as compared to control.

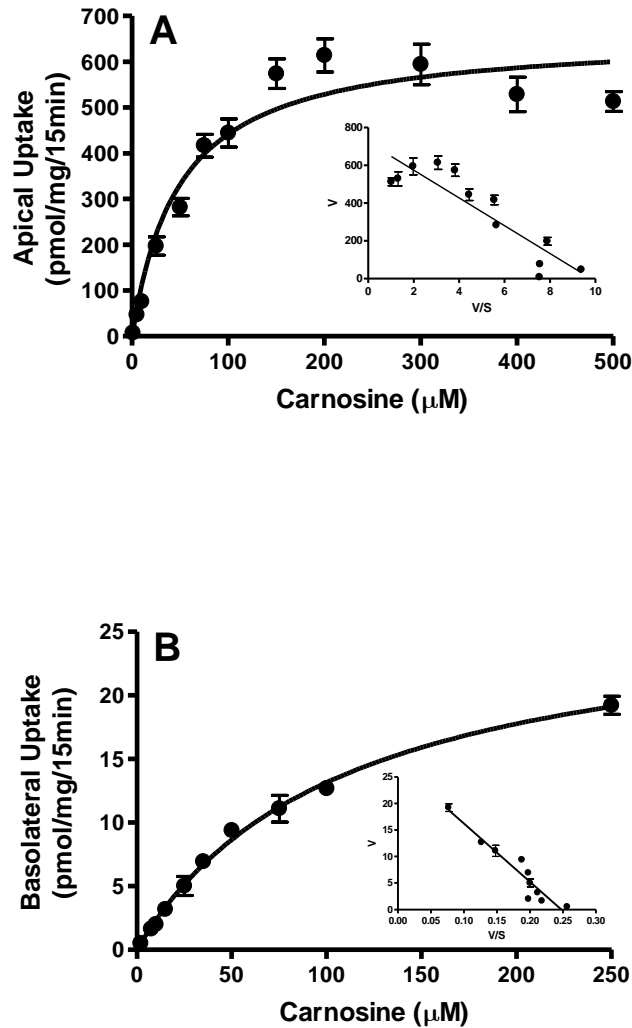


**Figure 3.6** Effect of concentration on the 15-min uptake of 1-500  $\mu\text{M}$  [ $^3\text{H}$ ]carnosine from the apical (A) and basolateral (B) sides of SKPT cell monolayers at 37°C. For all experiments, the buffer pH was 6.0 in the apical compartment and 7.4 in the basolateral compartment. Data are presented as mean  $\pm$  SE (n=3-6); the inset is a Woolf-Augustinsson-Hofstee plot of the transformed data (V, pmol/mg/15min versus V/S,  $\mu\text{l}/\text{mg}/15\text{min}$ ).



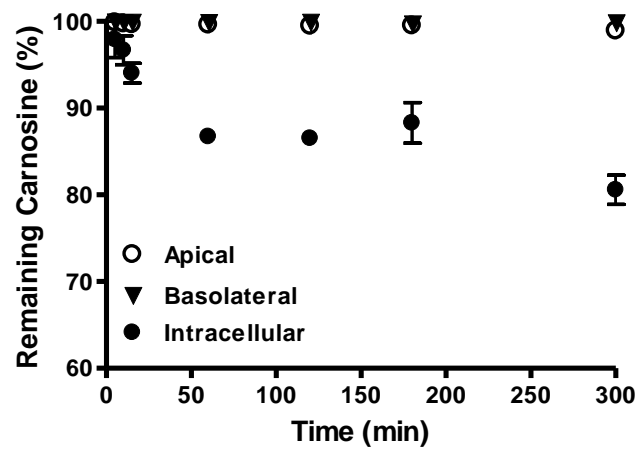


**Figure 3.7** Stability of carnosine in the apical, basolateral, and intracellular compartments of SKPT cell monolayers as a function of time (pH 6.0 buffer in apical side and pH 7.4 buffer in basolateral side). Data are presented as mean  $\pm$  SE (n=3).

**Table 3.1** PCR conditions for Proton-Coupled Oligopeptide Transporter and GAPDH

PEPT1	Sense:	GCCCTGATAGCCCTTGGTAC
	Antisense:	AGTCCAGCCAGTGGTTCCTC
PEPT2	Denaturing:	95°C for 2 min, 94°C for 1 min
	Annealing:	54°C for 45 sec
PHT1	Extension:	72°C for 1min
	Cycle #:	30
PEPT1	Sense:	TGAGTCTAATTGCTCTGGGAAC
	Antisense:	ATCTGCGATGAGATGCTTTG
PEPT2	Denaturing:	95°C for 2 min, 94°C for 1 min
	Annealing:	53°C for 45 sec
PHT2	Extension:	72°C for 1min
	Cycle #:	30
PHT1	Sense:	CGCTCGCGCTCTTTTCTCTG
	Antisense:	AGCAATGGCCACGCAGACTG
PHT2	Denaturing:	95°C for 2 min, 94°C for 1 min
	Annealing:	55°C for 45 sec
GAPDH	Extension:	72°C for 1min
	Cycle #:	34
PHT2	Sense:	TGCTGCTAGTGGAGATGCTG
	Antisense:	GATGGTGGTGGAGCAACAAGC
GAPDH	Denaturing:	95°C for 2 min, 94°C for 1 min
	Annealing:	53°C for 45 sec
GAPDH	Extension:	72°C for 1min
	Cycle #:	35
GAPDH	Sense:	CCAGTATGACTCTACCCACGG
	Antisense:	CAGGGATGATGTTCTGGGC
GAPDH	Denaturing:	95°C for 2 min, 94°C for 1 min
	Annealing:	54°C for 1 min
GAPDH	Extension:	72°C for 1.5 min
	Cycle #:	30

## REFERENCES

- Aruoma OI, Laughton MJ and Halliwell B (1989) Carnosine, homocarnosine and anserine: could they act as antioxidants in vivo? *Biochem J* **264**:863-869.
- Bhardwaj RK, Herrera-Ruiz D, Eltoukhy N, Saad M and Knipp GT (2006) The functional evaluation of human peptide/histidine transporter 1 (hPHT1) in transiently transfected COS-7 cells. *Eur J Pharm Sci* **27**:533-542.
- Brandsch M, Brandsch C, Ganapathy ME, Chew CS, Ganapathy V and Leibach FH (1997) Influence of proton and essential histidyl residues on the transport kinetics of the H<sup>+</sup>/peptide cotransport systems in intestine (PEPT 1) and kidney (PEPT 2). *Biochim Biophys Acta* **1324**:251-262.
- Brandsch M, Brandsch C, Prasad PD, Ganapathy V, Hopfer U and Leibach FH (1995) Identification of a renal cell line that constitutively expresses the kidney-specific high-affinity H<sup>+</sup>/peptide cotransporter. *FASEB J* **9**:1489-1496.
- Bravo SA, Nielsen CU, Amstrup J, Frokjaer S and Brodin B (2004) Epidermal growth factor decreases PEPT2 transport capacity and expression in the rat kidney proximal tubule cell line SKPT0193 cl.2. *Am J Physiol Renal Physiol* **286**:F385-393.
- Bravo SA, Nielsen CU, Frokjaer S and Brodin B (2005) Characterization of rPEPT2-mediated Gly-Sar transport parameters in the rat kidney proximal tubule cell line SKPT-0193 cl.2 cultured in basic growth media. *Mol Pharm* **2**:98-108.
- Daniel H and Kottra G (2004) The proton oligopeptide cotransporter family SLC15 in physiology and pharmacology. *Pflugers Arch* **447**:610-618.
- Fei YJ, Kanai Y, Nussberger S, Ganapathy V, Leibach FH, Romero MF, Singh SK, Boron WF and Hediger MA (1994) Expression cloning of a mammalian proton-coupled oligopeptide transporter. *Nature* **368**:563-566.
- Fujii T, Takaoka M, Muraoka T, Kurata H, Tsuruoka N, Ono H, Kiso Y, Tanaka T and Matsumura Y (2003) Preventive effect of L-carnosine on ischemia/reperfusion-induced acute renal failure in rats. *Eur J Pharmacol* **474**:261-267.
- Fujii T, Takaoka M, Tsuruoka N, Kiso Y, Tanaka T and Matsumura Y (2005) Dietary supplementation of L-carnosine prevents ischemia/reperfusion-induced renal injury in rats. *Biol Pharm Bull* **28**:361-363.

Ganapathy ME, Brandsch M, Prasad PD, Ganapathy V and Leibach FH (1995) Differential recognition of beta -lactam antibiotics by intestinal and renal peptide transporters, PEPT 1 and PEPT 2. *J Biol Chem* **270**:25672-25677.

Ganapathy ME, Huang W, Wang H, Ganapathy V and Leibach FH (1998) Valacyclovir: a substrate for the intestinal and renal peptide transporters PEPT1 and PEPT2. *Biochem Biophys Res Commun* **246**:470-475.

Ganapathy ME, Prasad PD, Mackenzie B, Ganapathy V and Leibach FH (1997) Interaction of anionic cephalosporins with the intestinal and renal peptide transporters PEPT 1 and PEPT 2. *Biochim Biophys Acta* **1324**:296-308.

Groneberg DA, Doring F, Eynott PR, Fischer A and Daniel H (2001) Intestinal peptide transport: ex vivo uptake studies and localization of peptide carrier PEPT1. *Am J Physiol Gastrointest Liver Physiol* **281**:G697-704.

Groneberg DA, Doring F, Theis S, Nickolaus M, Fischer A and Daniel H (2002) Peptide transport in the mammary gland: expression and distribution of PEPT2 mRNA and protein. *Am J Physiol Endocrinol Metab* **282**:E1172-1179.

Handler JS (1986) Studies of kidney cells in culture. *Kidney Int* **30**:208-215.

Hartman PE, Hartman Z and Ault KT (1990) Scavenging of singlet molecular oxygen by imidazole compounds: high and sustained activities of carboxy terminal histidine dipeptides and exceptional activity of imidazole-4-acetic acid. *Photochem Photobiol* **51**:59-66.

Herrera-Ruiz D and Knipp GT (2003) Current perspectives on established and putative mammalian oligopeptide transporters. *J Pharm Sci* **92**:691-714.

Hipkiss AR (1998) Carnosine, a protective, anti-ageing peptide? *Int J Biochem Cell Biol* **30**:863-868.

Hipkiss AR, Preston JE, Himsforth DT, Worthington VC, Keown M, Michaelis J, Lawrence J, Mateen A, Allende L, Eagles PA and Abbott NJ (1998) Pluripotent protective effects of carnosine, a naturally occurring dipeptide. *Ann N Y Acad Sci* **854**:37-53.

Inui K, Terada T, Masuda S and Saito H (2000) Physiological and pharmacological implications of peptide transporters, PEPT1 and PEPT2. *Nephrol Dial Transplant* **15 Suppl 6**:11-13.

Irie M, Terada T, Okuda M and Inui K (2004) Efflux properties of basolateral peptide transporter in human intestinal cell line Caco-2. *Pflugers Arch* **449**:186-194.

Janssen B, Hohenadel D, Brinkkoetter P, Peters V, Rind N, Fischer C, Rychlik I, Cerna M, Romzova M, de Heer E, Baelde H, Bakker SJ, Zirie M, Rondeau E, Mathieson P, Saleem MA, Meyer J, Koppel H, Sauerhoefer S, Bartram CR, Nawroth P, Hammes HP, Yard BA, Zschocke J and van der Woude FJ (2005) Carnosine as a protective factor in diabetic nephropathy: association with a leucine repeat of the carnosinase gene CNDP1. *Diabetes* **54**:2320-2327.

Kurata H, Fujii T, Tsutsui H, Katayama T, Ohkita M, Takaoka M, Tsuruoka N, Kiso Y, Ohno Y, Fujisawa Y, Shokoji T, Nishiyama A, Abe Y and Matsumura Y (2006) Renoprotective effects of l-carnosine on ischemia/reperfusion-induced renal injury in rats. *J Pharmacol Exp Ther* **319**:640-647.

Liu W, Liang R, Ramamoorthy S, Fei YJ, Ganapathy ME, Hediger MA, Ganapathy V and Leibach FH (1995) Molecular cloning of PEPT 2, a new member of the H<sup>+</sup>/peptide cotransporter family, from human kidney. *Biochim Biophys Acta* **1235**:461-466.

Neumann J, Bruch M, Gebauer S and Brandsch M (2004) Transport of the phosphonodipeptide alafosfalin by the H<sup>+</sup>/peptide cotransporters PEPT1 and PEPT2 in intestinal and renal epithelial cells. *Eur J Biochem* **271**:2012-2017.

Nielsen CU, Supuran CT, Scozzafava A, Frokjaer S, Steffansen B and Brodin B (2002) Transport characteristics of L-carnosine and the anticancer derivative 4-toluenesulfonylureido-carnosine in a human epithelial cell line. *Pharm Res* **19**:1337-1344.

Ocheltree SM, Shen H, Hu Y, Keep RF and Smith DE (2005) Role and relevance of peptide transporter 2 (PEPT2) in the kidney and choroid plexus: in vivo studies with glycylsarcosine in wild-type and PEPT2 knockout mice. *J Pharmacol Exp Ther* **315**:240-247.

Rubio-Aliaga I, Boll M and Daniel H (2000) Cloning and characterization of the gene encoding the mouse peptide transporter PEPT2. *Biochem Biophys Res Commun* **276**:734-741.

Sakata K, Yamashita T, Maeda M, Moriyama Y, Shimada S and Tohyama M (2001) Cloning of a lymphatic peptide/histidine transporter. *Biochem J* **356**:53-60.

Sawada K, Terada T, Saito H and Inui K (2001) Distinct transport characteristics of basolateral peptide transporters between MDCK and Caco-2 cells. *Pflugers Arch* **443**:31-37.

- Shen H, Ocheltree S, Hu Y, Keep R and Smith D (2007) Impact of Genetic Knockout of PEPT2 on Cefadroxil Pharmacokinetics, Renal Tubular Reabsorption and Brain Penetration in Mice. *Drug Metab Dispos*.
- Shen H, Smith DE, Yang T, Huang YG, Schnermann JB and Brosius FC, 3rd (1999) Localization of PEPT1 and PEPT2 proton-coupled oligopeptide transporter mRNA and protein in rat kidney. *Am J Physiol* **276**:F658-665.
- Shu C, Shen H, Hopfer U and Smith DE (2001) Mechanism of intestinal absorption and renal reabsorption of an orally active ace inhibitor: uptake and transport of fosinopril in cell cultures. *Drug Metab Dispos* **29**:1307-1315.
- Shu C, Shen H, Teuscher NS, Lorenzi PJ, Keep RF and Smith DE (2002) Role of PEPT2 in peptide/mimetic trafficking at the blood-cerebrospinal fluid barrier: studies in rat choroid plexus epithelial cells in primary culture. *J Pharmacol Exp Ther* **301**:820-829.
- Son DO, Satsu H, Kiso Y and Shimizu M (2004) Characterization of carnosine uptake and its physiological function in human intestinal epithelial Caco-2 cells. *Biofactors* **21**:395-398.
- Sugawara M, Huang W, Fei YJ, Leibach FH, Ganapathy V and Ganapathy ME (2000) Transport of valganciclovir, a ganciclovir prodrug, via peptide transporters PEPT1 and PEPT2. *J Pharm Sci* **89**:781-789.
- Sun H and Pang KS (2008) Permeability, transport, and metabolism of solutes in Caco-2 cell monolayers: a theoretical study. *Drug Metab Dispos* **36**:102-123.
- Takahashi K, Nakamura N, Terada T, Okano T, Futami T, Saito H and Inui KI (1998) Interaction of beta-lactam antibiotics with H<sup>+</sup>/peptide cotransporters in rat renal brush-border membranes. *J Pharmacol Exp Ther* **286**:1037-1042.
- Terada T and Inui K (2004) Peptide transporters: structure, function, regulation and application for drug delivery. *Curr Drug Metab* **5**:85-94.
- Terada T, Sawada K, Ito T, Saito H, Hashimoto Y and Inui K (2000) Functional expression of novel peptide transporter in renal basolateral membranes. *Am J Physiol Renal Physiol* **279**:F851-857.
- Terada T, Sawada K, Saito H, Hashimoto Y and Inui K (1999) Functional characteristics of basolateral peptide transporter in the human intestinal cell line Caco-2. *Am J Physiol* **276**:G1435-1441.

Teuscher NS, Keep RF and Smith DE (2001) PEPT2-mediated uptake of neuropeptides in rat choroid plexus. *Pharm Res* **18**:807-813.

Teuscher NS, Novotny A, Keep RF and Smith DE (2000) Functional evidence for presence of PEPT2 in rat choroid plexus: studies with glycylsarcosine. *J Pharmacol Exp Ther* **294**:494-499.

Teuscher NS, Shen H, Shu C, Xiang J, Keep RF and Smith DE (2004) Carnosine uptake in rat choroid plexus primary cell cultures and choroid plexus whole tissue from PEPT2 null mice. *J Neurochem* **89**:375-382.

Xiang J, Hu Y, Smith DE and Keep RF (2006) PEPT2-mediated transport of 5-aminolevulinic acid and carnosine in astrocytes. *Brain Res* **1122**:18-23.

Yamashita T, Shimada S, Guo W, Sato K, Kohmura E, Hayakawa T, Takagi T and Tohyama M (1997) Cloning and functional expression of a brain peptide/histidine transporter. *J Biol Chem* **272**:10205-10211.

## Chapter 4

### SIGNIFICANCE OF PEPT1 IN THE *IN SITU* INTESTINAL PERMEABILITY OF GLYCYLSARCOSINE IN WILD-TYPE AND PEPT1 KNOCKOUT MICE

#### ABSTRACT

**Purpose.** To define the *in situ* intestinal transport properties of glycylsarcosine (GlySar) in PEPT1<sup>+/+</sup> (wild-type) and PEPT1<sup>-/-</sup> (knockout) mice, and to delineate the relative importance of PEPT1 in the intestinal absorption of small peptides.

**Methods.** An *in situ* single-pass intestinal perfusion model was used to assess the effective permeability of GlySar in both wild-type and PEPT1 knockout mice. In particular, [<sup>3</sup>H]GlySar (10 μM) was perfused in 8 cm of proximal small intestine at a rate of 0.1 ml/min for 90 minute as a function of pH, potential inhibitors and substrate concentration. Permeability was calculated as:  $P_{\text{eff}} = -Q \cdot \ln(C_{\text{out}}/C_{\text{in}})/(2\pi RL)$ , after correcting for water flux with [<sup>14</sup>C]PEG 4000 (a nonabsorbable marker).

**Results.** Permeability of [<sup>3</sup>H]GlySar was dramatically reduced in PEPT1 knockout mice as compared to wild-type mice (>20-fold reduction; p<0.001). Further, the permeability of [<sup>3</sup>H]mannitol was not different between genotypes, demonstrating a lack of significant



change in the integrity of small intestinal epithelia in mice. GlySar uptake was found to be pH-stimulated in wild-type animals with a maximum permeability being observed at pH 5.5; no such pH effect was found in the PEPT1 knockout mice. Transport specificity was confirmed by evaluating the permeability of GlySar in the presence of potential inhibitors. In wild-type mice, GlySar permeability was significantly reduced by the dipeptides carnosine, GlySar and GlyPro, the ACE inhibitor captopril, the aminocephalosporin cefadroxil, and the antiviral prodrug valacyclovir ( $p < 0.01$ ). In contrast, the amino acids Gly and L-His, the active parent moiety acyclovir, and cefazolin (a cephalosporin lacking an  $\alpha$ -amino group) had no effect. Saturable kinetics was observed for GlySar in wild-type mice with a  $K_m$  value of about 10 mM.

**Conclusions.** PEPT1 is responsible for at least 90% of dipeptide uptake in the small intestine and exhibits low-affinity kinetics for GlySar, a finding that is consistent with previous *in vitro* studies. These results suggest that PEPT1 will play a crucial role in the uptake of dietary peptides, mimetics and peptide-like drugs.

## INTRODUCTION

Protein is an important part of our daily diet. A typical western diet usually contains 70-100 g protein per day. In addition to dietary protein, saliva and gastrointestinal tract secretions also contribute a significant amount of protein (~35g/day) (Ganapathy et al., 2006). In gastrointestinal lumen, the proteins are converted into large peptides by gastric and pancreatic proteases, which subsequently undergo further hydrolysis by various peptidases in the brush border membrane of intestinal epithelium into small peptides (80%) and free amino acids (20%) (Ganapathy et al., 2006). The final end products of protein digestion are absorbed into the enterocytes predominately in the form of di- and tripeptides as opposed to free amino acids (Matthews, 1975). Once inside the enterocytes, the majority of the di- and tripeptides undergo further hydrolysis into their constituent amino acids by cytoplasmic peptidases and exit the epithelial cells via different basolateral amino acid transporters. A small amount of small peptides that are resistant to cytoplasmic peptidases exit the enterocytes intact across the basolateral membrane through a basolateral peptide transporter that has yet to be cloned (Terada et al., 1999). Furthermore, there are regional differences in small intestinal epithelium in respect to their absorptive capacities for free amino acids and small peptides. While the proximal small intestine has a greater absorption capacity for small peptides compared to the distal small intestine, the distal intestine has a greater absorptive capacity for amino acids compared to the proximal small intestine (Matthews et al., 1971). In addition, the activities of brush border membrane peptidase are much higher in the ileum than in the jejunum (Silk et al., 1976), implying an increase in rate of appearance for single amino

acids as the luminal contents move along the intestine while the concentration of small peptides decrease.

Proton-coupled oligopeptide transporters (POTs) are membrane proteins that are responsible for translocating small peptides and peptidomimetics across a biological membrane via an inwardly-directed proton gradient and negative membrane potential. Thus far, four members of the POT superfamily, specifically PEPT1 (SLC15A1), PEPT2 (SLC15A2), PHT1 (SLCA4) and PHT2 (SLCA3), have been identified in mammals (Herrera-Ruiz and Knipp, 2003; Daniel and Kottra, 2004). PEPT1, being expressed on the apical membrane of enterocytes in small intestine (Ogihara et al., 1996; Walker et al., 1998; Groneberg et al., 2001), is believed to be the primary POT responsible for small intestinal absorption of di/tripeptides and peptide-like therapeutic agents. PEPT1 is characterized as a high-capacity, low-affinity transporter. It was first isolated and cloned from a rabbit intestine cDNA library (Fei et al., 1994), which subsequently lead to the cloning of PEPT1 from human (Liang et al., 1995), rat (Saito et al., 1995; Miyamoto et al., 1996) and mouse (Fei et al., 2000) intestinal cDNA libraries. It has been found that PEPT1 is highly homologous (~ 80%) across species (Liang et al., 1995; Miyamoto et al., 1996; Fei et al., 2000). PEPT1 is predicted to contain 12 transmembrane domains with both C and N terminals facing the cytosolic side, and protein sizes from 707 to 710 in amino acids depending on the species. The genomic organization of human PEPT1 shows high similarity with its mouse orthologue (Urtti et al., 2001). In addition, studies suggest that mouse and human have comparable intestinal expression patterns and levels, whereas PEPT1 expression level in the rat is several fold higher (Kim et al., 2007). PEPT1, in addition to transporting di- and tripeptides, also transports a number of

peptidomimetic therapeutic agents of different conformation, size, polarity and charge (e.g.,  $\beta$ -lactam antibiotics, ACE inhibitors, renin inhibitors, bestatin and antiviral prodrug valacyclovir), and acts as a vehicle for their effective intestinal absorption. Due to its broad substrate specificity and high capacity, PEPT1 is considered to be a very attractive target for drug delivery to improve the bioavailability of low permeable drugs.

Because of PEPT1's putative physiological and pharmacological importance in the absorption of di/tripeptides and peptidomimetic in the small intestine, PEPT1 is the most extensively studied transporter among the POT members. However, most of the previous studies were obtained from *in vitro* models such as cell transfection with PEPT1, Caco-2 cells, brush border membrane vesicles (BBMV) and Ussing chambers using non-physiological conditions that lack an intact blood supply. Moreover, both human and rat small intestine, in addition to expressing PEPT1, have been shown to express PHT1 and PHT2 transcripts (Herrera-Ruiz et al., 2001), where PHT1 is expressed in the villous epithelium of small intestine (Bhardwaj et al., 2006). Due to the existence of multiple peptide transport systems with overlapping substrate specificity in the small intestine, the previous *in situ* intestinal perfusion studies in rat do not isolate the individual role of a single gene product, PEPT1, in relation to other peptide transporters (or other processes). Thereby, by utilizing PEPT1 deficient mice, we can assess the relative role of PEPT1 under physiological conditions for the absorption of small peptides and peptidomimetics. Therefore, the aim of the present study is to delineate the relative importance of PEPT1 in the intestinal absorption of small peptides by defining the *in situ* intestinal transport properties of glycylsarcosine (GlySar) in the intestine of PEPT1<sup>+/+</sup> (wild-type) and PEPT1<sup>-/-</sup> (knockout) mice.

## MATERIALS AND METHODS

### Animals

Animals studies were carried out in accordance with the Guide for the Care and Use of Laboratory Animal as adopted and promulgated by the U.S National Institutes of Health. Gender matched 8-10 weeks old PEPT1<sup>+/+</sup> (wild-type) and PEPT1<sup>-/-</sup> (null) mice were used for all experiments. The mice were kept in temperature controlled environment with a 12-h light and 12-dark cycle, and received a standard diet and water *ad libitum* (Unit for Laboratory Animal Medicine, University of Michigan, Ann Arbor, MI).

### Chemicals

[<sup>3</sup>H]GlySar (0.5 Ci/mmol), [<sup>3</sup>H]metoprolol (64.6 Ci/mmol) and [<sup>14</sup>C]inulin (2 mCi/g) were purchased from Moravek Biochemicals and Radiochemicals (Brea, CA). [<sup>14</sup>C]PEG 4000 (1.5 mCi/g) and [<sup>3</sup>H]mannitol (20 Ci/mmol) were purchased from American Radiolabeled Compounds (St. Louis, MO). Unlabelled PEG 4000 was obtained from Mallinckrodt Baker, Inc (Phillipsburg, NJ). Acyclovir and valacyclovir were generous gifts from GlaxoSmithKline (Research Triangle Park, NC). All other chemicals were acquired from Sigma –Aldrich (St. Louis, MO).

### *In Situ* Single-Pass Intestinal Perfusion

Gender-matched mice of the genotype PEPT1<sup>+/+</sup> (wild-type) and PEPT1<sup>-/-</sup> (null) were fasted over night with free access to water prior to each experiment. Following anesthesia with sodium pentobarbital (40-60 mg/kg, I.P), surgery was performed on the animals on top of a heating pad to maintain the body temperature. Isopropyl alcohol was used to sterilize the abdominal area and a 1.5 cm of midline longitudinal incision was made to expose the small intestine. An 8 cm segment of the proximal jejunum (i.e., ~2 cm distal to the ligament of Treitz) was isolated followed by incisions at both the proximal and distal ends (8 cm separation) and the lumen was gently rinsed with warm isotonic saline solution. Glass cannulas (2.0 mm outer diameter) that were attached to rubber tubings were inserted at both ends of the jejunal segment and secured in place with silk sutures. Following the cannulation, the isolated intestinal segment was covered with saline-wetted gauze and parafilm to prevent dehydration. After the surgical procedure, the animals were transferred to a temperature-controlled Plexiglas perfusion chamber (31°C) to maintain the body temperature during the perfusion experiment. The inlet tubing was connected to a 10 ml syringe placed on a perfusion pump (Harvard Apparatus, Model 22, South Natick, MA) and the outlet tubing was placed in a collection vial. The perfusion solution contained 10 mM MES, 135 mM NaCl, 5 mM KCl and 0.01% (w/v) PEG 4000 at pH 6.5. [<sup>3</sup>H]GlySar (10 μM) was perfused through the proximal jejunal segment at a rate of 0.1 ml/min for 90 minutes as a function of pH, potential inhibitors, and substrate concentration. The exiting perfusate was collected at every 10 minutes for 90 minutes. A 100 μL aliquot of each collected sample was added a vial containing 5.5 ml of scintillation cocktail (Ecolite, MP Biomedicals, Solon, OH), and the samples were analyzed with a dual-channel liquid scintillation counter (Beckman LS

6000 SC; Beckman Coulter Inc., Fullerton, CA). Following the experiment, the animal were euthanized by pentobarbital overdose solution and disposed of according to the rules and regulations of Radiation Safety Service and ULAM. We used [<sup>3</sup>H]GlySar, a hydrolysis-resistant dipeptide, as our model compound. [<sup>14</sup>C]PEG 4000 was added to the perfusion buffer as a non-absorbable marker to measure water flux.

### Data Analysis

The effective permeability ( $P_{eff}$ ) was determined from the steady-state loss of drug from the perfusate as it flows through the intestine according to a complete radial mixing (parallel tube) model (Ho and Higuchi, 1974; Amidon et al., 1980) :

$$P_{eff}(cm/sec) = -\frac{Q * \ln (C_{out}/C_{in})}{2\pi RL} \quad (Eq. 1)$$

where  $Q$  is the perfusion rate (0.1 ml/min),  $R$  is the radius of the intestinal segment (0.1 cm) and  $L$  is the length of the perfused intestinal segment (8 cm). The  $C_{in}$  and  $C_{out}$  represent the inlet and outlet concentrations of drug.  $C_{out}$  was corrected for the water transport (flux) that occurs during the perfusion according to changes in concentration of non-absorbable compound PEG 4000:

$$C_{out} = \frac{C_{perfusate}}{PEG_{out}/PEG_{in}} \quad (Eq. 2)$$

where  $C_{perfusate}$  is the actual concentration of drug in the exiting perfusate, and  $PEG_{in}$  and  $PEG_{out}$  are the inlet and outlet concentrations of PEG 4000. Steady-state was assessed when the inlet over outlet concentrations of PEG 4000 approach a constant value, which occurred approximately 20-30 minutes after the start of perfusion.

Initially, PEG 4000 was used as the non-absorbable marker to correct for the water absorption/secretion during the mouse intestinal perfusion (Loria et al., 1976). However, based on a comparison study of different water flux measurements, PEG 4000 (compared to gravimetric method and inulin) appears to overestimate the water secretion by approximately 21% for mouse intestinal perfusion (Appendix B). Therefore, all of the water flux corrections assessed by PEG 4000 were adjusted by an average water flux correction of 14%, as determined by the 3 methods (i.e., non-absorbable markers PEG 4000 plus inulin plus gravimetric method).

### **Estimation of Intrinsic Membrane Parameters**

The effective permeability determined by Eq. 1 includes a combination of the unstirred aqueous layer permeability ( $P_{aq}$ ) and the intrinsic membrane permeability ( $P_w$ ).

$$\frac{1}{P_{eff}} = \frac{1}{P_w} + \frac{1}{P_{aq}} \quad (Eq. 3)$$

Therefore, it is critical to isolate the intrinsic membrane permeability in order to determine intrinsic membrane uptake parameters such as  $K_m$  and  $J_{max}$  due to a transporter(s) (e.g., PETP1). The aqueous and intrinsic (unbiased) membrane permeabilities were estimated using a modified boundary layer model (Johnson and Amidon, 1988).

$$P_{aq} = \left( A \frac{R}{D} G_z^{1/3} \right)^{-1} \quad (Eq. 4)$$



where  $D$  is the aqueous diffusion coefficient. Graetz number ( $Gz$ ) (the ratio of the mean tube residence time to the time required for radial diffusional equilibration ) and unitless constant  $A$  were estimated from the following expressions:

$$G_z = \frac{\pi DL}{2Q} \quad (Eq.5)$$

$$A = 10.0Gz + 1.01 \quad \text{where} \quad 0.004 \leq Gz < 0.01$$

$$A = 4.5Gz + 1.065 \quad \text{where} \quad 0.01 \leq Gz < 0.03$$

$$A = 2.5Gz + 1.125 \quad \text{where} \quad 0.03 \leq Gz$$

Drug concentrations at the membrane surface ( $C_w$ ) and the intrinsic membrane permeability ( $P_w$ ) were calculated as follows:

$$C_w = C_{in}(1 - P_{eff}/P_{aq}) \quad (Eq.6)$$

$$P_w = \frac{P_{eff}}{1 - P_{eff}/P_{aq}} \quad (Eq.7)$$

Regression of intrinsic membrane permeability ( $P_w$ ) vs. membrane surface concentration of drug ( $C_w$ ) can be used to determine the unbiased intrinsic membrane parameters:

$$P_w = \frac{J_{max}}{K_m + C_w} + P_m \quad (Eq.8)$$

where  $J_{max}$ , is the maximum flux,  $K_m$  is the intrinsic Michaelis constant, and  $P_m$  is the intrinsic passive membrane permeability.

The intrinsic membrane uptake parameters  $J_{max}$  and  $K_m$  can also be expressed as a function of flux  $J$  and membrane surface concentration.

$$J = \frac{J_{max} C_w}{K_m + C_w} + P_m C_w \quad (Eq. 9)$$

$$J = P_{eff} C_{in} \quad (Eq. 10)$$

The flux at steady-state is the product of the effective drug permeability,  $P_{eff}$ , and the bulk drug concentration,  $C_{in}$ .

The apparent biased kinetic parameters,  $J'_m$  and  $K'_m$  where the aqueous resistance is not subtracted from the total resistance, can be estimated as a function of effective permeability and inlet concentration.

$$P_{eff} = \frac{J'_{max}}{K'_m + C_{in}} + P'_m \quad (Eq. 11)$$

$$J = \frac{J'_{max} C_{in}}{K'_m + C_{in}} + P'_m C_{in} \quad (Eq. 12)$$

When the aqueous layer is ignored, the membrane parameters obtained are biased, and  $K_m$  is overestimated. Therefore, it is necessary to either eliminate or account for the effect of this aqueous layer resistance in order to obtain the true membrane parameters.

### **Estimation of Aqueous Diffusion Coefficient**

The diffusion coefficient ( $D$ ) of GlySar used in estimation of aqueous permeability (Eq. 4) was determined according to the Hayduck-Laudie's expression (Reid et al., 1977)

$$D = 13.26 \times 10^{-5} \eta^{-1.14} V_A^{-0.589} \quad (\text{Eq. 13})$$

Where  $\eta$  is the viscosity of water (0.6915 cP at 37°C),  $V_A$  is the solute molar volume at normal boiling point ( $\text{cm}^3/\text{g}/\text{mol}$ ), and  $D$  is the binary diffusion coefficient at infinite dilution ( $\text{cm}^2/\text{s}$ ). Molar volume ( $V_A$ ) for GlySar was estimated using Schroeder's additive method. The values for  $V_A$  and  $D$  for GlySar are  $140 \text{ cm}^3/\text{g}/\text{mol}$  and  $0.00066 \text{ cm}^2/\text{min}$ , respectively.

$$G_z = 0.08285$$

$$A = 1.3321$$

$$P_{\text{aq}} = 1.892 \times 10^{-4} \text{ cm/s}$$

### **Statistical Analysis**

Data were reported as mean  $\pm$  S.E. A two-tailed student t-test was used to compare statistical differences between two groups. For multiple comparisons, one-way analysis of variance (ANOVA) was used followed by *Dunnett's* test for pairwise comparisons with the control group (GraphPad Prism, v4.0; GraphPad Software, Inc., La Jolla, CA). A probability of  $p \leq 0.05$  was considered significant.

## RESULTS

### **GlySar Permeability in PEPT1<sup>+/+</sup> vs. PEPT1<sup>-/-</sup> Mice**

As observed in Fig. 4.1, permeability of 10  $\mu$ M GlySar in PEPT1<sup>-/-</sup> mice was about 20x lower than that of wild-type mice demonstrating the crucial role of PEPT1 transporter in absorption of GlySar.

### **Control for Passive and Paracellular Permeability**

To assess whether the deletion of PEPT1 had any influence on membrane integrity, permeability of 10  $\mu$ M mannitol and metoprolol were evaluated in PEPT1<sup>+/+</sup> vs. PEPT1<sup>-/-</sup> mice to investigate if any differences in paracellular and passive permeability occurred respectively, between the two genotypes. As depicted in Fig 4.2 and Fig 4.3, no significant differences were observed in permeability of mannitol or metoprolol between the two genotypes, demonstrating that differences in GlySar permeability in PEPT1<sup>+/+</sup> vs. PEPT1<sup>-/-</sup> mice are due to PEPT1-mediated transport rather than a change in integrity of brush border membrane in the small intestine.

### **pH-Dependent Studies**

Permeability of 10  $\mu$ M GlySar was evaluated at various pH values in order to test for a proton-dependent uptake of GlySar by PEPT1. As demonstrated in Fig. 4.3, there was a minor effect of pH on GlySar permeability in wild-type mice, the optimal uptake being at pH 5.5 (Fig 4.4A), and no effect of pH on PEPT1 deficient mice (Fig 4.4C), demonstrating the proton-substrate symport characteristics of PEPT1. However, the pH

effect on GlySar permeability *in-situ* was not as prominent as *in vitro* models because the microclimate pH is relatively insensitive to pH changes in the bulk phase (Lucas et al., 1980; Hogerle and Winne, 1983; Shiau et al., 1985). Dimethylamiloride (DMA), a  $\text{Na}^+/\text{H}^+$  exchanger inhibitor (Arakawa and Hara, 1999; Mirossay et al., 1999), decreases GlySar permeability in a dose dependent manner (Fig 4.4B). In the presence of 0.1 mM DMA, the GlySar permeability was not altered, whereas the presence of 1 and 2 mM DMA significantly reduced the GlySar permeability ( $p < 0.05$ ).

### **Concentration-Dependent Studies**

To determine the PEPT1-mediated uptake parameters of GlySar (i.e.,  $J_{max}$  and  $K_m$ ), dipeptide permeability was evaluated over a wide concentration range (0.01-200 mM total substrate in perfusate) in wild-type mice. As observed in Fig. 4.5, GlySar exhibited Michaelis-Menten uptake kinetics where the estimated apparent kinetic parameters were  $J'_{max} = 4.4 \text{ nmol/cm}^2/\text{sec}$  and  $K'_m = 19.8 \text{ mM}$  (Fig 4.5A). When intestinal wall concentrations of GlySar ( $C_w$ ) were used to estimate the kinetic parameters (after adjusting for the unstirred aqueous layer), the intrinsic absorption kinetics parameters for GlySar were  $J_{max} = 4.0 \text{ nmol/cm}^2/\text{sec}$  and  $K_m = 5.7 \text{ mM}$  (Fig 4.5B).

### **Specificity of PEPT1 Transporter**

Permeability of 10  $\mu\text{M}$  GlySar was determined in the presence of various potential inhibitors of PEPT1 to demonstrate the specificity of transport. As depicted in Fig. 4.6A, GlySar permeability in wild-type mice was significantly reduced by several dipeptides (GlySar, GlyPro and carnosine), the ACE inhibitor captopril, the  $\alpha$ -amino cephalosporin cefadroxil, and the antiviral prodrug valacyclovir. In contrast, single

amino acids (glycine and histidine), a cephalosporin without an  $\alpha$ -amino group (cephazolin) and the active antiviral species acyclovir had no effect. Moreover, in PEPT1 knockout mice, the potential inhibitors carnosine and cefadroxil had no influence on GlySar permeability. Absence of inhibition by histidine, an inhibitor of PHT-mediated transport, in wild-type mice suggests that PHT1 and PHT2 are not involved in the intestinal permeability of GlySar.

### **Comparison with Rat Permeability**

Since rat is the most commonly used animal in preclinical permeability studies and a good correlation has already been established between rat and human permeability for many drugs (Amidon et al., 1988; Fagerholm et al., 1996; Chiou and Barve, 1998; Salphati et al., 2001; Zhao et al., 2003), the permeability of GlySar was also measured in this rodent species. As observed in Fig 4.7, GlySar permeability in rat was about 2x lower than in mice ( $p < 0.001$ ).

## DISCUSSION

PEPT1 is believed to play an important role in the absorption of di/tripeptides and peptide-like drugs in small intestine. Previous *in vitro* studies on PEPT1 provided us with important information with respect to structure-functions, substrate specificity, substrate affinity, mechanism of transport, and localization. However, most studies were limited due to the lack of an intact blood supply, overlapping substrate specificities, and the contribution of multiple transport systems, thus, making it difficult to isolate the relative role of a single gene product, PEPT1, in relation to other possible transporters that are present in the small intestine. The recent generation of PEPT1 knockout mice (Hu et al., 2008) has provided a unique opportunity to probe the functional activity of PEPT1 under physiological conditions. In the present *in situ* study, we have validated the utility of using wild-type and PEPT1 knockout mice for intestinal perfusion by demonstrating the pH-stimulated uptake, specific inhibition, and low-affinity kinetics of a model dipeptide, GlySar.

Human and mouse PEPT1 share many similarities, suggesting that the findings from mouse PEPT1 can be extrapolated to human. At the molecular level, PEPT1 is highly homologous in amino acid sequence (~ 80%) across species (Liang et al., 1995; Miyamoto et al., 1996; Fei et al., 2000), having 83% amino acid identity between human and mouse PEPT1 (Fei et al., 2000). The genomic organization of human PEPT1 also shows high similarity with its mouse orthologue (Urtti et al., 2001). When expressed in *Xenopus laevis* oocytes and transfected cells, human and mouse PEPT1 share many molecular dynamic similarities with respect to their driving force (i.e., pH gradient and

membrane potential), substrate specificity, substrate affinity, and sensitivity (Liang et al., 1995; Mackenzie et al., 1996; Fei et al., 2000). In both species, PEPT1 transporter is expressed in small intestine and kidney (Liang et al., 1995; Zhang et al., 2004; Hu et al., 2008). With immunolocalization studies, it was demonstrated that PEPT1 is expressed in the apical membrane of small intestine (i.e., duodenum, jejunum and ileum), but not in colon for both human and mouse (Walker et al., 1998; Groneberg et al., 2001). Gene expression studies have shown that mouse and human have comparative intestinal expression levels, whereas PEPT1 expression levels in rat were several-fold higher (Kim et al., 2007), suggesting that the PEPT1-mediated intestinal absorption of peptide substrates in human is more similar to mouse than rat.

Although a good correlation has been established between rat and human permeability (Amidon et al., 1988; Fagerholm et al., 1996; Chiou and Barve, 1998; Salphati et al., 2001; Zhao et al., 2003), no such correlation has been determined between mouse and human permeability due to the sparse data available on mouse intestinal permeability.

The functional characteristics of PEPT1 obtained from the current *in situ* model were in parallel with those obtained from *in vitro* models. Based on a PEPT1-transfected cell model, PEPT1 was shown to be a low-affinity, high-capacity transporter, where  $K_m$  for GlySar was 0.29 -0.39 mM for human PEPT1 (Liang et al., 1995; Zhang et al., 2004), 0.35 mM for monkey PEPT1 (Zhang et al., 2004) and 1.1 mM for rat PEPT1 (Terada et al., 1997). Our current *in situ* intestinal perfusion model reported an intrinsic  $K_m$  of 5.7 mM for GlySar in wild-type mice, which is very similar to the PEPT1 affinity of GlySar in other species using *in vitro* models. It is important to note that the intrinsic affinity



used here is an estimated unbiased affinity after correcting for the effect of the unstirred aqueous layer on GlySar permeability.

In our concentration-dependent studies, we used GlySar concentrations up to 200 mM since the estimated concentration of dipeptides and tripeptides after the digestion of protein in the intestinal lumen can be as high as 100 mM (Ganapathy et al., 2006). The low-affinity and high-capacity characteristics of the PEPT1 transporter are quite suitable for its physiological function to absorb such a high concentration of small peptides in the intestinal lumen. Previous *in vitro* studies have shown that human PEPT1, in addition to recognizing di- and tri-peptides, also recognizes peptidomimetic therapeutic agents such as ACE inhibitors (i.e., captopril, enalapril),  $\beta$ -lactam antibiotics, bestatin and the antiviral prodrug valacyclovir (Liang et al., 1995; Han et al., 1998; Zhang et al., 2004). Our findings, based on the mouse *in situ* intestinal perfusion model, were consistent with those previous results in regard to PEPT1 substrate specificity. It is interesting to note that histidine, an inhibitor for PHTs, did not inhibit the permeability of GlySar suggesting that, despite their intestinal expression, PHT1 and PHT2 do not contribute to GlySar permeability at the apical surface of small intestine. It has already been confirmed that in PEPT1 null mice, PEPT2, PHT1 and PHT2 are not upregulated in small intestine as a compensatory response to deletion of PEPT1 gene (Hu et al., 2008).

The pH-stimulated transport of di/tripeptides has been shown for PEPT1 in rabbit, rat, mouse and human using several *in vitro* models such as intestinal brush border membrane vesicles (Ganapathy and Leibach, 1983; Ganapathy et al., 1984; Inui et al., 1988), *Xenopus laevis* oocytes (Fei et al., 1994; Saito et al., 1995; Steel et al., 1997; Fei et al., 2000), and PEPT1-transfected cells (Matsumoto et al., 1994; Liang et al., 1995;

Fujisawa et al., 2006). In addition, uptake was shown to have a bell-shaped curve vs. pH with the optimal transport activity occurring at pH 5.5-6.0. Although the optimal pH of GlySar permeability was observed at pH 5.5 in our *in situ* intestinal perfusion model, the magnitude of change for proton dependency was not as remarkable as shown by *in vitro* models. The reduced effect of pH-dependent uptake was most likely due to the fact that changes in luminal bulk pH do not necessarily translate to significant changes in pH at the vicinity of the intestinal membrane where a low microclimate pH is maintained (Lucas et al., 1980; Hogerle and Winne, 1983; Shiau et al., 1985). Lucas and his coworkers have demonstrated that when the pH of luminal bulk phase was varied from 5.5 to 8.5, the surface microclimate pH was only 5.5 to 6.2, a pH change less than one unit (Lucas et al., 1980).

Immunoblot and immunofluorescence localization studies in rat have revealed that PEPT1 protein was expressed in apical membranes of the duodenum, jejunum, and ileum, and that the strongest staining was observed in the jejunal segment (Ogihara et al., 1996). Similarly, PEPT1 was also found in the apical membrane of all segments of mouse small intestine (i.e., duodenum, jejunum and ileum) (Groneberg et al., 2001). When expression patterns of PEPT1 were evaluated in human intestine, a similar finding was found where PEPT1 mRNA was highly expressed in small intestine with the expression ranking: duodenum>jejunum>ileum. Additionally, immunoblot analyses have revealed that PEPT1 protein is expressed in the duodenum, jejunum and ileum of human intestine (Terada et al., 2005). In all of the studies mentioned above, PEPT1 expression was not found in colon. Decreased activity of PEPT1 in ileum, compared to jejunum, is physiologically sound since peptidase activity along the small intestine is much higher in

ileum than jejunum (Silk et al., 1976) suggesting a gradual decrease in the concentration of small peptides while the concentration of single amino acids increase as luminal contents move along the intestine. Interestingly, expression of the amino acid transporter B<sup>0</sup>AT1 (SLC6A19) also increases from duodenum to ileum (Terada et al., 2005). The reciprocal expression of PEPT1 and B<sup>0</sup>AT1, and the increased activity of brush border membrane peptidase from the jejunum to ileum may play an important role in maintaining the efficient absorption of end products from a protein meal.

In conclusion, in the present study we have demonstrated that 1) PEPT1 is responsible for at least 90% of dipeptide uptake in the small intestine; 2) that PEPT1 exhibits a pH-stimulated uptake of dipeptide; 3) that the inhibition of dipeptide uptake is specific; 4) that transport of GlySar exhibited low-affinity kinetics, which is reflective of PEPT1 transport kinetics. Taken together, these results suggest that PEPT1 will play a crucial role in the uptake of dietary peptides, mimetics and peptide-like drugs in the small intestine. Future studies will focus on elucidating the role of PEPT1 in the regional permeability of peptide-like therapeutic drugs/prodrug such as cefadroxil and valacyclovir, using an *in situ* intestinal perfusion model.

## FIGURES

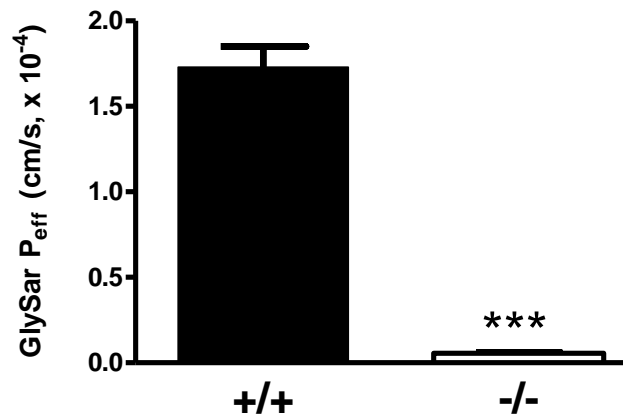


**Figure 4.1** Effective permeability (P<sub>eff</sub>) of 10 μM [<sup>3</sup>H]GlySar during jejunal perfusion of PEPT1<sup>+/+</sup> and PEPT1<sup>-/-</sup> mice. Studies were performed in pH 6.5 perfusion buffer. Data are presented as mean ± SE (n=6-9). \*\*\* p < 0.001, for PEPT1 null vs. wild-type.

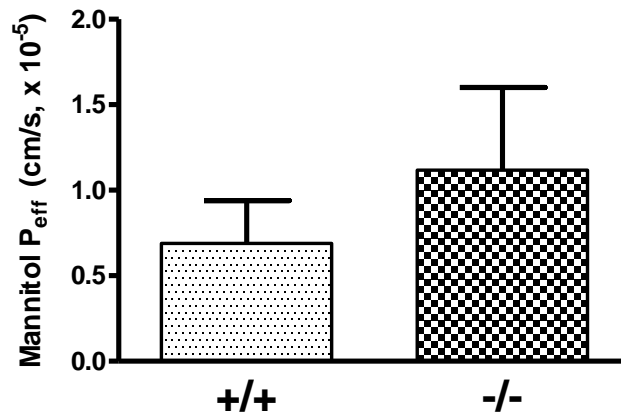


**Figure 4.2** Effective permeability (P<sub>eff</sub>) of 10 μM [<sup>3</sup>H]mannitol during jejunal perfusion of PEPT1<sup>+/+</sup> and PEPT1<sup>-/-</sup> mice. Studies were performed in pH 6.5 perfusion buffer. Data are presented as mean ± SE (n=4-6).

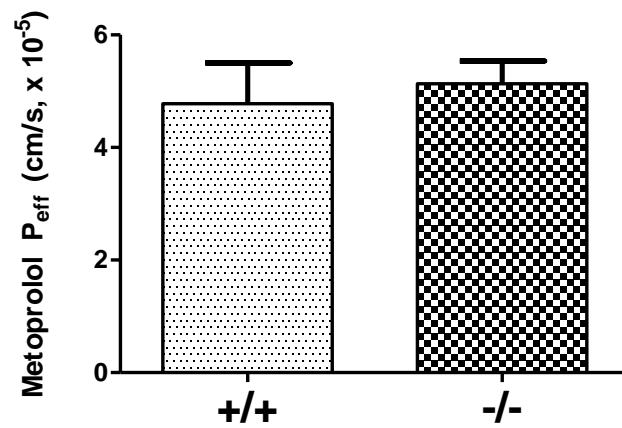


**Figure 4.3** Effective permeability (P<sub>eff</sub>) of 10 μM [<sup>3</sup>H]metoprolol during jejunal perfusion of PEPT1<sup>+/+</sup> and PEPT1<sup>-/-</sup> mice. Studies were performed in pH 6.5 perfusion buffer. Data are presented as mean ± SE (n=4-6).

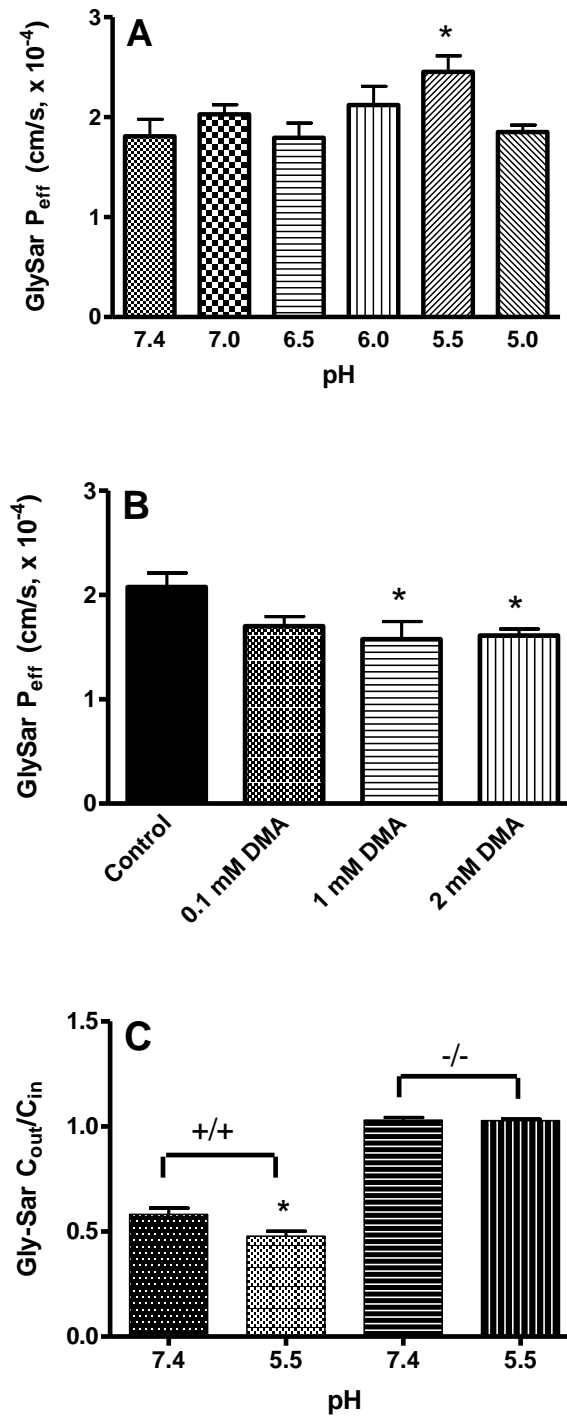


**Figure 4.4** Effect of pH on effective permeability ( $P_{eff}$ ) of 10  $\mu$ M [ $^3$ H]GlySar during jejunal perfusion of wild-type (+/+) mice (A) and PEPT1 null (-/-) mice (C). \*  $p < 0.05$ , compared to pH 7.4. Effect of dimethylamiloride (DMA) (B) on the  $P_{eff}$  of 10  $\mu$ M [ $^3$ H]GlySar during jejunal perfusion of wild-type mice. Studies were performed in pH 6.5 perfusion buffer (n=4, mean  $\pm$  SE). \*  $p < 0.05$ , compared to control values.

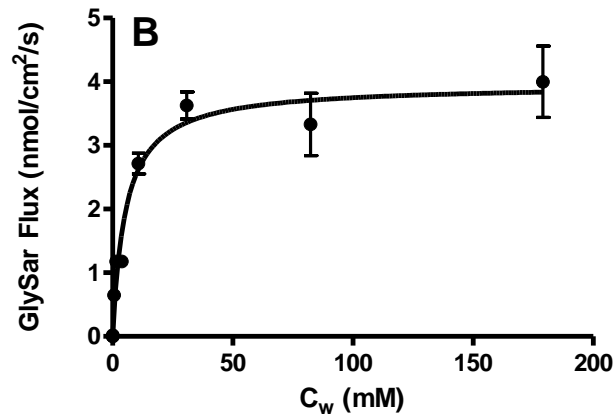
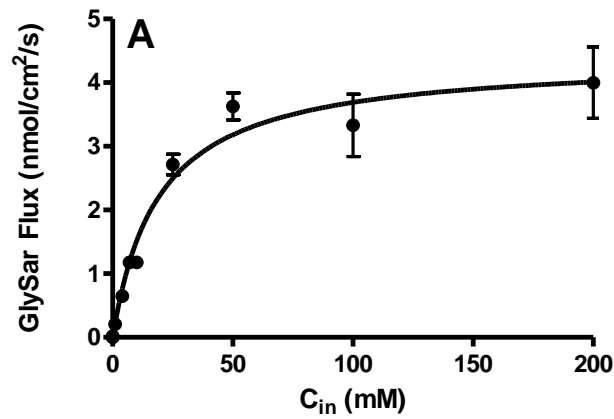


**Figure 4.5** Concentration-dependent flux of [<sup>3</sup>H]GlySar (0.01-20 mM total substrate in perfusate) during jejunal perfusion of wild-type mice. Studies were performed in pH 6.5 buffer (n=4, mean ± SE). In panel A, C<sub>in</sub> represents perfusate concentration of GlySar. In panel B, C<sub>w</sub> represent mean “estimated” concentration of GlySar at the intestinal wall.



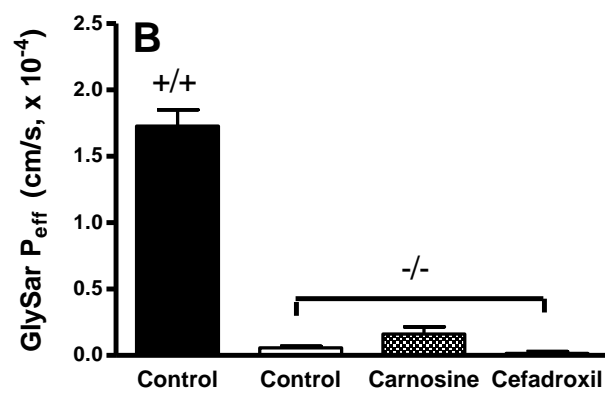
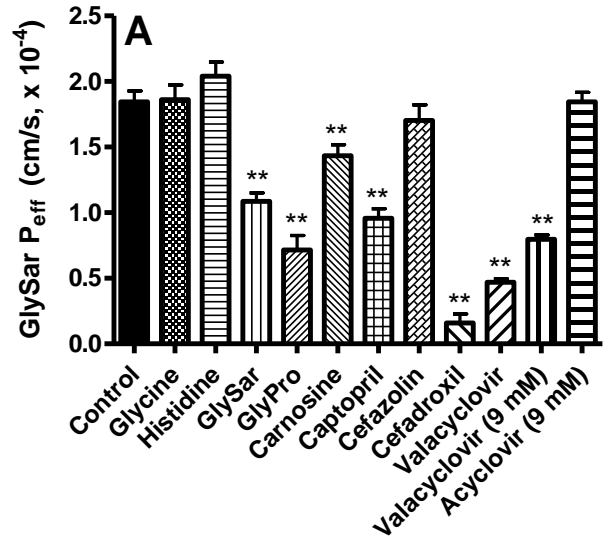


**Figure 4.6** Effect of potential inhibitors (25 mM) on the P<sub>eff</sub> of 10 μM [<sup>3</sup>H]GlySar during jejunal perfusion of wild-type (+/+) mice (A) and PEPT1 null (-/-) mice (B). Studies were performed in pH 6.5 perfusion buffer (n=4, mean ± SE). \*\* p < 0.01, compared to control values.

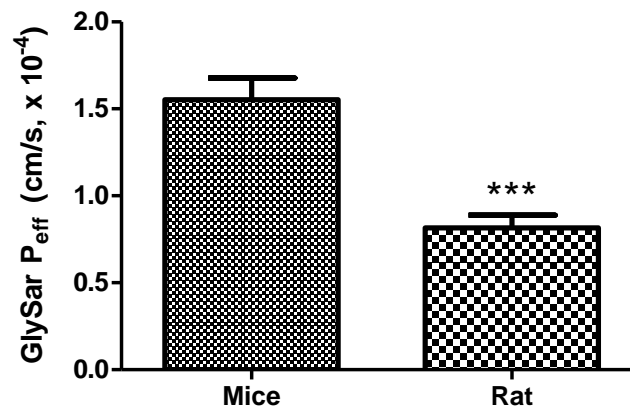


**Figure 4.7** Effective permeability (P<sub>eff</sub>) of 10  $\mu$ M [<sup>3</sup>H]GlySar during jejunal perfusion of mice and rats. Studies were performed in pH 6.5 perfusion buffer. Data are presented as mean  $\pm$  SE (n=5-6). \*\*\* p < 0.001 for rat vs. mouse.

## REFERENCES

Amidon GL, Kou J, Elliott RL and Lightfoot EN (1980) Analysis of models for determining intestinal wall permeabilities. *J Pharm Sci* **69**:1369-1373.

Amidon GL, Sinko PJ and Fleisher D (1988) Estimating human oral fraction dose absorbed: a correlation using rat intestinal membrane permeability for passive and carrier-mediated compounds. *Pharm Res* **5**:651-654.

Arakawa J and Hara A (1999) Effect of 5-(N,N-Dimethyl)-amiloride, a specific inhibitor of Na(+)/H(+) exchanger, on the palmitoyl-L-carnitine-induced mechanical and metabolic derangements in the isolated perfused rat heart. *Pharmacology* **59**:239-248.

Bhardwaj RK, Herrera-Ruiz D, Eltoukhy N, Saad M and Knipp GT (2006) The functional evaluation of human peptide/histidine transporter 1 (hPHT1) in transiently transfected COS-7 cells. *Eur J Pharm Sci* **27**:533-542.

Chiou WL and Barve A (1998) Linear correlation of the fraction of oral dose absorbed of 64 drugs between humans and rats. *Pharm Res* **15**:1792-1795.

Daniel H and Kottra G (2004) The proton oligopeptide cotransporter family SLC15 in physiology and pharmacology. *Pflugers Arch* **447**:610-618.

Fagerholm U, Johansson M and Lennernas H (1996) Comparison between permeability coefficients in rat and human jejunum. *Pharm Res* **13**:1336-1342.

Fei YJ, Kanai Y, Nussberger S, Ganapathy V, Leibach FH, Romero MF, Singh SK, Boron WF and Hediger MA (1994) Expression cloning of a mammalian proton-coupled oligopeptide transporter. *Nature* **368**:563-566.

Fei YJ, Sugawara M, Liu JC, Li HW, Ganapathy V, Ganapathy ME and Leibach FH (2000) cDNA structure, genomic organization, and promoter analysis of the mouse intestinal peptide transporter PEPT1. *Biochim Biophys Acta* **1492**:145-154.

Fujisawa Y, Tateoka R, Nara T, Kamo N, Taira T and Miyauchi S (2006) The extracellular pH dependency of transport activity by human oligopeptide transporter 1 (hPEPT1) expressed stably in Chinese hamster ovary (CHO) cells: a reason for the bell-shaped activity versus pH. *Biol Pharm Bull* **29**:997-1005.

Ganapathy V, Burckhardt G and Leibach FH (1984) Characteristics of glycylsarcosine transport in rabbit intestinal brush-border membrane vesicles. *J Biol Chem* **259**:8954-8959.

Ganapathy V, Gupta N and Martindale RG (2006) Protein Digestion and Absorption, in: *Physiology of the Gastrointestinal Tract* (Johnson LR ed), pp 1667-1692, Elsevier, Burlington.

Ganapathy V and Leibach FH (1983) Role of pH gradient and membrane potential in dipeptide transport in intestinal and renal brush-border membrane vesicles from the rabbit. Studies with L-carnosine and glycyl-L-proline. *J Biol Chem* **258**:14189-14192.

Groneberg DA, Doring F, Eynott PR, Fischer A and Daniel H (2001) Intestinal peptide transport: ex vivo uptake studies and localization of peptide carrier PEPT1. *Am J Physiol Gastrointest Liver Physiol* **281**:G697-704.

Han H, de Vruhe RL, Rhie JK, Covitz KM, Smith PL, Lee CP, Oh DM, Sadee W and Amidon GL (1998) 5'-Amino acid esters of antiviral nucleosides, acyclovir, and AZT are absorbed by the intestinal PEPT1 peptide transporter. *Pharm Res* **15**:1154-1159.

Herrera-Ruiz D and Knipp GT (2003) Current perspectives on established and putative mammalian oligopeptide transporters. *J Pharm Sci* **92**:691-714.

Herrera-Ruiz D, Wang Q, Gudmundsson OS, Cook TJ, Smith RL, Faria TN and Knipp GT (2001) Spatial expression patterns of peptide transporters in the human and rat gastrointestinal tracts, Caco-2 in vitro cell culture model, and multiple human tissues. *AAPS PharmSci* **3**:E9.

Ho NF and Higuchi WI (1974) Theoretical model studies of intestinal drug absorption. IV. Bile acid transport at pre-micellar concentrations across diffusion layer-membrane barrier. *J Pharm Sci* **63**:686-690.

Hogerle ML and Winne D (1983) Drug absorption by the rat jejunum perfused in situ. Dissociation from the pH-partition theory and role of microclimate-pH and unstirred layer. *Naunyn Schmiedebergs Arch Pharmacol* **322**:249-255.

Hu Y, Smith DE, Ma K, Jappar D, Thomas W and Hillgren KM (2008) Targeted Disruption of Peptide Transporter Pept1 Gene in Mice Significantly Reduces Dipeptide Absorption in Intestine. *Mol Pharm.*

Inui K, Okano T, Maegawa H, Kato M, Takano M and Hori R (1988) H<sup>+</sup> coupled transport of p.o. cephalosporins via dipeptide carriers in rabbit intestinal brush-border

membranes: difference of transport characteristics between cefixime and cephadrine. *J Pharmacol Exp Ther* **247**:235-241.

Johnson DA and Amidon GL (1988) Determination of intrinsic membrane transport parameters from perfused intestine experiments: a boundary layer approach to estimating the aqueous and unbiased membrane permeabilities. *J Theor Biol* **131**:93-106.

Kim HR, Park SW, Cho HJ, Chae KA, Sung JM, Kim JS, Landowski CP, Sun D, Abd El-Aty AM, Amidon GL and Shin HC (2007) Comparative gene expression profiles of intestinal transporters in mice, rats and humans. *Pharmacol Res* **56**:224-236.

Liang R, Fei YJ, Prasad PD, Ramamoorthy S, Han H, Yang-Feng TL, Hediger MA, Ganapathy V and Leibach FH (1995) Human intestinal H<sup>+</sup>/peptide cotransporter. Cloning, functional expression, and chromosomal localization. *J Biol Chem* **270**:6456-6463.

Loria RM, Kayne HL, Kibrick S and Broitman SA (1976) Measurement of intestinal absorption in mice by a double-label radioisotope perfusion technic. *Lab Anim Sci* **26**:603-606.

Lucas ML, Lei FH and Blair JA (1980) The influence of buffer pH, glucose and sodium ion concentration on the acid microclimate in rat proximal jejunum in vitro. *Pflugers Arch* **385**:137-142.

Mackenzie B, Loo DD, Fei Y, Liu WJ, Ganapathy V, Leibach FH and Wright EM (1996) Mechanisms of the human intestinal H<sup>+</sup>-coupled oligopeptide transporter hPEPT1. *J Biol Chem* **271**:5430-5437.

Matsumoto S, Saito H and Inui K (1994) Transcellular transport of oral cephalosporins in human intestinal epithelial cells, Caco-2: interaction with dipeptide transport systems in apical and basolateral membranes. *J Pharmacol Exp Ther* **270**:498-504.

Matthews DM (1975) Intestinal absorption of peptides. *Physiol Rev* **55**:537-608.

Matthews DM, Crampton RF and Lis MT (1971) Sites of maximal intestinal absorptive capacity for amino acids and peptides: evidence for an independent peptide uptake system or systems. *J Clin Pathol* **24**:882-883.

Mirossay L, Mirossay A, Kocisova E, Radvakova I, Miskovsky P and Mojzis J (1999) Hypericin-induced phototoxicity of human leukemic cell line HL-60 is potentiated by omeprazole, an inhibitor of H<sup>+</sup>K<sup>+</sup>-ATPase and 5'-(N,N-dimethyl)-amiloride, an inhibitor of Na<sup>+</sup>/H<sup>+</sup> exchanger. *Physiol Res* **48**:135-141.

Miyamoto K, Shiraga T, Morita K, Yamamoto H, Haga H, Taketani Y, Tamai I, Sai Y, Tsuji A and Takeda E (1996) Sequence, tissue distribution and developmental changes in rat intestinal oligopeptide transporter. *Biochim Biophys Acta* **1305**:34-38.

Ogihara H, Saito H, Shin BC, Terado T, Takenoshita S, Nagamachi Y, Inui K and Takata K (1996) Immuno-localization of H<sup>+</sup>/peptide cotransporter in rat digestive tract. *Biochem Biophys Res Commun* **220**:848-852.

Reid RC, Prausnitz JM and Sherwood TK (1977) *The properties of gases and liquids*. McGraw-Hill, New York.

Saito H, Okuda M, Terada T, Sasaki S and Inui K (1995) Cloning and characterization of a rat H<sup>+</sup>/peptide cotransporter mediating absorption of beta-lactam antibiotics in the intestine and kidney. *J Pharmacol Exp Ther* **275**:1631-1637.

Salphati L, Childers K, Pan L, Tsutsui K and Takahashi L (2001) Evaluation of a single-pass intestinal-perfusion method in rat for the prediction of absorption in man. *J Pharm Pharmacol* **53**:1007-1013.

Shiau YF, Fernandez P, Jackson MJ and McMonagle S (1985) Mechanisms maintaining a low-pH microclimate in the intestine. *Am J Physiol* **248**:G608-617.

Silk DB, Nicholson A and Kim YS (1976) Hydrolysis of peptides within lumen of small intestine. *Am J Physiol* **231**:1322-1329.

Steel A, Nussberger S, Romero MF, Boron WF, Boyd CA and Hediger MA (1997) Stoichiometry and pH dependence of the rabbit proton-dependent oligopeptide transporter PepT1. *J Physiol* **498** ( Pt 3):563-569.

Terada T, Saito H, Mukai M and Inui K (1997) Recognition of beta-lactam antibiotics by rat peptide transporters, PEPT1 and PEPT2, in LLC-PK1 cells. *Am J Physiol* **273**:F706-711.

Terada T, Sawada K, Saito H, Hashimoto Y and Inui K (1999) Functional characteristics of basolateral peptide transporter in the human intestinal cell line Caco-2. *Am J Physiol* **276**:G1435-1441.

Terada T, Shimada Y, Pan X, Kishimoto K, Sakurai T, Doi R, Onodera H, Katsura T, Imamura M and Inui K (2005) Expression profiles of various transporters for oligopeptides, amino acids and organic ions along the human digestive tract. *Biochem Pharmacol* **70**:1756-1763.

Urtti A, Johns SJ and Sadee W (2001) Genomic structure of proton-coupled oligopeptide transporter hPEPT1 and pH-sensing regulatory splice variant. *AAPS PharmSci* **3**:E6.

Walker D, Thwaites DT, Simmons NL, Gilbert HJ and Hirst BH (1998) Substrate upregulation of the human small intestinal peptide transporter, hPepT1. *J Physiol* **507** (Pt 3):697-706.

Zhang EY, Emerick RM, Pak YA, Wrighton SA and Hillgren KM (2004) Comparison of human and monkey peptide transporters: PEPT1 and PEPT2. *Mol Pharm* **1**:201-210.

Zhao YH, Abraham MH, Le J, Hersey A, Luscombe CN, Beck G, Sherborne B and Cooper I (2003) Evaluation of rat intestinal absorption data and correlation with human intestinal absorption. *Eur J Med Chem* **38**:233-243.

## Chapter 5

# SIGNIFICANCE OF PEPT1 ON THE *IN VIVO* ORAL ABSORPTION AND DISPOSITION OF GLYCYLSARCOSINE IN WILD-TYPE AND PEPT1 KNOCKOUT MICE

### ABSTRACT

**Purpose.** Genetically-modified mice have become a useful tool to elucidate the function and significance of specific proteins in the body. Although the proton-oligopeptide cotransporter PEPT1 (SLC15A1) is known to transport a variety of peptides, peptidomimetics and peptide-like drugs, its relative importance in intestinal absorption *in vivo* is unknown. Thus, this study examined the dose-dependent absorption profiles of a model dipeptide, glycylsarcosine (GlySar), in *Pept1*<sup>+/+</sup> (WT) and *Pept1*<sup>-/-</sup> (KO) mice, along with its tissue distribution.

**Methods.** [<sup>3</sup>H]GlySar was administered by gavage to WT and KO mice at doses of 1, 10, 100, 1000, and 5000 nmol/g body weight. Blood samples were obtained serially over 480 min, the plasma harvested, and area under the plasma concentration-time curve (AUC) determined. Tissue distribution studies were also performed where samples were obtained from both genotypes 1 and 8 h after a 10 nmol/g dose of [<sup>3</sup>H]GlySar.



[<sup>14</sup>C]Dextran MW 70,000 (0.15 μCi/mouse) was administered by tail vein injection 5 min prior to harvesting the tissues to correct for vascular space.

**Results.** For all five doses, the systemic exposure (AUC) of GlySar was about 50% lower in KO mice than in WT animals ( $p < 0.01$ ). With respect to the absorption profile in KO mice, plasma levels of GlySar reached a plateau at 90 min and then rose to a second plateau at 240 min. In WT mice, the plasma levels rose continuously to reach a single plateau at 90 min. When partial AUC (0-120min) was used as an indicator of rate of absorption, there was a 60% reduction in rate of GlySar absorption in KO mice compared to WT animals. A linear correlation was also observed between AUC and dose for both genotypes in the dose ranges of 1-100 nmol/g. Tissue accumulation of GlySar was significantly lower in KO versus WT mice. However, when tissue concentrations of GlySar were corrected for corresponding plasma levels, no statistical differences were observed, except for intestine.

**Conclusions.** PEPT1 ablation significantly reduced the rate and extent of *in vivo* oral absorption of GlySar in KO mice as compared to WT animals. With the exception of small intestine, the effect of PEPT1 on GlySar tissue distribution was unremarkable.

## INTRODUCTION

Following the ingestion of dietary protein (70-100 g per day), proteins are converted into large peptides by gastric and pancreatic proteases in the gastrointestinal lumen followed by a further hydrolysis into small peptides (80%) and free amino acids (20%) by various peptidases in the brush border membrane of intestinal epithelium (Ganapathy et al., 2006). The final end products of protein digestion are absorbed into the enterocytes predominately in the form of di- and tripeptides as supposed to free amino acids (Matthews, 1975). Once inside the enterocytes, the majority of the di- and tripeptides undergo further hydrolysis into their constituent amino acids by cytoplasmic peptidases and exit the epithelial cells via different basolateral amino acid transporters. A small amount of di- and tripeptides that are resistant to cytoplasmic peptidases exit the enterocytes intact across the basolateral membrane through a basolateral peptide transporter that has yet to be cloned (Terada et al., 1999).

PEPT1, a member of proton-coupled oligopeptide transporter (POT) family (i.e., PEPT1, PEPT2, PHT1 and PHT2) is an electrogenic symporter that translocates small peptides/mimetics along with protons across a biological membrane via an inwardly-directed proton gradient and negative membrane potential (Herrera-Ruiz and Knipp, 2003; Daniel and Kottra, 2004). PEPT1 is strongly expressed on the apical membrane of enterocytes in the small intestine (i.e., duodenum, jejunum, and ileum) with little or no expression in normal colon (Ogihara et al., 1996; Walker et al., 1998; Groneberg et al., 2001). In addition to PEPT1, human and rat small intestine have been shown to express PHT1 and PHT2 transcripts (Herrera-Ruiz et al., 2001), where PHT1 is expressed in the

villous epithelium of small intestine (Bhardwaj et al., 2006). However, PEPT1 is believed to be the primary POT responsible for small intestinal absorption of di/tripeptides and peptide-like therapeutic agents. PEPT1 is characterized as a high-capacity, low-affinity transporter. It was first isolated and cloned from a rabbit intestine cDNA library (Fei et al., 1994), which subsequently lead to the cloning of PEPT1 from human (Liang et al., 1995), rat (Saito et al., 1995; Miyamoto et al., 1996) and mouse (Fei et al., 2000) intestinal cDNA libraries. It has been found that PEPT1 is highly homologous across species (~ 80%) (Liang et al., 1995; Miyamoto et al., 1996; Fei et al., 2000). PEPT1 is predicted to contain 12 transmembrane domains with both C and N terminals facing the cytosolic side, and protein sizes ranging from 707 to 710 amino acids depending on the species. The genomic organization of human PEPT1 shows high similarity with its mouse orthologue (Urtti et al., 2001). In addition, studies suggest that mouse and human have comparable intestinal expression patterns and levels, whereas PEPT1 expression level in the rat is several fold higher (Kim et al., 2007). PEPT1, in addition to transporting di- and tripeptides, also transports a number of peptidomimetic therapeutic agents with different conformations, size, polarity and charge (e.g.,  $\beta$ -lactam antibiotics, ACE inhibitors, renin inhibitors, bestatin, and antiviral prodrug valacyclovir), and acts as a vehicle for their effective intestinal absorption. Due to its broad substrate specificity and high capacity, PEPT1 is considered to be a very attractive target for drug delivery to improve the bioavailability of low permeable drugs.

PEPT1, in addition to be highly expressed in small intestine, is also expressed in apical membrane of S1 segments of the kidney proximal tubule (i.e., kidney cortex), (Liang et al., 1995; Shen et al., 1999; Lu and Klaassen, 2006), followed by expression of

the low-capacity, high-affinity peptide transporter PEPT2 that is localized in the brush border of S3 segments in proximal tubule (i.e., outer stripe of outer medulla) (Liu et al., 1995; Shen et al., 1999; Rubio-Aliaga et al., 2000). In spite of the sequential expression of PEPT1 and PEPT2 in renal proximal tubules, studies have definitively shown that PEPT2 accounts for the vast majority of reabsorption for the model dipeptide glycylsarcosine (GlySar) and the  $\beta$ -lactam antibiotic cefadroxil in kidney (Takahashi et al., 1998; Inui et al., 2000; Ocheltree et al., 2005; Shen et al., 2007). PEPT1 is also expressed in other tissues such as liver, pancreas, lung, bile duct, ovary, placenta, testis, and prostate (Fei et al., 1994; Liang et al., 1995; Knutter et al., 2002; Lu and Klaassen, 2006), suggesting a possible role of PEPT1 in disposition of small peptide/mimetics in those tissues. Using immunofluorescence microscopy and transport studies, PEPT1 was demonstrated to be expressed in the lysosomal membrane of liver cells (Thamotharan et al., 1997), renal cells (Zhou et al., 2000), and pancreatic cells (Bockman et al., 1997), rather than being exclusively confined to the plasma membrane.

Due to the physiological and pharmacological importance of PEPT1 in the absorption of di/tripeptides and peptidomimetic drugs in the small intestine, PEPT1 is the most extensively studied transporter among the POT members. However, the previous studies were based on non-physiological *in vitro* models that lack an intact blood supply. In addition, PEPT1 is also expressed in other tissues such as kidney, lung, and liver where multiple POT members are expressed with overlapping substrate specificities, thus confounding an accurate assessment of PEPT1's significance in these tissues. Utilizing PEPT1 deficient mice will offer a powerful tool to assess the relative importance of PEPT1, under physiological conditions, for small peptide/mimetic absorption in the small

intestine as well as disposition in other tissues. Previously, we have investigated the role of PEPT1 in the absorption of small peptides by evaluating the *in situ* intestinal permeability of GlySar in wild-type and PEPT1 knockout mice, and have found that PEPT1 is responsible for at least 90% of dipeptide uptake in the small intestine (Chapter 4). However, results from the *in situ* intestinal perfusion model may not necessarily reflect what actually occurs *in vivo* where gastric emptying, intestinal transit, and intestinal residence time may influence the rate and extent of oral absorption. Therefore, the aim of the present study is to delineate the relative importance of PEPT1 in the *in vivo* absorption and disposition of small peptide/mimetic substrates by using glycylsarcosine (GlySar) as a model compound in PEPT1<sup>+/+</sup> (wild-type) and PEPT1<sup>-/-</sup> (knockout) mice.

## MATERIALS AND METHODS

### Materials

[<sup>3</sup>H]GlySar (14.4 Ci/mmol), [<sup>14</sup>C]GlySar (98 mCi/mmol), [<sup>14</sup>C]glycine (56 mCi/mmol), [<sup>14</sup>C]dextran-carboxyl 70,000 (1.1 mCi/g) were obtained from Moravek Biochemicals and Radiochemicals (Brea, CA). Unlabelled GlySar (mol. wt. = 146.1) was supplied by Sigma-Aldrich (St. Louis, MO). Hyamine hydroxide was purchased from ICN Radiochemicals (Irvine, CA) and hydrogen peroxide was obtained from Sigma-Aldrich (St. Louis, MO). All other chemicals were acquired from standard sources.

### Animals

Animal studies were carried out in accordance with the Guide for the Care and Use of Laboratory Animal as adopted and promulgated by the U.S National Institutes of Health. Gender matched 8-10 week old PEPT1<sup>+/+</sup> (wild-type) and PEPT1<sup>-/-</sup> (null) mice were used for all experiments. The mice were kept in temperature controlled environment with a 12-h light and 12-h dark cycle, and received a standard diet and water *ad libitum* (Unit for Laboratory Animal Medicine, University of Michigan, Ann Arbor, MI).

### Systemic Exposure of Orally Administered GlySar

PEPT1<sup>+/+</sup> and PEPT1<sup>-/-</sup> mice were fasted overnight prior to each experiment. The drug was dissolved in normal saline and administered to the mice in aqueous solution.

Gastric gavage (20G needle) was used to orally administer a solution of [<sup>3</sup>H]GlySar (0.5 μCi/g body weight, 10 μl/g body weight) for all doses. Serial blood samples (Peng et al., 2009) were collected by tail nicks at 0.5, 5, 10, 20, 30, 45, 60, 75, 90, 120, 180, 240, 360, and 480 min after the initial oral dose. The blood samples (~ 20 μL) were transferred to a 0.2 ml thin walled PCR tube containing 3 μl of 7.5% potassium EDTA and centrifuged at 3300 g for 3 min at ambient temperature to obtain the plasma. 5-10 μl of plasma was transferred into a scintillation vial, and 6 mL of CytoScint scintillation fluid (MP Biomedicals, Solon, OH) was added to the plasma sample. The radioactivity of plasma sample was measured with a dual-channel liquid scintillation counter (Beckman LS 6000 SC; Beckman Coulter Inc., Fullerton, CA). Animals were returned to their cages in between blood sampling where they had free access to water. Food was provided in their cages four hours after the initial dose. The cage was equipped with heating pad to maintain the mice body temperature. After 1 and 4 h of oral gavage, 250 μL of warm saline was given by I.P as the supplemental fluid in order to prevent dehydration.

After the last blood sample was obtained (8 h), several organs/tissues (e.g., kidney, liver, lung, pancreas, spleen, small and large intestines, bile ducts, ovary, testis, prostate, skeletal muscle, heart, eye, and cerebral cortex) were collected. One kidney was collected intact, and the other kidney was separated into renal cortex, outer medulla, and inner medulla. The small intestine was cut into duodenum, proximal jejunum, mid-small intestine, distal ileum, proximal colon, and distal colon; each segment was washed with pre-warmed saline solution to remove the fecal material and then blotted dry prior to weighing. A larger blood volume (30 μL) was collected at the end of experiment to correct for the vascular space using dextran 70,000, along with the GlySar plasma

concentration. Tissue samples were then solubilized in 0.5 ml of 1 M hyamine hydroxide (tissue solubilizer) (ICN Radiochemicals, Irvine, CA) for 24 h at 37°C. After the tissue solubilization, 40 µl hydrogen peroxide (30 wt%) (Sigma Aldrich, St. Louis, MO) was added to each sample for color treatment and incubated at 37°C for 24 h. A 6 mL aliquot of CytoScint scintillation fluid (MP Biomedicals, Solon, OH) was added to the tissue and blood samples, and the radioactivity of each sample was measured with a dual-channel liquid scintillation counter. At 5 min prior to tissue harvesting, [<sup>14</sup>C]dextran MW 70,000 (0.15 µCi/mouse) was administered via tail vein injection to determine the vascular space of tissues, and all tissue concentrations of GlySar were corrected for this values.

Corrected tissue concentrations of GlySar ( $C_{tiss,corr}$ , nmol/g wet tissue) were calculated (Ocheltree et al., 2005; Shen et al., 2007) as:

$$C_{tiss,corr} = C_{tiss} - V \times C_b$$

where  $C_{tiss}$  is the uncorrected GlySar tissue concentration (nmol/g wet tissue),  $V$  is the vascular space determined by dextran in the tissue (ml/g), and  $C_b$  is the GlySar blood concentration (nmol/ml).

A separate tissue distribution study was also performed after orally dosing [<sup>3</sup>H] GlySar by gavage at 10 nmol/g body weight (0.5 µCi/g body weight, 10 µl/g body weight). However in this study, organ/tissue and blood samples were collected one hour after the initial dose. All other aspects of sample treatment and analysis were described previously.

### **Systemic Exposure of Intravenously Administered GlySar**



PEPT1<sup>+/+</sup> and PEPT1<sup>-/-</sup> mice were fasted overnight prior to each experiment. The drug was dissolved in normal saline and administered to the mice in aqueous solution. The animals were anesthetized with sodium pentobarbital (40-60 mg/kg, i.p.). Following anesthesia, the mice were given [<sup>3</sup>H]GlySar (10 nmol/g body weight, 0.25 μCi/g body weight) via tail vein injection (5 μl/g body weight). Serial blood samples (Peng et al., 2009) were collected by tail nicks at 0.25, 2, 5, 15, 30, 60, 120, 180, 240, 360, and 480 min after the initial intravenous bolus dose. The blood samples (~ 20 μL) were transferred to a 0.2 ml thin walled PCR tube containing 3 μl of 7.5% potassium EDTA and centrifuged at 3300 g for 3 min at ambient temperature to obtain the plasma. 5-10 μl of plasma was transferred into a scintillation vial, and 6 mL of CytoScint scintillation fluid was added to the plasma sample. The radioactivity of plasma sample was measured with a dual-channel liquid scintillation counter. Animals were returned to their cages in between blood sampling where they had free access to water. Food was provided in their cages four hours after the initial dose. The cage was equipped with a heating pad to maintain the mice body temperature. After 1 and 4 h of I.V administration, 250 μL of warm saline was given by I.P as the supplemental fluid in order to prevent dehydration. After the last blood sample was obtained (8 h), several organs/tissues were collected, as described previously (Systemic Exposure of Orally Administered GlySar).

### **Metabolic Stability of GlySar after Oral Administration**

PEPT1<sup>+/+</sup> and PEPT1<sup>-/-</sup> mice were fasted overnight prior to the each experiment. The drug was dissolved in normal saline and administered to the mice in aqueous solution. Gastric gavage (20G needle) was used to orally administer a solution of [<sup>14</sup>C]GlySar (10 nmol/g body weight, 0.5 μCi/g body weight, 10 μl/g body weight). Each

mouse was placed separately in a Nalgene metabolic cage with diuresis adapter (Harvard Apparatus Inc., Holliston, MA) for 24 h, where they have free access to water. Food was provided in their cages four hours after the initial oral dose. Urine samples were collected at 8 and 24 h. The urine samples were centrifuged at 15,000 g for 10 min at room temperature, and the supernatants were then frozen at -80°C until analysis by high-performance liquid chromatography (HPLC). Prior to HPLC analysis, the urine samples were diluted 2-fold in water, then analyzed by HPLC (Model 515 Pump, Water, Milford, MA) with radiochromatographic detection (Flo-One 500TR, PerkinElmer Life and Analytical Sciences, Boston, MA). Sample components were separated using a reversed-phase column (Supelco Discovery® C-18, 5 µm, 250 cm × 4.6 mm, Supelco Park, Bellefonte, PA) subjected to a mobile phase of 0.01 M phosphate buffer (pH = 2.0) and 0.1% heptafluorobutyric acid, pumped isocratically at 1 ml /min under ambient temperature. Retention times for glycine and GlySar were 4.8 min and 9.8 min, respectively, under ambient conditions. Stability of GlySar was determined by its recovery and by the appearance of glycine in urine samples.

## **Data Analysis**

Data are reported as mean  $\pm$  SE, unless otherwise noted. Statistical differences between the wild-type and PEPT1 null mice were determined using a two sample student's t-test; for multiple comparisons, one-way variance of analysis (ANOVA) was performed followed by *Dunnett's* test for pairwise comparison with the control group (GraphPad Prism, v4.0; GraphPad Software, Inc., La Jolla, CA).  $p < 0.05$  was considered statistically significant.

## RESULTS

### Dose Dependency of Orally Administered GlySar

In order to probe whether PEPT1 deletion had any effect on the *in vivo* oral absorption of small peptides, GlySar was administered orally over the dose range of 1 to 5000 nmol/g body weight to wild-type and PEPT1 knockout mice (Figs 5.1-5.5). Since it takes approximately 20-30 min for the ingested luminal contents to move 50% of the small intestine length in mouse (Nagakura et al., 1996; Pol et al., 1996; Nagakura et al., 1997; El-Salhy, 2001), and the entire gastrointestinal transit time in mouse is approximately 150-200 min (Nagakura et al., 1996; Nagakura et al., 1997; Schwarz et al., 2002; Friebe et al., 2007; Yamamoto et al., 2008), the oral absorption profiles of GlySar were examined at 120 min, 240 min, and 480 min. With respect to the absorption profile in wild-type mice, GlySar plasma levels rose rapidly and reached a single plateau level at about 90 min for the 1, 10, 100, and 1000 nmol/g doses, and at about 30 min for the 5000 nmol/g dose (Figs 5.1-5.5). For PEPT1 null mice, GlySar plasma levels reached a first plateau at about 90 min and then rose to a second plateau at about 240 min for all 5 doses. As demonstrated in Figs 5.1-5.5, the extent of oral systemic exposure of GlySar was significantly reduced in PEPT1 null mice compared to wild-type mice (especially during the first 2 h) for all tested doses ( $p < 0.01$ ). The extent of GlySar absorption in PEPT1 null mice is approximately 40%, 55% and 70% of that achieved in the wild-type during the 2, 4, and 8 h absorption profile periods, respectively, for all 5 doses (Table 5.1), suggesting a significant role of PEPT1 in the intestinal absorption of GlySar.

GlySar was administered orally over a 5000-fold dose range to explore whether or not there is saturation of the PEPT1 transporter. Dose-corrected AUCs (area under the plasma concentration-time curve) at different doses were compared with 1 nmol/g dose as a control (ANOVA followed by *Dunnett's* test for pairwise comparison). As demonstrated in Fig 5.6, there is dose linearity over doses of 1-100 nmol/g for both genotypes. At doses of 1000 and 5000 nmol/g, dose-corrected AUCs decreased in the same direction for both genotypes, although they have some statistical differences for different AUC calculations. There were 13-20% and 25-35% reductions in dose-corrected AUC values at doses of 1000 and 5000 nmol/g, respectively, when compared to the 1 nmol/g dose for both genotypes. However, reductions in the extent of absorption at both doses are most likely due to GlySar precipitation in the gastrointestinal tract, because of rapid water absorption in the jejunum (Masaoka et al., 2006), as opposed to PEPT1 saturation. We have observed that at the 10,000 nmol/g dose, GlySar had solubility issues in solution (data not shown).

As a method to illustrate potential differences in absorption rate between genotypes, cumulative partial AUC vs. time profiles for the 5 doses of GlySar are shown in Figs 5.7-5.11. As observed in the graphs, for wild-type mice, the curve had a single slope from 20 to 480 min. However, for PEPT null mice, the curves had 2 distinct slopes from 20 to 480 min; a slower slope was observed from 20-120 min and a faster slope was observed from 240-480 min, which was parallel to that of wild-type mice. The transition point for the two slopes in PEPT1 null mice appears to be at about 180 min. As shown in Table 5.2, at 20-120 min, there was approximately a 60% reduction in slope in PEPT1 null mice compared to wild-type mice. In contrast, at 240-480 min, the slope in PEPT1

null mice was very similar to that of wild-type (< 10% difference). We believe these differing slopes represent absorption rate differences between genotypes over the first 2 h followed by similar disposition profiles at later times for PEPT1 null and wild-type mice.

Overall, results from the oral studies suggest that deletion of PEPT1 significantly reduces the rate and extent of oral GlySar absorption during *in vivo* conditions, which is consistent with the findings from *in situ* model (Chapter 4). A linear correlation was also observed between AUC and dose for both genotypes in the dose range of 1-100 nmol/g.

### **Systemic Exposure of Intravenously Administered GlySar**

Fig 5.12 depicts the plasma-concentration profile of GlySar in wild-type and PEPT1 null mice after an i.v. bolus administration of dipeptide at 10 nmol/g dose. As demonstrated, there is a very rapid initial decline in plasma concentration (0-120 min) followed by an extremely slow terminal disposition phase (120-480 min) for both genotypes. The very slow terminal phase could be due to a very efficient reabsorption of GlySar via peptide transporters in kidney (PEPT1 and/or PEPT2) resulting in prolonged recirculation of dipeptide in the body. Notwithstanding the mechanism, the very slow terminal phase precluded an accurate estimate of GlySar terminal half-life and  $AUC_{(0-inf)}$ , along with model fitting of the data. Therefore, AUC values were determined noncompartmentally for the experimental data observed.

### **Tissue Distribution of GlySar**

Due to the expression of PEPT1 in many tissues, in addition to its presence in small intestine, tissue distribution of GlySar was evaluated at 1 and 8 h following its

administration in wild-type and PEPT1 null mice. Fig 5.13 displays the concentration of GlySar in selected tissues 60 min following an oral dose. Comparison of GlySar tissue concentration in PEPT1 null mice to wild-type mice shows that PEPT1 has a major impact on tissue accumulation of GlySar. In particular, wild-type mice had about 7-fold higher tissue accumulation of GlySar in duodenum compared to PEPT1 null mice. Tissue concentrations of GlySar in other tissues were 2 to 4 fold greater in wild-type mice than PEPT1 null mice (Fig 5.13 A). Since the plasma concentrations of GlySar were significantly different between the two genotypes at 60 min (Fig 5.2), the source of GlySar for all tissues except the intestine after oral dosing, the tissue concentrations of dipeptide were corrected by their corresponding plasma concentrations for all tissue other than intestine in order to rule out differences being due to systemic exposure alone (Fig 5.13B). No statistical differences were observed between genotypes in the tissue/plasma concentration ratios of GlySar for all tissues (Fig 5.13 B).

Tissue accumulation of GlySar was also evaluated 8 h after both oral and i.v. bolus administrations. When administered orally, GlySar accumulation was 9.4-fold ( $p < 0.001$ ) and 1.5-fold ( $p < 0.5$ ) higher in duodenum and distal ileum, respectively, in wild-type mice compared to PEPT1 null mice, demonstrating the functional role of PEPT1 in the small intestine (Fig 5.14A). No statistical differences were observed in all other tissues between the two genotypes (Fig 5.14A). When tissue accumulation of GlySar was corrected by its corresponding plasma level for all tissues (intestine omitted), no statistically significant differences between the genotypes were observed either (Fig 5.14B). The consistency between the tissue concentration and tissue/plasma concentration ratio of GlySar at 8 h after oral administration is probably due to the

similarity in GlySar plasma concentrations in the two genotypes at 8 h after the oral gavage (Fig 5.2C). When GlySar was administered by i.v. bolus, wild-type mice had about 1.3 to 9.6 times greater tissue accumulation of dipeptide in selected tissues (i.e., testis, pancreas, heart, small and large intestine, skeletal muscle, eyes, and cerebral cortex) compared to PEPT1 null mice (Fig 5.15A). When the tissue concentration of GlySar was normalized by its corresponding plasma level for all tissues including intestine, no statistically significant differences between the genotypes were observed, except for mid small intestine ( $p < 0.05$ ) (Fig 5.15B).

### **Metabolic Stability of GlySar**

Metabolic stability of GlySar following oral gavage administration was evaluated by high-performance liquid chromatography with radiochemical detection, coupled to liquid scintillation counting spectrometry. At 8 h following the oral administration, 85% and 80% of GlySar was recovered intact in the urine for wild-type and PEPT1 null mice, respectively (Fig 5.16A). Approximately 77% of GlySar was recovered in the urine intact 24 h after dosing for the genotypes (Fig 5.16B). No statistical differences were observed between the two genotypes for GlySar stability. Therefore, GlySar instability was not a confounding issue in these studies, and no further correction of the data was performed.

Previously in our laboratory, we investigated the stability of GlySar following an i.v. bolus dose of dipeptide and demonstrated that 95% of GlySar was recovered in the urine intact 24 h after dosing for wild-type mice (Ocheltree et al., 2005). The difference in metabolic stability of GlySar between the oral (77%) and i.v (95%) administrations



after 24 h suggests a possible metabolism of GlySar in the gastrointestinal tract (e.g., brush border membrane peptidase, enterocyte cytoplasmic peptidases).

## DISCUSSION

PEPT1 is believed to play an important role in the absorption of di/tripeptides, peptidomimetics and peptide-like drugs in the intestine. Previous *in vitro* studies provided important information with respect to PEPT1 structure-function, substrate specificity, substrate affinity, mechanism of transport, and localization. However, most studies were often limited due to a lack of intact blood supply, overlapping substrate specificities, and contribution of multiple transport systems, thus, making it difficult to isolate the relative role of a single gene product (i.e., PEPT1) in relation to other possible transporters that are present in the small intestine. The recent generation of PEPT1 knockout mice (Hu et al., 2008) has provided a unique opportunity to probe the functional activity of PEPT1 under physiological and pathophysiological conditions. Previously, we have investigated the role of PEPT1 in dipeptide (i.e., GlySar) absorption using an *in situ* intestinal perfusion model and found that PEPT1 is responsible for at least 90% of dipeptide uptake in the small intestine (Chapter 4). Although the *in situ* intestinal perfusion model may be reflective of *in vivo* physiological conditions following an oral administration (i.e., intact blood supply, preserved microclimate, brush border enzymes, and transporters) and is widely used in preclinical settings to predict human drug absorption, it also has many limitations (e.g., not having an appropriate intestinal residence time, lacking intestinal motility, and perfused drug not traveling through the whole length of intestine), thus limiting the extrapolation of its finding to the *in vivo* setting. As a result, we have attempted to confirm our findings from the *in situ* model with *in vivo* studies. By using PEPT1 knockout mice under physiological *in vivo* conditions, we were able to demonstrate that PEPT1 ablation significantly reduces the

rate and extent of *in vivo* oral absorption of GlySar in PEPT1 knockout mice as compared to wild-type animals. Moreover, with the exception of small intestine, PEPT1 does not appear to affect the systemic tissue distribution of GlySar.

Human and mouse PEPT1 share many similarities, suggesting that the findings from mouse PEPT1 can be extrapolated to human. At the molecular level, PEPT1 is highly homologous in amino acid sequence (~ 80%) across species (Liang et al., 1995; Miyamoto et al., 1996; Fei et al., 2000), having 83% amino acid identity between human and mouse PEPT1 (Fei et al., 2000). The genomic organization of human PEPT1 also shows high similarity with its mouse orthologue (Urtti et al., 2001). When expressed in *Xenopus laevis* oocytes and transfected cells, human and mouse PEPT1 share many molecular dynamic similarities with respect to their driving force (i.e., pH gradient and membrane potential), substrate specificity, substrate affinity, and sensitivity (Liang et al., 1995; Mackenzie et al., 1996; Fei et al., 2000). In both species, the PEPT1 transporter is expressed in small intestine and kidney (Liang et al., 1995; Zhang et al., 2004; Hu et al., 2008). With immunolocalization studies, it was demonstrated that PEPT1 is expressed in the apical membrane of small intestine (i.e., duodenum, jejunum and ileum), but not in colon for both human and mouse (Walker et al., 1998; Groneberg et al., 2001). Gene expression studies have shown that mouse and human have comparative intestinal expression levels, whereas PEPT1 expression levels in rat were several-fold higher (Kim et al., 2007), suggesting that the PEPT1 mediated intestinal absorption of peptide substrates in human is more similar to mouse than rat.

In the current study, we administered GlySar over a 1-5000 nmol/g dose range, which reflects the physiological range of daily protein consumption. According to

Ganapathy *et. al.* (2006), the estimated concentration of dipeptides and tripeptides after the digestion of protein in the intestinal lumen can reach as high as 100 mM. In the present study, the volume of oral gavage was 200  $\mu$ l/20 g body weight at every dose. Studies by McConnell and coworkers (2008) have suggested that the water content of mouse gastrointestinal tract is approximately 0.4 g, which would correspond to 0.4 ml (assuming 1 g/ml density approximation). Thus, with an average body weight of 20 g/mouse, current doses of 1, 10, 100, 1000 and 5000 nmol/g of GlySar would approximate to 0.033, 0.33, 3.3, 33, and 167 mM, respectively, in the small intestine.

Absorption in the intestine is influenced by many factors including the intrinsic permeability of compounds, surface area of the intestinal membrane, drug concentration in the intestinal lumen, pore radius for paracellular pathways, thickness of the mucus layer, membrane fluidity that affects the passive permeability, and the gastrointestinal transit time that controls the residence time of the compound in the intestine (Masaoka *et al.*, 2006). Among these factors, permeability through the membrane, luminal drug concentration, and residence time are considered the most important factors for oral drug absorption (Kimura and Higaki, 2002; Masaoka *et al.*, 2006). Luminal drug concentration following oral administration changes due to its absorption in each intestinal segment as well as because of changes in fluid volume of each intestinal segment. In wild-type mice, the concentration of GlySar probably decreases rapidly as it travels through the intestine due to a rapid absorption via PEPT1. As a result, we might not observe a noticeable saturation of PEPT1 even at a high oral dose of 1000 or 5000 nmol/g (equates to 33 and 167 mM, respectively) which are estimated to be above the  $K_m$  value of GlySar in mouse small intestine (i.e., intrinsic  $K_m = 5.5$  mM and apparent  $K_m =$

19 mM for GlySar in mouse *in situ* intestinal perfusion model, Chapter 4). In contrast, in PEPT1 knockout mice, due to the lack of GlySar absorption via PEPT1, higher concentrations of GlySar might become available at later intestinal segments, thus having higher driving force for passive permeability in these regions than in wild-type. The increased role of passive permeability at the later intestinal segments might explain the second rise in GlySar plasma concentrations from 120-240 min in PEPT1 null mice (Figs 5.1-5.5).

We believe that the reduction in dose-corrected AUCs in both genotypes at 1000 and 5000 nmol/g doses (Fig 5.6) are most likely due to the precipitation of GlySar in the gastrointestinal tract because of rapid water absorption in the jejunum, especially in PEPT1 null mice. If it was only due to saturation of the PEPT1 transporter, we would not have observed a similar reduction in dose-corrected AUCs in PEPT1 knockout mice. Masaoka and coworkers (2006) have reported that for a poorly permeable compound, drug concentrations in the small intestine could get 2-5 fold higher than the administered dose concentration due a quick absorption of ingested water in the jejunum. This phenomenon could be the case in PEPT1 null mice at high GlySar concentrations (i.e., 1000 and 5000 nmol/g doses), resulting in precipitation of GlySar and, consequently, a reduction in the dose-corrected AUCs. In wild-type mice, the reduction in dose-corrected AUCs at 1000 and 5000 nmol/g doses could be due to a combined effect of GlySar precipitation at those doses (because of a rapid water absorption) and partial saturation of PEPT1 transporter.

Although there is general consensus about using AUC as an indicator of extent of absorption, there are several indirect measures for assessment of absorption rate such

$C_{\max}$ ,  $t_{\max}$ , and partial AUC (Chen et al., 2001). Among these, partial AUC has been suggested to be a more sensitive measure of absorption rate than  $C_{\max}$  and/or  $t_{\max}$  (Chen, 1992). In the current study, the ratio of  $AUC_{0-8h}$  of PEPT1 knockout mice to wild-type mice is about 0.7-0.75 (Table 5.1, Figs 5.1-5.5), suggesting a 25-30% decrease in extent of GlySar absorption due to PEPT1 deletion. When partial AUCs (0-2 h) were compared as a mean of assessment of rate of absorption, there was a 60% reduction in absorption rate of GlySar due to deletion of PEPT1 (Table 5.1, Figs 5.1-5.5). When incremental accumulative partial AUC was plotted versus time, there was a 60% decrease in the slope (0-2 h) of the plot in the PEPT1 null mice compared to that of wild-type (Table 5.2, Figs 5.7-5.11), again suggesting an approximately 60% reduction in rate of GlySar absorption due to the deletion of PEPT1 transporter. However, when rates of accumulative partial AUC increase were compared at 240-480 min, the two genotypes had very similar slopes, suggesting a similar disposition profile at these later time points.

When GlySar was administered by i.v. bolus, there was an exceptionally slow terminal elimination phase (120-480 min) for both wild-type and PEPT1 null mice (Fig 5.12). The very slow terminal elimination phase could be due to an efficient reabsorption of GlySar via peptide transporters in kidney (PEPT1 and/or PEPT2) causing a recirculation of dipeptide in the body. When GlySar plasma levels are compared between wild-type and PEPT1 null mice, there is a 25% reduction in GlySar plasma level in PEPT1 knockout mice in terminal phase (120-480 min) compared to wild-type mice (Fig 5.12). The slow terminal phase could be due to a number of other factors such as reabsorption of GlySar in kidney by processes other than PEPT1/PEPT2 and equilibration of GlySar in peripheral tissues and plasma.

The relative importance of PEPT1 was quite dramatic during *in situ* single-pass perfusions of GlySar in jejunal tissue, in which a > 90% reduction in GlySar permeability was observed in PEPT1 knockout mice compared to wild-type mice (Chapter 4). Although the current *in vivo* studies corroborate the *in situ* findings, the magnitude of PEPT1's relevance was much smaller during the *in vivo* studies, in which an approximate 50% reduction in the extent of GlySar absorption was observed in PEPT1 null mice compared to wild-type mice over 8 h (Table 5.1). Other mechanisms (e.g., passive permeability, paracellular permeability) may play a bigger role in the *in vivo* absorption of GlySar than previously believed. A possible compensatory response to deletion of PEPT1 by up-regulation of PEPT2, PHT1 and PHT2 has already been ruled out during the initial development and validation of PEPT1 deficient mice (Hu et al., 2008). The difference we observed between the *in situ* and *in vivo* conditions may reflect the residual length of the entire intestine such that the longer residence time of a drug may increase its passive permeability, thereby, diminishing the role of the active transporter PEPT1. Additionally, passive permeability might play an even larger role in the absence of PEPT1 transport in the null mice. This speculation is in agreement with the findings from Hironaka and coworkers' (2009) where PEPT1 contributed to one-half of total absorption of cephalexin and its function was compensated by passive diffusion if PEPT1 does not function properly.

In conclusion, the current study demonstrates that ablation of PEPT1 significantly reduced the *in vivo* rate and extent of oral absorption of dipeptides (i.e., GlySar) in PEPT1 null compared to wild-type mice following an oral administration. However, the extent of PEPT1's relevance during the *in vivo* oral absorption studies of dipeptide is not

as remarkable as previously thought based on *in vitro* and *in situ* models. Other than small intestine, PEPT1 does not appear to affect the tissue distribution of GlySar.

Further studies will be directed at understanding the effect of PEPT1 on the oral absorption of peptidomimetic therapeutic agents such as cefadroxil and valacyclovir during *in vivo* conditions. In addition, the effect of PEPT1 deletion on intestinal motility, intestinal transient time, and food effects on drug absorption should be examined.



## FIGURES

1 nmol/g

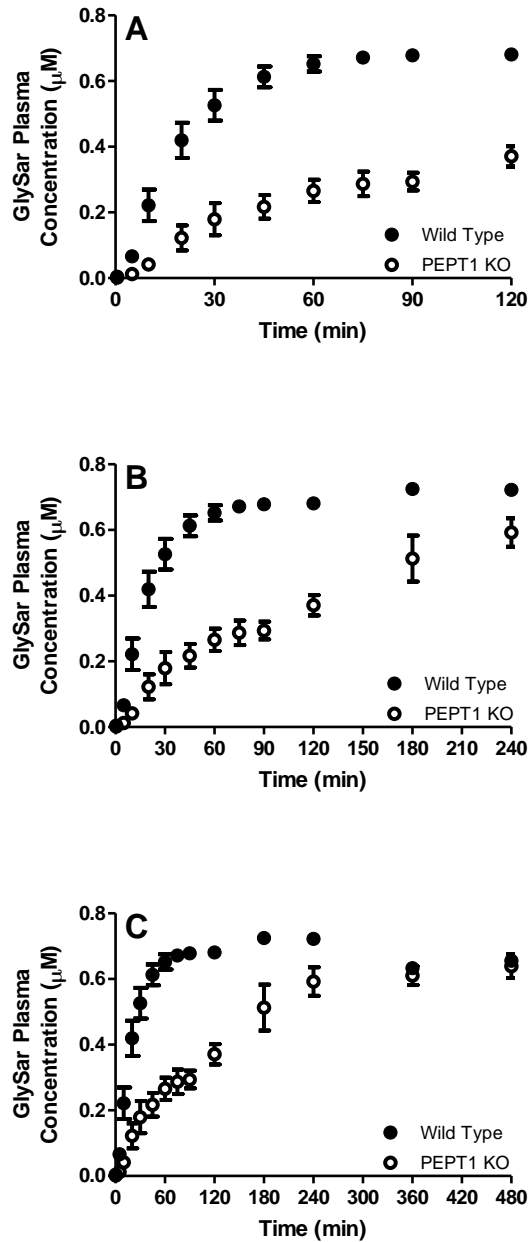


**Figure 5.1** Plasma concentrations of GlySar as a function of time over 120 min (A), 240 min (B), and 480 min (C) in PEPT1<sup>+/+</sup> (wild-type) and PEPT1<sup>-/-</sup> (KO) mice following a 1 nmol/g oral gavage dose. Data are expressed as mean ± S.E. (n = 4).

10 nmol/g

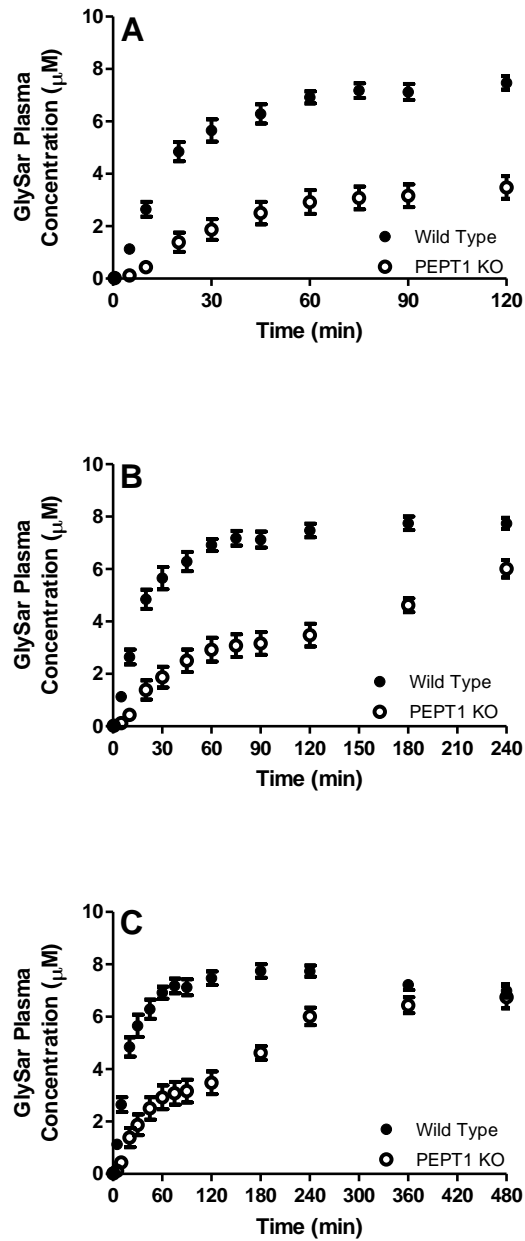


**Figure 5.2** Plasma concentrations of GlySar as a function of time over 120 min (A), 240 min (B), and 480 min (C) in PEPT1<sup>+/+</sup> (wild-type) and PEPT1<sup>-/-</sup> (KO) mice following a 10 nmol/g oral gavage dose. Data are expressed as mean  $\pm$  S.E. (n = 6).

100 nmol/g

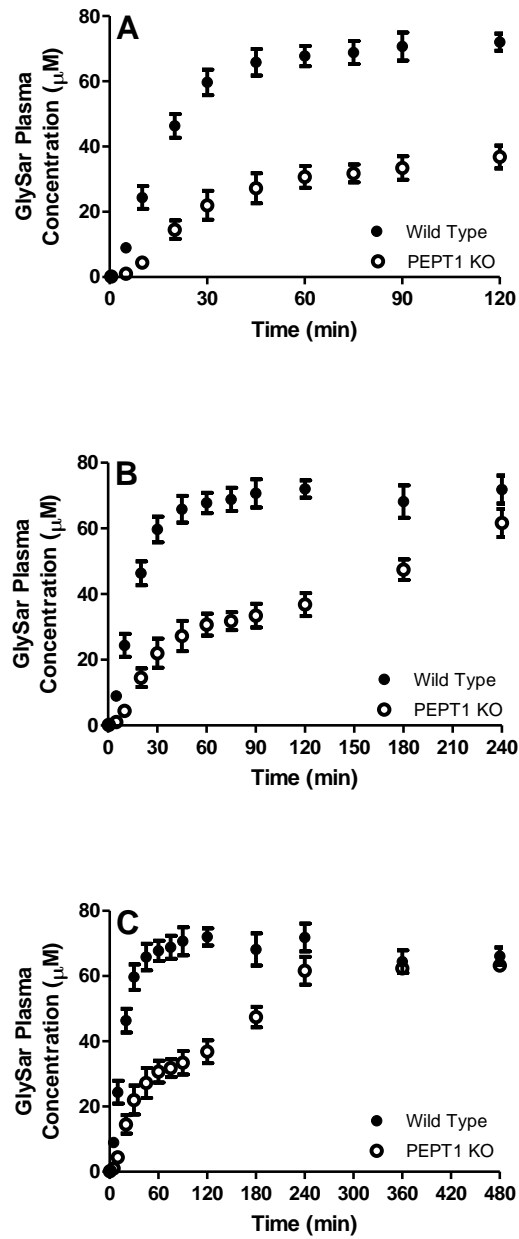


**Figure 5.3** Plasma concentrations of GlySar as a function of time over 120 min (A), 240 min (B), and 480 min (C) in PEPT1<sup>+/+</sup> (wild-type) and PEPT1<sup>-/-</sup> (KO) mice following a 100 nmol/g oral gavage dose. Data are expressed as mean  $\pm$  S.E. (n = 4).

1000 nmol/g

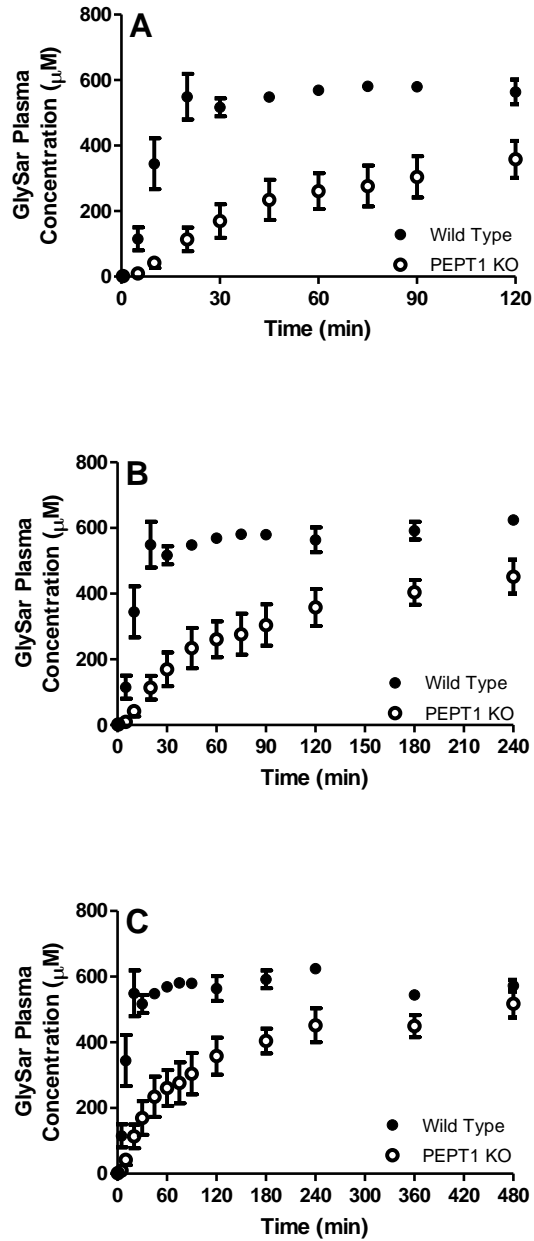


**Figure 5.4** Plasma concentrations of GlySar as a function of time over 120 min (A), 240 min (B), and 480 min (C) in PEPT1<sup>+/+</sup> (wild-type) and PEPT1<sup>-/-</sup> (KO) mice following a 1000 nmol/g oral gavage dose. Data are expressed as mean ± S.E. (n = 5).

5000 nmol/g

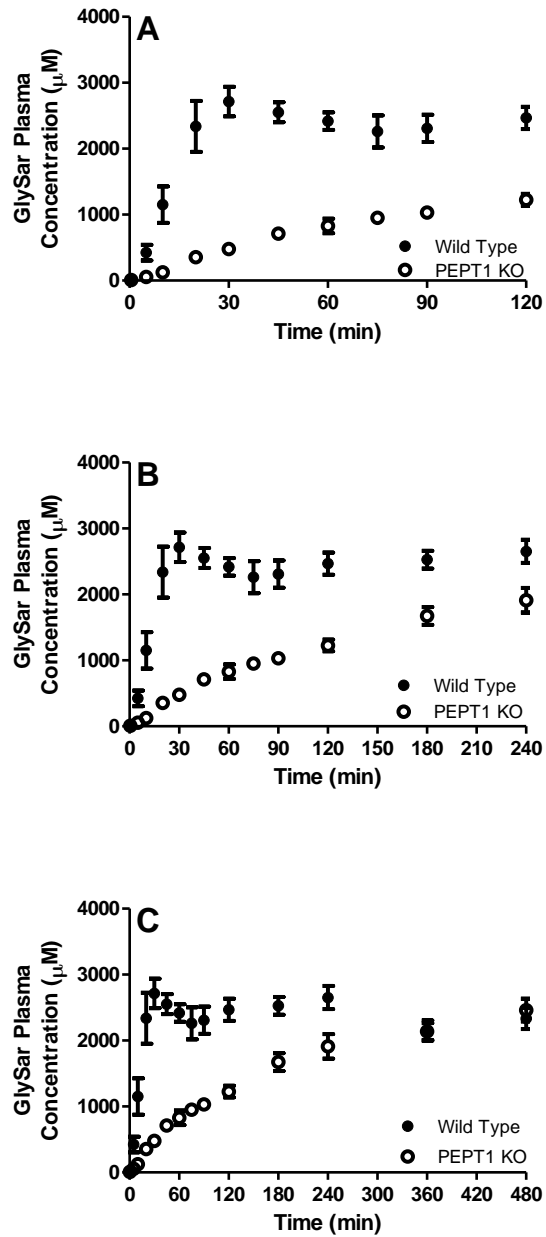


**Figure 5.5** Plasma concentrations of GlySar as a function of time over 120 min (A), 240 min (B), and 480 min (C) in PEPT1<sup>+/+</sup> (wild-type) and PEPT1<sup>-/-</sup> (KO) mice following a 5000 nmol/g oral gavage dose. Data are expressed as mean  $\pm$  S.E. (n = 4).

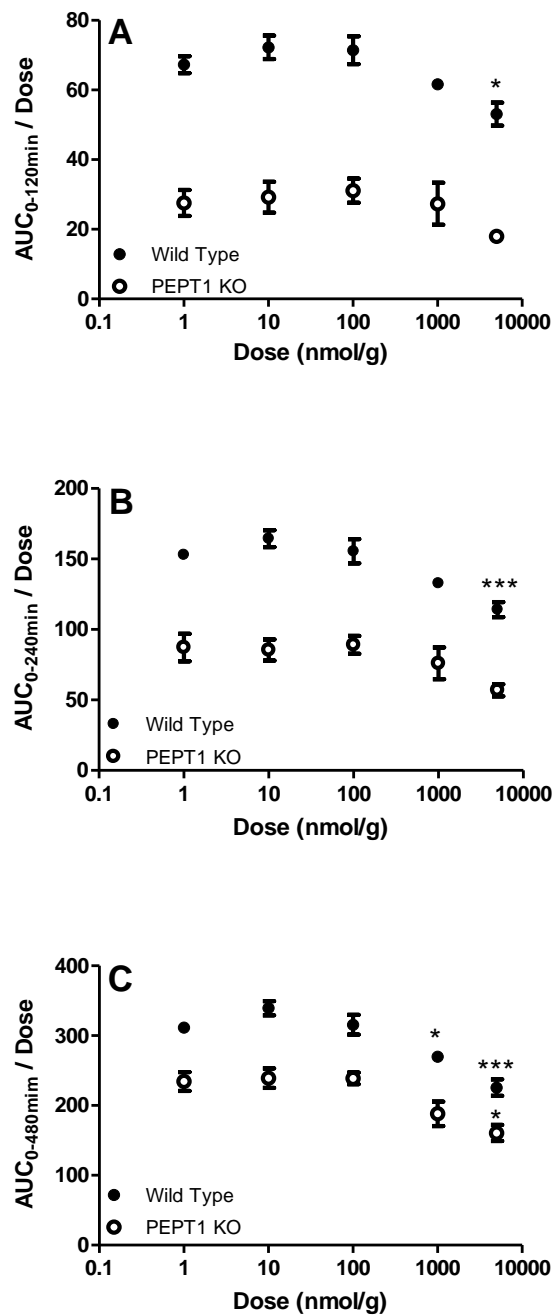


**Figure 5.6** Dose-corrected cumulative partial area under the plasma concentration-time curves vs. dose of GlySar in PEPT1<sup>+/+</sup> (wild-type) and PEPT1<sup>-/-</sup> (KO) mice after an oral gavage administration. Data are expressed as mean  $\pm$  S.E. (n = 4-6). \* p < 0.05; \*\*\* p < 0.001 compared with 1 nmol/g dose.

1 nmol/g

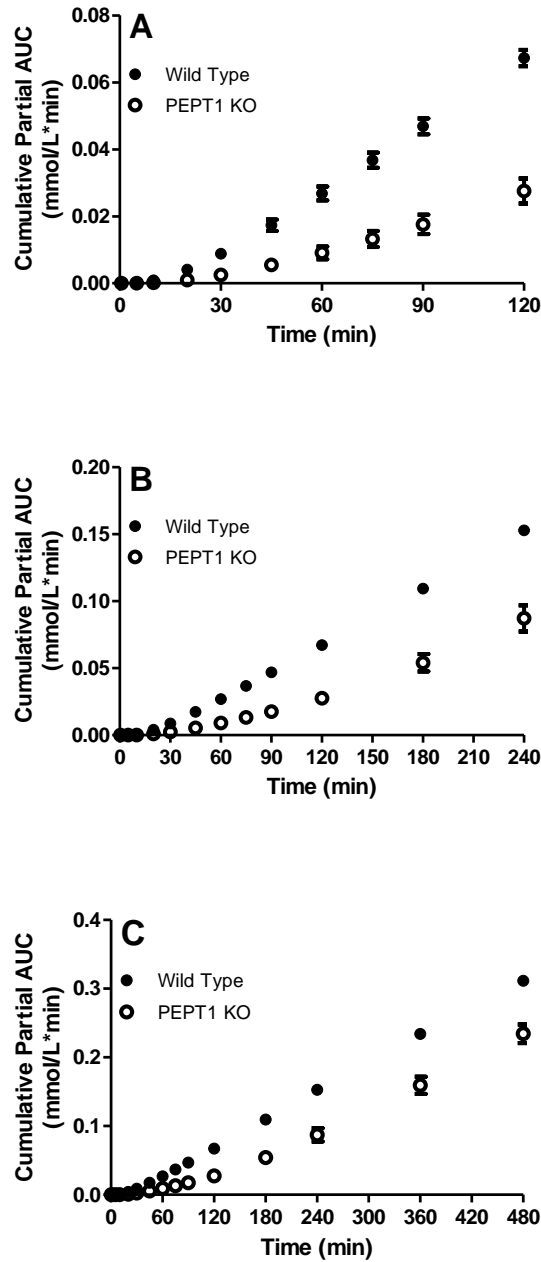


**Figure 5.7** Cumulative partial AUCs (area under the plasma concentration-time curves) of GlySar as a function of time over 120 min (A), 240 min (B), and 480 min (C) in PEPT1<sup>+/+</sup> (wild-type) and PEPT1<sup>-/-</sup> (KO) mice following a 1 nmol/g oral gavage dose. Data are expressed as mean ± S.E. (n = 4).

10 nmol/g

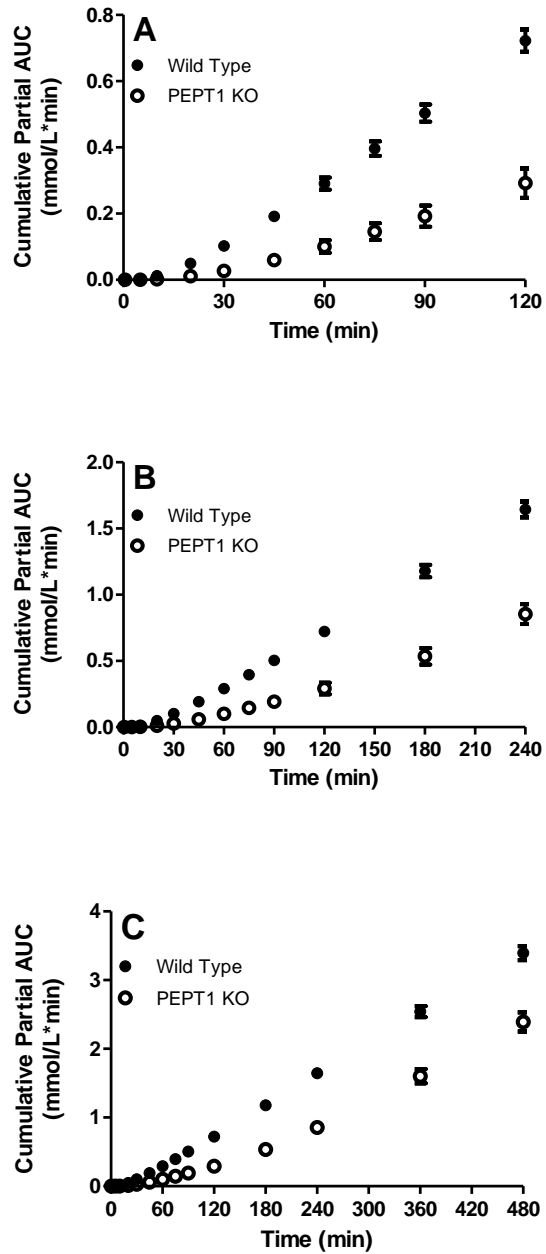


**Figure 5.8** Cumulative partial AUCs (area under the plasma concentration-time curves) of GlySar as a function of time over 120 min (A), 240 min (B), and 480 min (C) in PEPT1<sup>+/+</sup> (wild-type) and PEPT1<sup>-/-</sup> (KO) mice following a 10 nmol/g oral gavage dose. Data are expressed as mean  $\pm$  S.E. (n = 6).



100 nmol/g

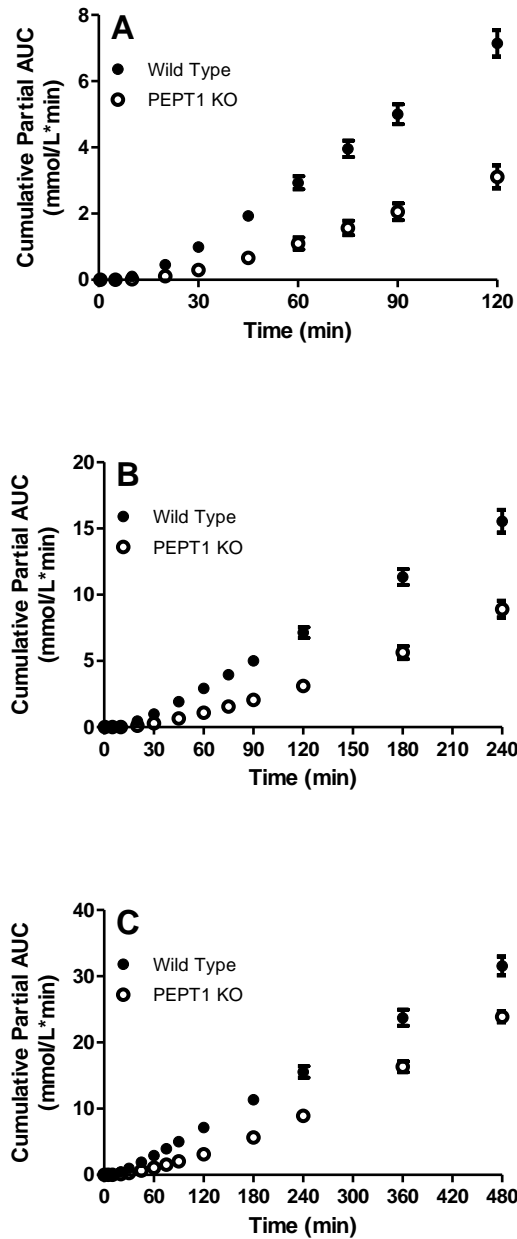


**Figure 5.9** Cumulative partial AUCs (area under the plasma concentration-time curves) of GlySar as a function of time over 120 min (A), 240 min (B), and 480 min (C) in PEPT1<sup>+/+</sup> (wild-type) and PEPT1<sup>-/-</sup> (KO) mice following a 100 nmol/g oral gavage dose. Data are expressed as mean  $\pm$  S.E. (n = 4).

1000 nmol/g

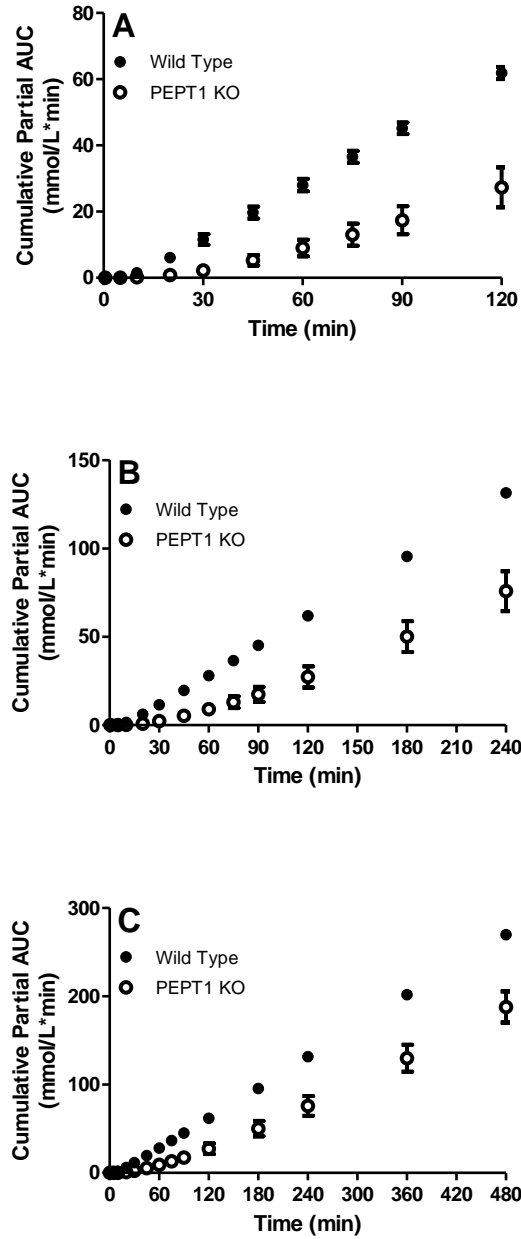


**Figure 5.10** Cumulative partial AUCs (area under the plasma concentration-time curves) of GlySar as a function of time over 120 min (A), 240 min (B), and 480 min (C) in PEPT1<sup>+/+</sup> (wild-type) and PEPT1<sup>-/-</sup> (KO) mice following a 1000 nmol/g oral gavage dose. Data are expressed as mean  $\pm$  S.E. (n = 5).

5000 nmol/g

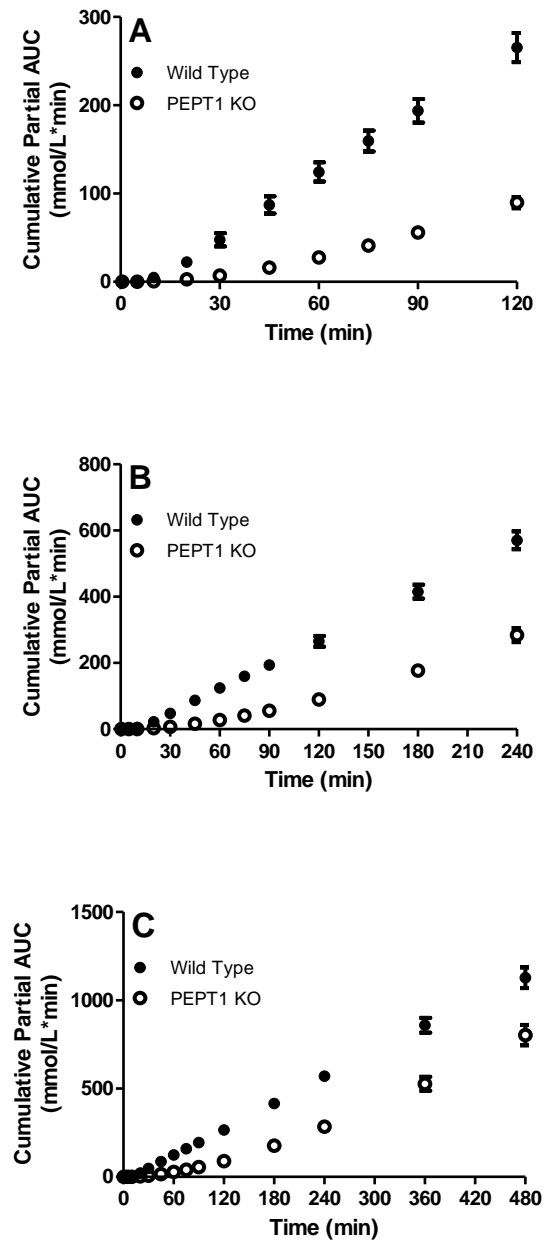


**Figure 5.11** Cumulative partial AUCs (area under the plasma concentration-time curves) of GlySar as a function of time over 120 min (A), 240 min (B), and 480 min (C) in PEPT1<sup>+/+</sup> (wild-type) and PEPT1<sup>-/-</sup> (KO) mice following a 5000 nmol/g oral gavage dose. Data are expressed as mean  $\pm$  S.E. (n = 4).

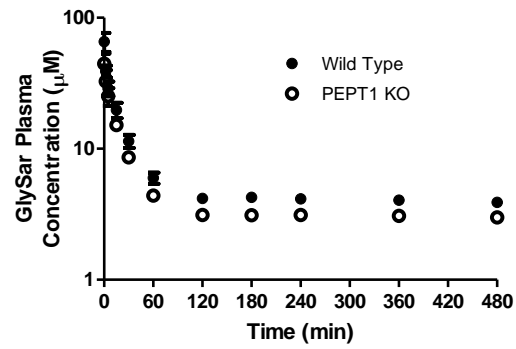


**Figure 5.12** Plasma concentration-time profiles of GlySar in PEPT1<sup>+/+</sup> (wild-type) and PEPT1<sup>-/-</sup> (KO) mice after intravenous bolus administration of dipeptide at a dose of 10 nmol/g. Data are expressed as mean  $\pm$  S.E. (n=4-8)

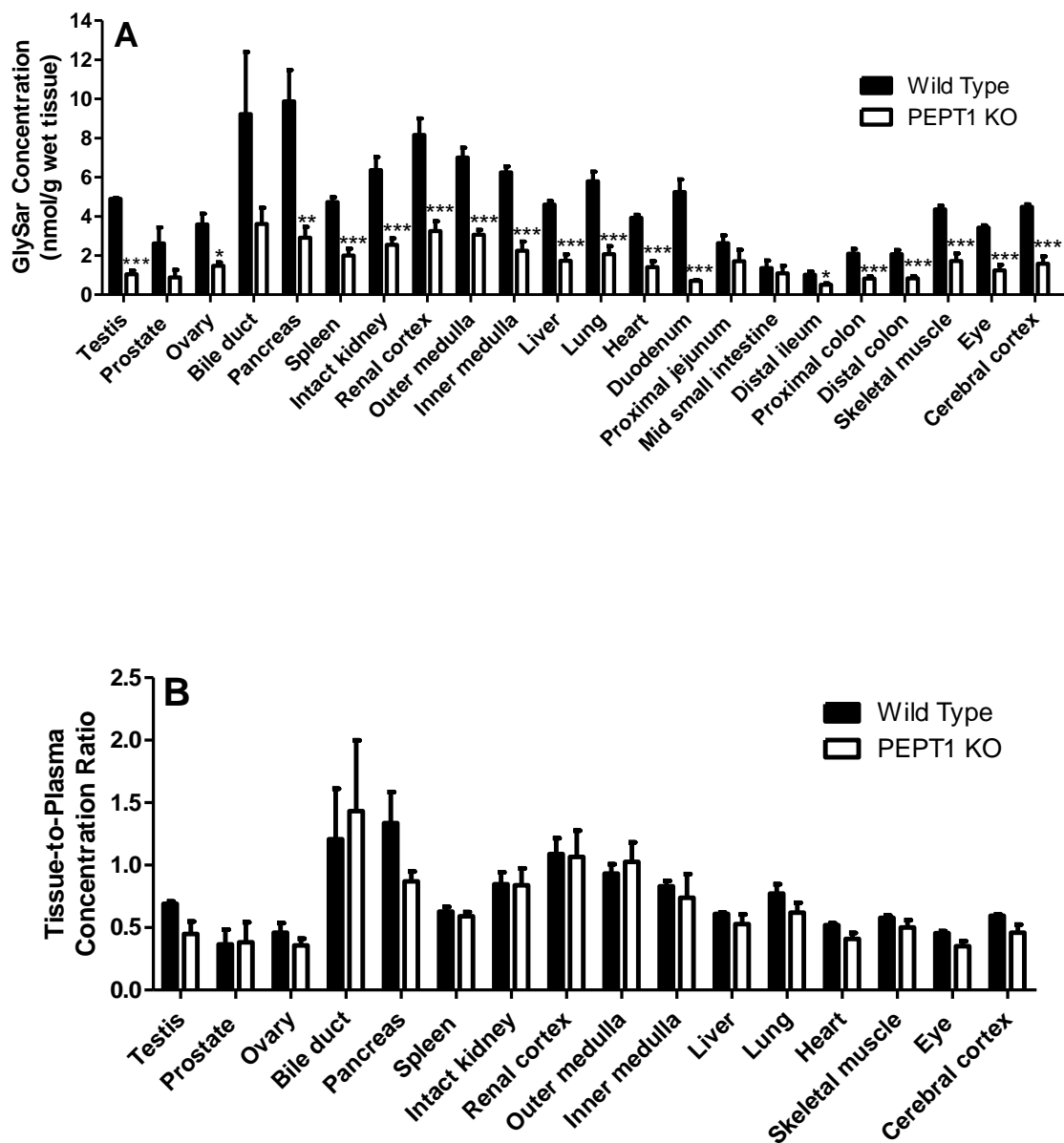


**Figure 5.13** Tissue concentration (A) and tissue-to-plasma concentration ratio (B) of GlySar in PEPT1<sup>+/+</sup> (wild-type) and PEPT1<sup>-/-</sup> (KO) mice, 60 min after oral gavage administration of dipeptide at 10 nmol/g. Data are expressed as mean ± S.E. (n=6). \* p < 0.05; \*\* p < 0.01; \*\*\* p < 0.001 compared with wild-type mice.

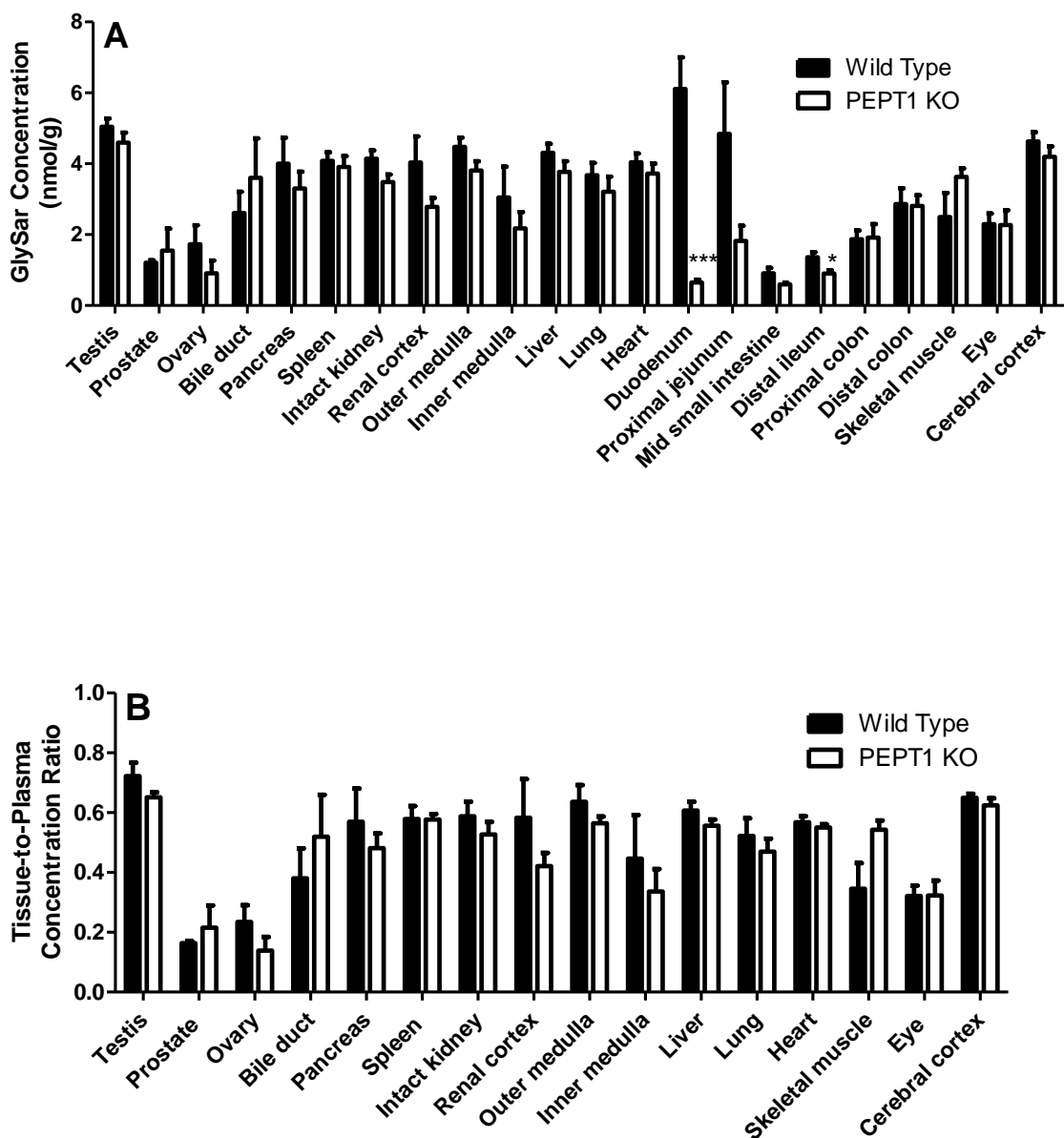


**Figure 5.14** Tissue concentration (A) and tissue-to-plasma concentration ratio (B) of GlySar in PEPT1<sup>+/+</sup> (wild-type) and PEPT1<sup>-/-</sup> (KO) mice, 8 h after oral gavage administration of dipeptide at 10 nmol/g. Data are expressed as mean  $\pm$  S.E. (n=6). \* p < 0.05; \*\* p < 0.01; \*\*\* p < 0.001 compared with wild-type mice.

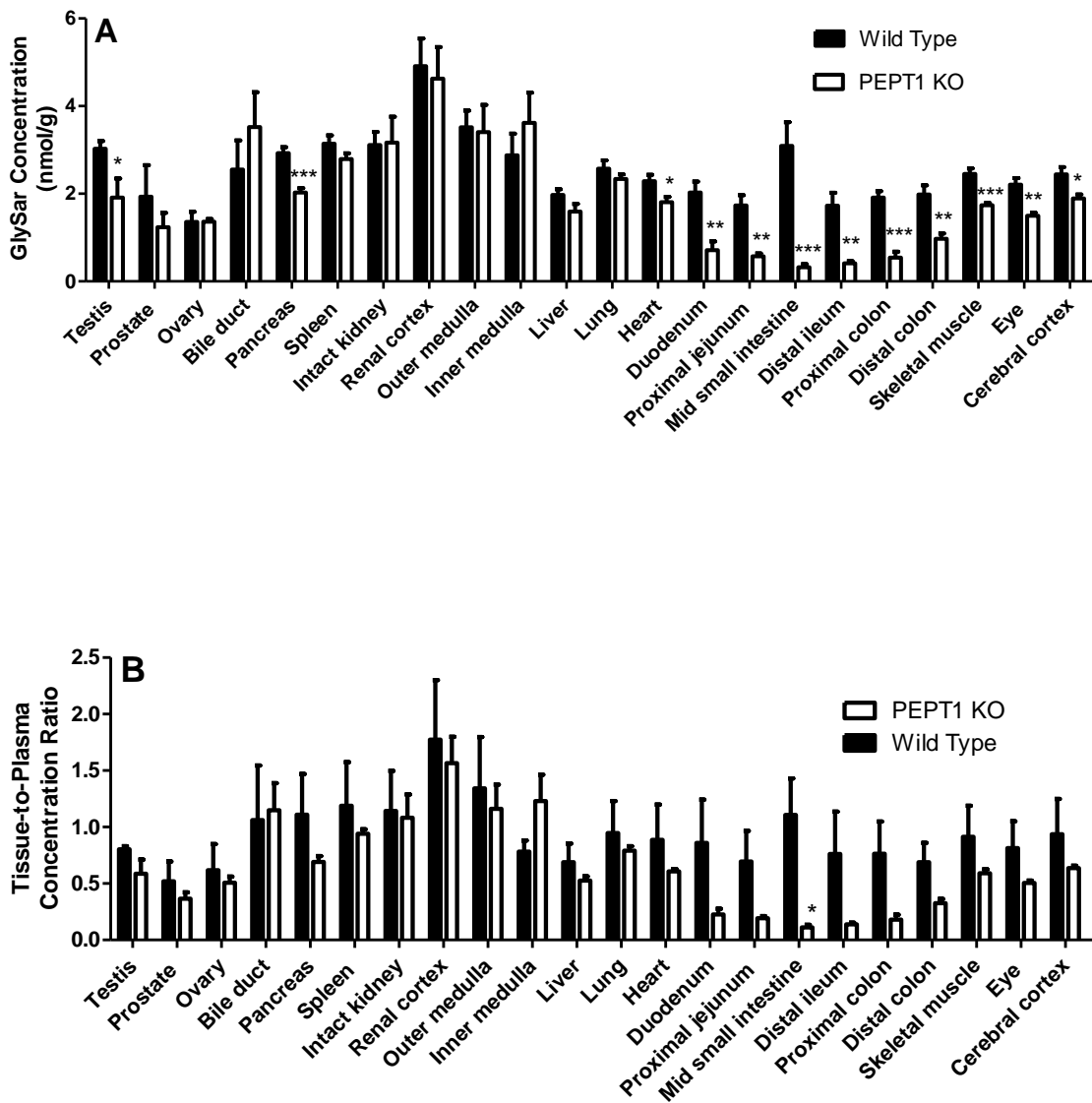


**Figure 5.15** Tissue concentration (A) and tissue-to-plasma concentration ratio (B) of GlySar in PEPT1<sup>+/+</sup> (wild-type) and PEPT1<sup>-/-</sup> (KO) mice, 8 h after intravenous bolus administration of dipeptide at 10 nmol/g. Data are expressed as mean ± S.E. (n=6). \* p < 0.05; \*\* p < 0.01; \*\*\* p < 0.001 compared with wild-type mice.

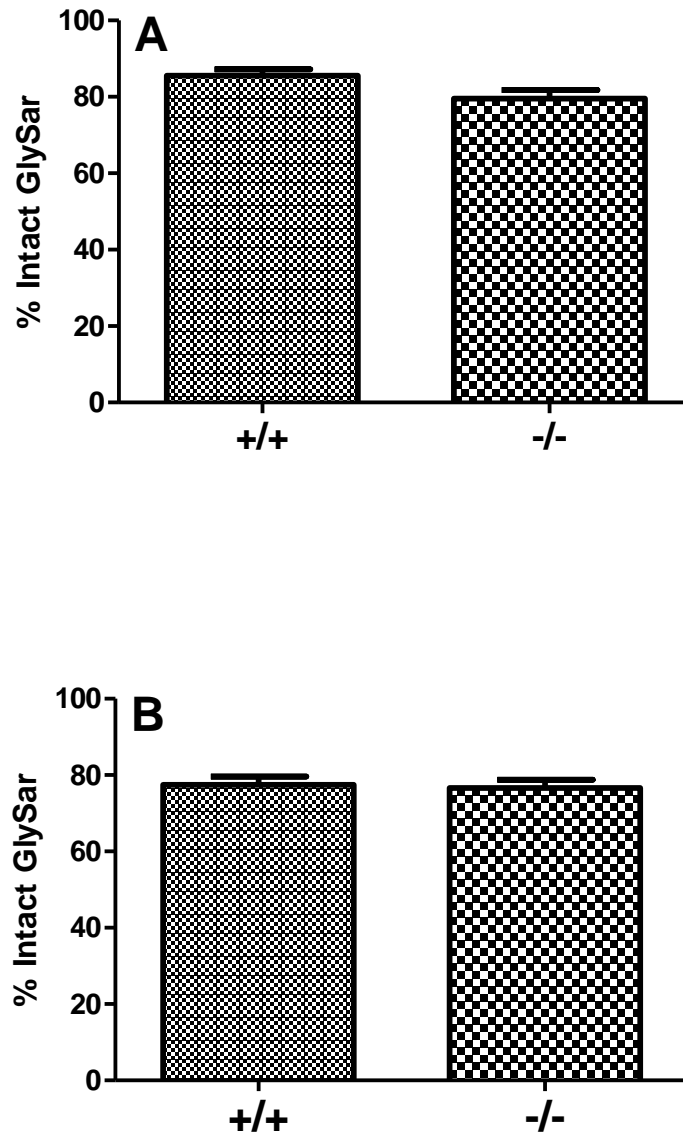


**Figure 5.16** Metabolic stability of GlySar in PEPT1<sup>+/+</sup> (wild-type) and PEPT1<sup>-/-</sup> (KO) mice urine over 8 hours (A) and over 24 hours (B) after oral dose administration of dipeptide at 10 nmol/g body weight. Data are presented as mean  $\pm$  SE (n=4).



**Table 5.1** Ration of extent of GlySar systemic exposure in PEPT1 null mice to wild-type at different time point with respect to dose following oral administration (corresponds to Fig 5.1-5.5).

Dose (nmol/g)	AUC <sub>KO</sub> /AUC <sub>WT</sub>		
	0-120 min	0-240 min	0-480 min
1	0.41	0.57	0.75
10	0.40	0.52	0.70
100	0.44	0.57	0.76
1000	0.44	0.57	0.70
5000	0.34	0.50	0.71

**Table 5.2** Dose-corrected slopes of accumulative partial AUC vs. time (Corresponds to Fig 5.7-5.11)

Dose (nmol/g)	20-120 min			240-480 min		
	Wild-type	PEPT1 KO	Ratio	Wild-type	PEPT1 KO	Ratio
1	0.64	0.27	0.42	0.66	0.61	0.93
10	0.68	0.28	0.42	0.73	0.64	0.88
100	0.67	0.30	0.45	0.67	0.62	0.94
1000	0.56	0.27	0.48	0.57	0.47	0.82
5000	0.49	0.17	0.36	0.46	0.43	0.93

## REFERENCES

Bhardwaj RK, Herrera-Ruiz D, Eltoukhy N, Saad M and Knipp GT (2006) The functional evaluation of human peptide/histidine transporter 1 (hPHT1) in transiently transfected COS-7 cells. *Eur J Pharm Sci* **27**:533-542.

Bockman DE, Ganapathy V, Oblak TG and Leibach FH (1997) Localization of peptide transporter in nuclei and lysosomes of the pancreas. *Int J Pancreatol* **22**:221-225.

Chen ML (1992) An alternative approach for assessment of rate of absorption in bioequivalence studies. *Pharm Res* **9**:1380-1385.

Chen ML, Lesko L and Williams RL (2001) Measures of exposure versus measures of rate and extent of absorption. *Clin Pharmacokinet* **40**:565-572.

Daniel H and Kottra G (2004) The proton oligopeptide cotransporter family SLC15 in physiology and pharmacology. *Pflugers Arch* **447**:610-618.

El-Salhy M (2001) Gastrointestinal transit in nonobese diabetic mouse: an animal model of human diabetes type 1. *J Diabetes Complications* **15**:277-284.

Fei YJ, Kanai Y, Nussberger S, Ganapathy V, Leibach FH, Romero MF, Singh SK, Boron WF and Hediger MA (1994) Expression cloning of a mammalian proton-coupled oligopeptide transporter. *Nature* **368**:563-566.

Fei YJ, Sugawara M, Liu JC, Li HW, Ganapathy V, Ganapathy ME and Leibach FH (2000) cDNA structure, genomic organization, and promoter analysis of the mouse intestinal peptide transporter PEPT1. *Biochim Biophys Acta* **1492**:145-154.

Friebe A, Mergia E, Dangel O, Lange A and Koesling D (2007) Fatal gastrointestinal obstruction and hypertension in mice lacking nitric oxide-sensitive guanylyl cyclase. *Proc Natl Acad Sci U S A* **104**:7699-7704.

Ganapathy V, Gupta N and Martindale RG (2006) Protein Digestion and Absorption, in: *Physiology of the Gastrointestinal Tract* (Johnson LR ed), pp 1667-1692, Elsevier, Burlington.

Groneberg DA, Doring F, Eynott PR, Fischer A and Daniel H (2001) Intestinal peptide transport: ex vivo uptake studies and localization of peptide carrier PEPT1. *Am J Physiol Gastrointest Liver Physiol* **281**:G697-704.

- Herrera-Ruiz D and Knipp GT (2003) Current perspectives on established and putative mammalian oligopeptide transporters. *J Pharm Sci* **92**:691-714.
- Herrera-Ruiz D, Wang Q, Gudmundsson OS, Cook TJ, Smith RL, Faria TN and Knipp GT (2001) Spatial expression patterns of peptide transporters in the human and rat gastrointestinal tracts, Caco-2 in vitro cell culture model, and multiple human tissues. *AAPS PharmSci* **3**:E9.
- Hironaka T, Itokawa S, Ogawara K, Higaki K and Kimura T (2009) Quantitative evaluation of PEPT1 contribution to oral absorption of cephalexin in rats. *Pharm Res* **26**:40-50.
- Hu Y, Smith DE, Ma K, Jappar D, Thomas W and Hillgren KM (2008) Targeted Disruption of Peptide Transporter Pept1 Gene in Mice Significantly Reduces Dipeptide Absorption in Intestine. *Mol Pharm.*
- Inui K, Terada T, Masuda S and Saito H (2000) Physiological and pharmacological implications of peptide transporters, PEPT1 and PEPT2. *Nephrol Dial Transplant* **15 Suppl 6**:11-13.
- Kim HR, Park SW, Cho HJ, Chae KA, Sung JM, Kim JS, Landowski CP, Sun D, Abd El-Aty AM, Amidon GL and Shin HC (2007) Comparative gene expression profiles of intestinal transporters in mice, rats and humans. *Pharmacol Res* **56**:224-236.
- Kimura T and Higaki K (2002) Gastrointestinal transit and drug absorption. *Biol Pharm Bull* **25**:149-164.
- Knutter I, Rubio-Aliaga I, Boll M, Hause G, Daniel H, Neubert K and Brandsch M (2002) H<sup>+</sup>-peptide cotransport in the human bile duct epithelium cell line SK-ChA-1. *Am J Physiol Gastrointest Liver Physiol* **283**:G222-229.
- Liang R, Fei YJ, Prasad PD, Ramamoorthy S, Han H, Yang-Feng TL, Hediger MA, Ganapathy V and Leibach FH (1995) Human intestinal H<sup>+</sup>/peptide cotransporter. Cloning, functional expression, and chromosomal localization. *J Biol Chem* **270**:6456-6463.
- Liu W, Liang R, Ramamoorthy S, Fei YJ, Ganapathy ME, Hediger MA, Ganapathy V and Leibach FH (1995) Molecular cloning of PEPT 2, a new member of the H<sup>+</sup>/peptide cotransporter family, from human kidney. *Biochim Biophys Acta* **1235**:461-466.
- Lu H and Klaassen C (2006) Tissue distribution and thyroid hormone regulation of Pept1 and Pept2 mRNA in rodents. *Peptides* **27**:850-857.

- Mackenzie B, Loo DD, Fei Y, Liu WJ, Ganapathy V, Leibach FH and Wright EM (1996) Mechanisms of the human intestinal H<sup>+</sup>-coupled oligopeptide transporter hPEPT1. *J Biol Chem* **271**:5430-5437.
- Masaoka Y, Tanaka Y, Kataoka M, Sakuma S and Yamashita S (2006) Site of drug absorption after oral administration: assessment of membrane permeability and luminal concentration of drugs in each segment of gastrointestinal tract. *Eur J Pharm Sci* **29**:240-250.
- Matthews DM (1975) Intestinal absorption of peptides. *Physiol Rev* **55**:537-608.
- McConnell EL, Basit AW and Murdan S (2008) Measurements of rat and mouse gastrointestinal pH, fluid and lymphoid tissue, and implications for in-vivo experiments. *J Pharm Pharmacol* **60**:63-70.
- Miyamoto K, Shiraga T, Morita K, Yamamoto H, Haga H, Taketani Y, Tamai I, Sai Y, Tsuji A and Takeda E (1996) Sequence, tissue distribution and developmental changes in rat intestinal oligopeptide transporter. *Biochim Biophys Acta* **1305**:34-38.
- Nagakura Y, Ito H, Kiso T, Naitoh Y and Miyata K (1997) The selective 5-hydroxytryptamine (5-HT)<sub>4</sub>-receptor agonist RS67506 enhances lower intestinal propulsion in mice. *Jpn J Pharmacol* **74**:209-212.
- Nagakura Y, Naitoh Y, Kamato T, Yamano M and Miyata K (1996) Compounds possessing 5-HT<sub>3</sub> receptor antagonistic activity inhibit intestinal propulsion in mice. *Eur J Pharmacol* **311**:67-72.
- Ocheltree SM, Shen H, Hu Y, Keep RF and Smith DE (2005) Role and relevance of peptide transporter 2 (PEPT2) in the kidney and choroid plexus: in vivo studies with glycylsarcosine in wild-type and PEPT2 knockout mice. *J Pharmacol Exp Ther* **315**:240-247.
- Ogihara H, Saito H, Shin BC, Terado T, Takenoshita S, Nagamachi Y, Inui K and Takata K (1996) Immuno-localization of H<sup>+</sup>/peptide cotransporter in rat digestive tract. *Biochem Biophys Res Commun* **220**:848-852.
- Peng SX, Rockafellow BA, Skedzielewski TM, Huebert ND and Hageman W (2009) Improved pharmacokinetic and bioavailability support of drug discovery using serial blood sampling in mice. *J Pharm Sci* **98**:1877-1884.
- Pol O, Valle L, Ferrer I and Puig MM (1996) The inhibitory effects of alpha(2)-adrenoceptor agonists on gastrointestinal transit during croton oil-induced intestinal inflammation. *Br J Pharmacol* **119**:1649-1655.

- Rubio-Aliaga I, Boll M and Daniel H (2000) Cloning and characterization of the gene encoding the mouse peptide transporter PEPT2. *Biochem Biophys Res Commun* **276**:734-741.
- Saito H, Okuda M, Terada T, Sasaki S and Inui K (1995) Cloning and characterization of a rat H<sup>+</sup>/peptide cotransporter mediating absorption of beta-lactam antibiotics in the intestine and kidney. *J Pharmacol Exp Ther* **275**:1631-1637.
- Schwarz R, Kaspar A, Seelig J and Kunnecke B (2002) Gastrointestinal transit times in mice and humans measured with <sup>27</sup>Al and <sup>19</sup>F nuclear magnetic resonance. *Magn Reson Med* **48**:255-261.
- Shen H, Ocheltree SM, Hu Y, Keep RF and Smith DE (2007) Impact of genetic knockout of PEPT2 on cefadroxil pharmacokinetics, renal tubular reabsorption, and brain penetration in mice. *Drug Metab Dispos* **35**:1209-1216.
- Shen H, Smith DE, Yang T, Huang YG, Schnermann JB and Brosius FC, 3rd (1999) Localization of PEPT1 and PEPT2 proton-coupled oligopeptide transporter mRNA and protein in rat kidney. *Am J Physiol* **276**:F658-665.
- Takahashi K, Nakamura N, Terada T, Okano T, Futami T, Saito H and Inui KI (1998) Interaction of beta-lactam antibiotics with H<sup>+</sup>/peptide cotransporters in rat renal brush-border membranes. *J Pharmacol Exp Ther* **286**:1037-1042.
- Terada T, Sawada K, Saito H, Hashimoto Y and Inui K (1999) Functional characteristics of basolateral peptide transporter in the human intestinal cell line Caco-2. *Am J Physiol* **276**:G1435-1441.
- Thamotharan M, Lombardo YB, Bawani SZ and Adibi SA (1997) An active mechanism for completion of the final stage of protein degradation in the liver, lysosomal transport of dipeptides. *J Biol Chem* **272**:11786-11790.
- Urtti A, Johns SJ and Sadee W (2001) Genomic structure of proton-coupled oligopeptide transporter hPEPT1 and pH-sensing regulatory splice variant. *AAPS PharmSci* **3**:E6.
- Walker D, Thwaites DT, Simmons NL, Gilbert HJ and Hirst BH (1998) Substrate upregulation of the human small intestinal peptide transporter, hPepT1. *J Physiol* **507** ( Pt 3):697-706.
- Yamamoto T, Watabe K, Nakahara M, Ogiyama H, Kiyohara T, Tsutsui S, Tamura S, Shinomura Y and Hayashi N (2008) Disturbed gastrointestinal motility and decreased interstitial cells of Cajal in diabetic db/db mice. *J Gastroenterol Hepatol* **23**:660-667.

Zhang EY, Emerick RM, Pak YA, Wrighton SA and Hillgren KM (2004) Comparison of human and monkey peptide transporters: PEPT1 and PEPT2. *Mol Pharm* **1**:201-210.

Zhou X, Thamotharan M, Gangopadhyay A, Serdikoff C and Adibi SA (2000) Characterization of an oligopeptide transporter in renal lysosomes. *Biochim Biophys Acta* **1466**:372-378.

## APPENDIX A

### MEASUREMENT OF SKPT INTRACELLULAR VOLUME

The intracellular volume of SKPT cells was measured by the 3-*O*-methyl-D-glucose method (Kletzien et al., 1975; Pollock et al., 1986) in glucose-free media. The cell monolayers were washed and preincubated apically with 0.4 ml of pH 6.0 buffer and basolaterally with 1.2 ml of pH 7.4 buffer for 10 min at 37°C. The buffers were then removed and fresh buffer (0.4 ml pH 6.0 or 1.2 ml pH 7.4 containing [<sup>3</sup>H]3-*O*-methyl-D-glucose (3-OMG) and [<sup>14</sup>C]mannitol; 1 mM, 5 mM, and 10 mM of each) was added to the apical and basolateral compartments, respectively, in presence of 200 μM of phloridzin (an inhibitor of Na<sup>+</sup>-coupled glucose cotransport). After 300 minutes of incubation (determined from Fig A.1) at 37°C, the uptake buffers were aspirated from both compartments and the monolayers were washed 5 times from both sides with ice-cold buffer containing 100 μM of phloretin (an inhibitor of facilitated diffusion). The filters with monolayers were then detached from the chamber, placed in a scintillation vial, and the cells were solubilized with 0.2 M NaOH and 1% SDS. Radioactivity was measured in solubilized cells with a dual-channel liquid scintillation counter (Beckman LS 6000 SC; Beckman Coulter Inc., Fullerton, CA). Uptake of 3-*O*-methyl-D-glucose was normalized for amount of protein per well, and the slope of uptake vs. concentration was taken as the intracellular volume of SKPT cells. Thus the intracellular volume of SKPT cells was determined to be 2.0±0.1 μl/mg of protein (Fig A.2).



## REFERENCES:

Kletzien RF, Pariza MW, Becker JE and Potter VR (1975) A method using 3-O-methyl-D-glucose and phloretin for the determination of intracellular water space of cells in monolayer culture. *Anal Biochem* **68**:537-544.

Pollock AS, Warnock DG and Strewler GJ (1986) Parathyroid hormone inhibition of Na<sup>+</sup>-H<sup>+</sup> antiporter activity in a cultured renal cell line. *Am J Physiol* **250**:F217-225.

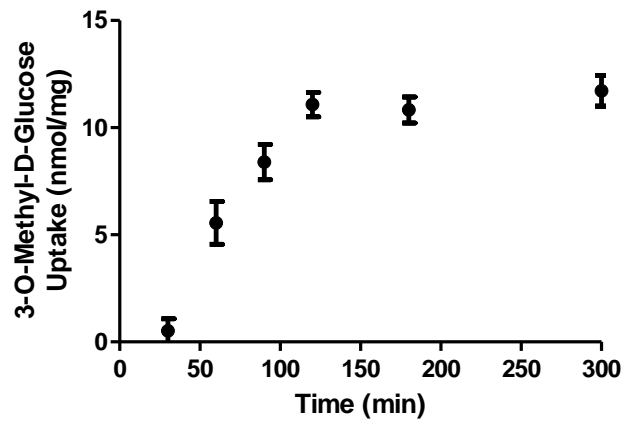


**Figure A.1** Intracellular accumulation of 5 mM  $^3\text{H}$ -3-OMG ((1.6  $\mu\text{Ci}/\text{well}$ ) and  $^{14}\text{C}$ -mannitol (0.5  $\mu\text{Ci}/\text{well}$ ) as a function of time in SKPT cell monolayers at 37°C. The apical compartment buffer pH was 6.0 and basolateral compartment buffer was 7.4. Data are expressed as mean  $\pm$  SE (n=4).

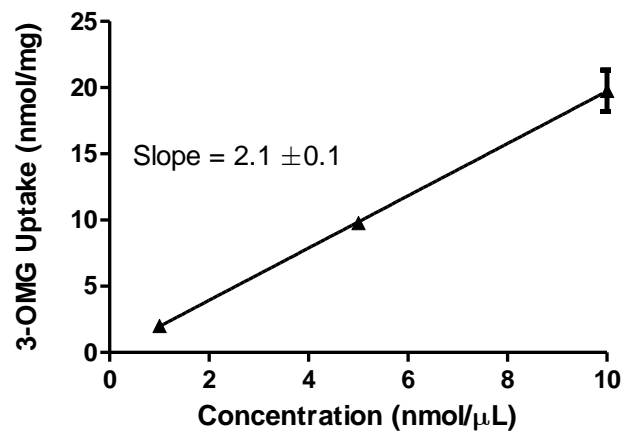


**Figure A.2** Intracellular accumulation of  $^3\text{H}$ -3-OMG ((1.6  $\mu\text{Ci}$ /well) and  $^{14}\text{C}$ -mannitol (0.5  $\mu\text{Ci}$ /well) as a function of concentration (i.e., 1, 5, and 10 mM) in SKPT cell monolayers at 37°C for 300 minutes. The apical compartment buffer pH was 6.0 and basolateral compartment buffer was 7.4. Data are expressed as mean  $\pm$  SE (n=4).

## APPENDIX B

### COMPARISON OF WATER FLUX MEASUREMENTS FOR MOUSE *IN SITU* SINGLE-PASS INTESTINAL PERFUSION

In order to evaluate the use of PEG 4000 as a non-absorbable marker, 3 different methods of estimation for water absorption/secretion (PEG 4000, inulin and gravimetric) during mouse *in situ* single-pass intestinal perfusion were compared in wild-type and PEPT1 knockout mice. Concentration of drug coming out of perfused intestine is corrected for water flux by a correction factor according to Eq. 2, 4 and 6. The correction factors for water absorption/secretion were estimated by Eq. 1 for non-absorbable marker PEG 4000, by Eq. 3 for non-absorbable marker inulin 5000, and by Eq. 5 for gravimetric method. (Refer to chapter 4, method section for experimental procedure.)

#### Use of non-absorbable marker PEG 4000

$$\text{Correction factor} = \frac{PEG_{out}}{PEG_{in}} \quad \text{Eq. 1}$$

$$C_{out} = \frac{C_{perfusate}}{PEG_{out} / PEG_{in}} \quad \text{Eq. 2}$$

### Use of non-absorbable marker inulin

$$\text{Correction factor} = \frac{\text{Inulin}_{out}}{\text{Inulin}_{in}} \quad \text{Eq. 3}$$

$$C_{out} = \frac{C_{perfusate}}{\text{Inulin}_{out} / \text{Inulin}_{in}} \quad \text{Eq. 4}$$

### Use of gravimetric method

$$\text{Correction factor} = \frac{V_{in-total}}{V_{out-total}} \quad \text{Eq. 5}$$

$$C_{out} = \frac{C_{perfusate}}{V_{in-total} / V_{out-total}} \quad \text{Eq. 6}$$

where  $C_{perfusate}$  is the actual concentration of drug in the exiting perfusate, and  $PEG_{in}$  and  $PEG_{out}$  are the inlet and outlet concentrations of PEG 4000 and  $Inulin_{in}$  and  $Inulin_{out}$  are the inlet and outlet concentrations of Inulin 5000.  $V_{in-total}$  and  $V_{out-total}$  are the total volume of solution entered and exited the perfused intestinal segments.  $C_{out}$  represents the corrected outlet concentrations of drug.

If correction factor  $> 1$ , then there is some loss of water due to water absorption from the lumen to intestine, thus  $C_{out}$  is more concentrated and thus should be corrected to a lower concentration by dividing by the correction factor of  $> 1$

If correction factor  $< 1$ , then there is some gain of water due water secretion from the intestine into the lumen, thus  $C_{out}$  is more diluted and should be corrected to a higher concentration by dividing by the correction factor of  $< 1$

Based on the results from the comparison study of different water flux measurements, PEG 4000 (compared to gravimetric method and inulin) appears to overestimate the water secretion by approximately 21% for mouse intestinal perfusion in both wild-type and PEPT1 knockout mice (Fig. B.1). Therefore, all of the water flux corrections assessed by PEG 4000 (in Chapter 4) were adjusted by an average water flux correction of 14%, as determined by the 3 methods (i.e., non-absorbable markers PEG 4000 plus inulin plus gravimetric method).

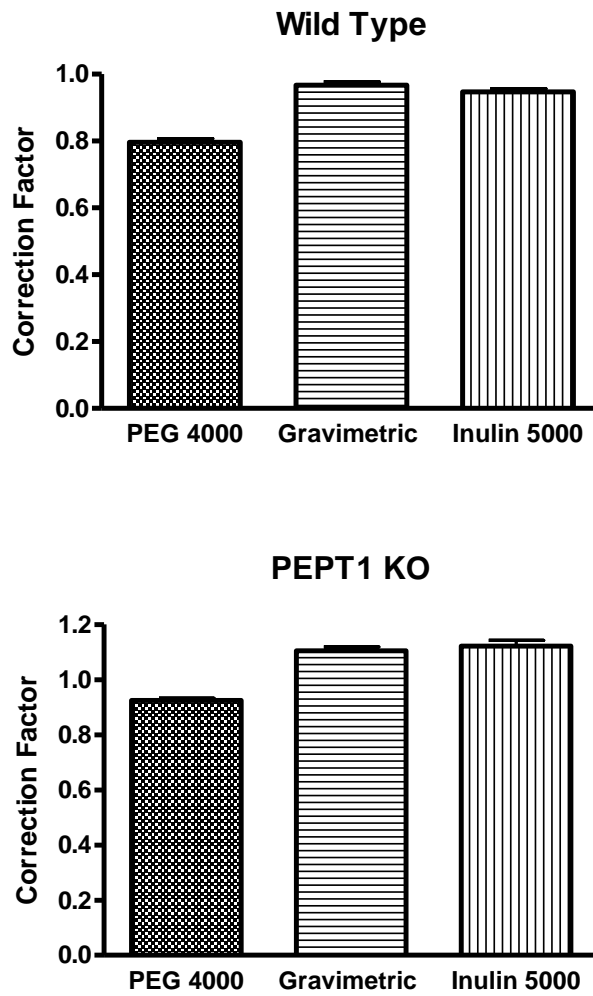


**Figure B.1** Correction factors for water absorption/secretion during the mouse *in situ* intestinal perfusion estimated by non-absorbable markers (i.e., PEG 4000, inulin 5000) and gravimetric methods in wild-type and PEPT1 knockout mice. Data are expressed as mean  $\pm$  SE (n=4-8).